INFORMATION TO USERS

This manuscript has been reproduced from the microfilm master. UMI films the text directly from the original or copy submitted. Thus, some thesis and dissertation copies are in typewriter face, while others may be from any type of computer printer.

The quality of this reproduction is dependent upon the quality of the copy submitted. Broken or indistinct print, colored or poor quality illustrations and photographs, print bleedthrough, substandard margins, and improper alignment can adversely affect reproduction.

In the unlikely event that the author did not send UMI a complete manuscript and there are missing pages, these will be noted. Also, if unauthorized copyright material had to be removed, a note will indicate the deletion.

Oversize materials (e.g., maps, drawings, charts) are reproduced by sectioning the original, beginning at the upper left-hand corner and continuing from left to right in equal sections with small overlaps. Each original is also photographed in one exposure and is included in reduced form at the back of the book.

Photographs included in the original manuscript have been reproduced xerographically in this copy. Higher quality 6" x 9" black and white photographic prints are available for any photographs or illustrations appearing in this copy for an additional charge. Contact UMI directly to order.

U·M·I

University Microfilms International
A Bell & Howell Information Company
300 North Zeeb Road, Ann Arbor, MI 48106-1346 USA
313/761-4700 800/521-0600

Reproduced with permission of the copyright owner. Further reproduction prohibited without permission.

Reproduced with permission of the copyright owner. Further reproduction prohibited without permission.

Order Number 9308417

Synthesis of state feedback laws for end-point optimization in batch processes

Palanki, Srinivas, Ph.D.

The University of Michigan, 1992

Copyright ©1992 by Palanki, Srinivas. All rights reserved.

U·M·I
300 N. Zeeb Rd.
Ann Arbor, MI 48106

Reproduced with permission of the copyright owner. Further reproduction prohibited without permission.

Reproduced with permission of the copyright owner. Further reproduction prohibited without permission.

SYNTHESIS OF STATE FEEDBACK LAWS FOR END-POINT OPTIMIZATION IN BATCH PROCESSES

by

Srinivas Palanki

A dissertation submitted in partial fulfillment
of the requirements for the degree of
Doctor of Philosophy
(Chemical Engineering)
in The University of Michigan
1992

Doctoral Committee:

Associate Professor Costas Kravaris, Co-chairperson
Professor Henry Y. Wang, Co-chairperson
Assistant Professor Jennifer J. Linderman
Professor Katta G. Murty

Reproduced with permission of the copyright owner. Further reproduction prohibited without permission.

Reproduced with permission of the copyright owner. Further reproduction prohibited without permission.

असतोमा सद्गमय
तमसोमा ज्योतिर्गमय
मृत्योर्मा अमृतंगमय

Lead me from ignorance to knowledge.
Lead me from darkness to light.
Lead me from death to eternal life.

(Vedic Prayer)

Reproduced with permission of the copyright owner. Further reproduction prohibited without permission.

RULES REGARDING THE USE OF

MICROFILMED DISSERTATIONS

Microfilmed or bound copies of doctoral dissertations submitted to The University of Michigan and made available through University Microfilms International or The University of Michigan are open for inspection, but they are to be used only with due regard for the rights of the author. Extensive copying of the dissertation or publication of material in excess of standard copyright limits, whether or not the dissertation has been copyrighted, must have been approved by the author as well as by the Dean of the Graduate School. Proper credit must be given to the author if any material from the dissertation is used in subsequent written or published work.

Reproduced with permission of the copyright owner. Further reproduction prohibited without permission.

© Srinivas Palanki 1992
All Rights Reserved

Reproduced with permission of the copyright owner. Further reproduction prohibited without permission.

To my parents Nagamani and Ramakrishna Rao

Reproduced with permission of the copyright owner. Further reproduction prohibited without permission.

ACKNOWLEDGEMENTS

I wish to express my deep gratitude to Professors Costas Kravaris and Henry Y. Wang who gave me the unique opportunity to work in the areas of Process Control and Biochemical Engineering. Their valuable advice and insightful comments are sincerely appreciated. I would also like to thank my committee members Professors Jennifer Linderman and Katta G. Murty for their suggestions and continuing interest in my research work. I am indebted to Dr. Robert Stieber and Dr. Abhay Kirpekar from whom - during two interships at Merck and Co. - I learnt many aspects of bioreactor operation. I owe a special note of appreciation to Professors Spillios Fassois and Dr. Barry Buckland who provided guidence during the early stages of this thesis. Financial support by the National Science Foundation for this work is gratefully acknowledged.

I had the good fortune to work with a number of talented collegues and friends who helped me maintain my course often through difficult times. I am indebted to Somesh Nigam who introduced me to the exciting world of Biotechnology. I would also like to extend my heartfelt gratitude to Nitin Anturkar, Tom Naglak, Masoud Soroush, Prodromos Daoutidis, Krishna Mohan, Amit Varma, Sadanand Deshpande, Min Zhang and Mike Bly for their friendship and constant support.

I am grateful to my parents without whose encouragement this endeavor would not have been possible. Finally, to my wife Subhadra, whose love and support brightens my life, I give my gratitude for her faith in me.

Reproduced with permission of the copyright owner. Further reproduction prohibited without permission.

TABLE OF CONTENTS

DEDICATION ii

ACKNOWLEDGEMENTS iii

LIST OF FIGURES vii

LIST OF TABLES x

LIST OF APPENDICES xii

ABSTRACT xiii

CHAPTER

I. INTRODUCTION 1

1.1 Motivation 1
1.2 Scope and Objectives 3

II. MODELING CONSIDERATIONS 6

2.1 Model Development 6
2.2 Model Reduction 7
2.3 Models with Affine Manipulated Input 9
2.4 Nomenclature 11

III. THE CLASSICAL OPTIMAL CONTROL PERSPECTIVE 12

3.1 Introduction 12
3.2 Formulation of the End-Point Optimization Problem 12
3.2.1 Necessary Conditions for Optimality on the Unconstrained Arc 13
3.2.2 Necessary Conditions for Optimality on the Constrained Arc 16
3.3 Difficulties in Using the Classical Approach in End-Point Optimization 16

Reproduced with permission of the copyright owner. Further reproduction prohibited without permission.

IV. STATE FEEDBACK LAWS FOR END-POINT OPTIMIZATION: FIXED FINAL TIME AND NO STATE CONSTRAINTS 18

4.1 Introduction 18
4.2 End-Point Optimization of Time Invariant Systems 19
4.3 Singular Extremal as a State Feedback Law Independent of the Adjoint States 22
4.4 End-Point Optimization for Time-Varying Systems 26
4.5 Implementation 31
4.6 Illustrative Examples 33
4.6.1 Example 1: Linear System 34
4.6.2 Example 2: s = infinity 39
4.6.3 Example 3: Static State Feedback 48
4.6.4 Example 4: Dynamic State Feedback 58
4.7 Nomenclature 66

V. STATE FEEDBACK LAWS FOR END-POINT OPTIMIZATION: FREE FINAL TIME AND A STATE INEQUALITY CONSTRAINT 69

5.1 Introduction 69
5.2 End Point Optimization of Time Invariant Systems 70
5.2.1 Optimal State Feedback Laws on Unconstrained Arcs 71
5.2.2 Optimal State Feedback Laws on Constrained Arcs 76
5.3 End-Point Optimization of Time Varying Systems 78
5.3.1 Optimal State Feedback Laws on Unconstrained Arcs 78
5.3.2 Optimal State Feedback Laws on Constrained Arcs 80
5.4 Implementation 81
5.5 Illustrative Examples 82
5.5.1 Example 1 82
5.5.2 Example 2 92
5.5.3 Example 3 101
5.6 Nomenclature 120

VI. REGULATION OF TIME-VARYING SYSTEMS 123

6.1 Introduction 123
6.2 Mathematical Preliminaries 125
6.2.1 Relative Order 125
6.3 Zero Dynamics 126
6.3.1 Linear Independence of Vector Fields 127
6.3.2 Invertible Transformations 128
6.3.3 Linear Independence of Scalar Fields 129
6.4 State Feedback 138

Reproduced with permission of the copyright owner. Further reproduction prohibited without permission.

6.4.1 Linear Controller Design with State Feedback . . . 139
6.4.2 Internal Stability . . . 140
6.5 Output Feedback Controller Synthesis via GLC . . . 144
6.5.1 Reduced Order Realization . . . 146
6.6 Linear Time-Varying Systems . . . 147
6.6.1 Zero Dynamics of Linear Time-Varying Systems . . 149
6.7 Illustrative Example . . . 150
6.8 Nomenclature . . . 161

VII. MODELING AND YIELD OPTIMIZATION OF CEPHAMYCIN C FERMENTATION . . . 162

7.1 Introduction . . . 162
7.2 Microbial Cell Metabolism for Synthesis of Beta-Lactam Antibiotics . . . 163
7.3 A Mathematical Model for Synthesis of Beta-Lactam Antibiotics . . . 168
7.3.1 Cell Growth . . . 169
7.3.2 Substrate Utilization . . . 169
7.3.3 Synthesis of Enzymes Necessary for Synthesis of Cephamycin C . . . 170
7.3.4 Synthesis of Intermediates and Product of Secondary Metabolism . . . 170
7.4 Yield Optimization of Cephamycin C . . . 172
7.4.1 Effect of Feeding Glucose . . . 173
7.4.2 Effect of Feeding Amino Acids . . . 176
7.4.3 Effect of Changing Temperature . . . 179
7.4.4 Effect of Changing Temperature on Amino Acid Feeding . . . 185
7.5 Conclusions . . . 185

VIII. CONCLUSIONS AND FUTURE WORK . . . 188

APPENDICES . . . 191

BIBLIOGRAPHY . . . 205

Reproduced with permission of the copyright owner. Further reproduction prohibited without permission.

LIST OF FIGURES

Figure

4.1 Profile of switching function $\lambda^T g(x)$ (example 1) 37

4.2 Optimal time profile of species B (example 1) 38

4.3 Profile of time-varying parameter $\mu_m(t)$ (example 2) 40

4.4 Optimal input profile (example 2) 43

4.5 Optimal cell mass and substrate profiles (example 2) 44

4.6 Profile of switching function $\lambda^T g(x,t)$ (example 2) 47

4.7 Profile of time-varying parameters $\mu_0(t)$ and $\nu_0(t)$ (example 3) . . . 49

4.8 Optimal input profile (example 3) 53

4.9 Optimal time profile of ethanol (example 3) 54

4.10 Profile of switching function $\lambda^T g(x,t)$ and second order condition $\lambda^T[g, \overline{ad}_f^1 g](x,t)$ (example 3) 55

4.11 Optimal input profile (example 4) 63

4.12 (Optimal time profile of species B example 4) 64

4.13 Profile of switching function $\lambda^T g(x)$ and second order condition $\lambda^T[g, ad_f^1 g](x)$ (example 4) 65

5.1 Optimal temperature profile (example 1) 86

5.2 Optimal cooling rate profile (example 1) 87

5.3 Profile of objective function (example 1) 88

5.4 First order condition (example 1) 89

Reproduced with permission of the copyright owner. Further reproduction prohibited without permission.

5.5 Hamiltonian (example 1) 90

5.6 Optimal input profile (example 2) 96

5.7 Profile of objective function (example 2) 97

5.8 First order condition (example 2) 98

5.9 Second order condition (example 2) 99

5.10 Hamiltonian (example 2) 100

5.11 Optimal input profile (example 3, Case I) 106

5.12 Profile of objective function (example 3, Case I) 107

5.13 First order condition (example 3, Case I) 108

5.14 Second order condition (example 3, Case I) 109

5.15 Hamiltonian (example 3, Case I) 110

5.16 Optimal input profile (example 3, Case II) 114

5.17 Profile of objective function (example 3, Case II) 115

5.18 First order condition (example 3, Case II) 116

5.19 Second order condition (example 3, Case II) 117

5.20 Hamiltonian (example 3, Case II) 118

6.1 A Schematic of the System 152

6.2 Time Profile of Activity of Catalytic Sites 153

6.3 Closed Loop Response for Perfect Model 156

6.4 Time Varying Parameter Da_3 157

6.5 Robustness Analysis 158

6.6 Comparison with Adaptive Control 160

Reproduced with permission of the copyright owner. Further reproduction prohibited without permission.

7.1 Key Metabolic Processes in a Microbial Cell 164

7.2 Biosynthetic Pathway for α-aminoadipate, Cysteine, and Valine . . 166

7.3 Biosynthetic Pathway for β-lactam Antibiotics 167

7.4 Effect of Glucose Feeding on Product 175

7.5 Effect of Feeding Amino Acids on Product 177

7.6 Effect of Enzyme Activity on Product 180

7.7 Effect of Changing Temperature on Product 183

7.8 Optimal Temperature and Product Profiles 184

7.9 Optimal Temperature and Product Profiles (Constrained Optimization) 186

Reproduced with permission of the copyright owner. Further reproduction prohibited without permission.

LIST OF TABLES

Table

4.1 Model Parameters 36

4.2 Initial Conditions 36

4.3 Model Parameters 42

4.4 Initial Conditions 45

4.5 Robustness Analysis 46

4.6 Open Loop vs. Closed Loop Implementation 46

4.7 Model Parameters 52

4.8 Initial Conditions 52

4.9 Sensitivity of error in switching time on performance index 56

4.10 Open-loop Vs. Closed-loop Implementation 57

4.11 Model Parameters 62

4.12 Initial Conditions 62

4.13 Sensitivity of error in initial condition of $u(t)$ on performance index 62

4.14 Robustness Analysis 63

5.1 Model Parameters (example 1) 85

5.2 Initial Conditions (example 1) 85

5.3 Constrained vs. Unconstrained Optimization (example 1) 91

5.4 Robustness Analysis (example 1) 92

Reproduced with permission of the copyright owner. Further reproduction prohibited without permission.

5.5 Model Parameters (example 2) 95

5.6 Initial Conditions (example 2) 95

5.7 Constrained Optimization (example 2) 95

5.8 Sensitivity of error in switching time on performance index 101

5.9 Model Parameters (example 3) 105

5.10 Initial Conditions (example 3) 105

5.11 Constrained Optimization (example 3, Case I) 105

5.12 Robustness Analysis 111

5.13 Sensitivity of error in initial condition of $u(t)$ on performance index 112

5.14 Constrained Optimization (example 3, Case II) 113

5.15 Sensitivity of error in initial condition of $u(t)$ on performance index 113

5.16 Robustness Analysis 119

7.1 Model Parameters 187

Reproduced with permission of the copyright owner. Further reproduction prohibited without permission.

LIST OF APPENDICES

Appendix

A. PROOFS OF THEOREMS IN CHAPTER IV 192

A.1 Proof of Theorem 4.1 192
A.2 Proof of Corollary 4.1 193
A.3 Proof of Corollary 4.2 193
A.4 Proof of Theorem 4.2 194
A.5 Proof of Theorem 4.3 195
A.6 Proof of Theorem 4.4 196
A.7 Proof of Theorem 4.5 197

B. PROOFS OF CHAPTER V 199

B.1 Proof of Theorem 5.1 199
B.2 Proof of Theorem 5.2 200
B.3 Proof of Theorem 5.3 201
B.4 Proof of Theorem 5.4 202

Reproduced with permission of the copyright owner. Further reproduction prohibited without permission.

ABSTRACT

SYNTHESIS OF STATE FEEDBACK LAWS FOR END-POINT OPTIMIZATION IN BATCH PROCESSES

by
Srinivas Palanki

Co-chairpersons: Costas Kravaris, Henry Y. Wang

This thesis studies the class of singular optimal control problems, where a performance index must be optimized at the final time of operation of a batch process. It is shown that geometric tools can be used to obtain a more concrete and transparent representation of the necessary conditions for optimality. Optimal state feedback laws for the singular region of operation are derived for the first time. The existence of a singular region as well as the nature of the feedback law (static or dynamic) are completely characterized in terms of the Lie bracket structure of the system dynamics. Explicit synthesis formulae for the state feedback laws are first obtained for the case where the final time is fixed and there are no state inequality constraints. Utilizing the same methodology, these results are extended to include the case where the final time is free and there is a state inequality constraint. As illustrative examples of application of the proposed methodology, several end-point optimization problems in batch chemical and biochemical reactors are considered. It is observed that under certain conditions the end-point optimization problem is equivalent to a

Reproduced with permission of the copyright owner. Further reproduction prohibited without permission.

regulation problem in a time-varying system. Feedback laws are derived to solve this regulation problem. A nonlinear transformation is derived which provides a linear time-invariant input-output response. A standard linear controller with integral action is then used for offsetless tracking of the desired trajectory. Internal stability results under the state feedback are provided. Then, a dynamic output feedback controller for the time-varying system is synthesized. Finally, end-point optimization of cephamycin C, an industrially important β-lactam antibiotic, is considered. Three different manipulated inputs, namely, glucose feeding, amino acids feeding and temperature, are considered. It is shown how the theory developed in this thesis can be used for end-point optimization for each case.

Reproduced with permission of the copyright owner. Further reproduction prohibited without permission.

CHAPTER I

INTRODUCTION

The study of the application of science is easy for anyone who is master of the theory of it.

Louis Pasteur

1.1 Motivation

Batch and semi-batch processes are of great importance to the chemical industry. A wide variety of specialty chemicals such as antibiotics and polymers are produced in batch reactors; they are preferred due to their ease and flexibility of operation. Batch reactors are used when there are many processing steps in the chemical process, when isolation is required for reasons of sterility or safety and when the materials involved are hard to handle.

The first step to rational design of a batch chemical reactor generally consists of guaranteeing safety and operability objectives. Once these goals are achieved, the next step is to make its operation profitable. Since batch processes typically produce low-volume-high-value products, optimal operation is extremely important. Every small improvement in the process may result in considerable reduction in production costs. Batch processes are *transient* in nature; the process variables

Reproduced with permission of the copyright owner. Further reproduction prohibited without permission.

undergo significant changes during the batch cycle and there is no process steady state. Generally, the major objective is *not* to keep the system at a set point but to *maximize* the product of interest at the *end* of the batch cycle. Thus, in this situation, the role of control is to optimize a performance index at the final time rather than to regulate of the process.

There is a wide body of literature dealing with the solution of end-point optimization problems on a case-by-case basis for specific batch processes. There are two different approaches that have been used.

1. Open-Loop Optimization: In this approach, the optimal trajectory of the manipulated input is first calculated off-line via optimal control theory and then implemented on the process in an open-loop fashion. There have been a plethora of articles in using this approach, primarily because of its simplicity in implementation. Hicks *et al.* (1969) applied Pontryagin's principle to a free radical polymerization reactor to minimize a performance index which was a function of deviations of conversion, number average degree of polymerization and polydispersity from their desired values. Sacks *et al.* (1972) used Pontryagin's principle to calculate the optimal temperature and initiator addition policy to achieve a given conversion in a free radical polymerization batch reactor. Chen and Jeng (1978) studied batchwise bulk polymerizations operated under optimal temperature and initial initiator concentration. Thomas and Kiparissides (1984) applied the Pontryagin Minimum Principle to a batch polymerization reactor to calculate the optimal temperature and initiator policies that are required to produce a polymer with a desired final conversion, and desired number average and weight average molecular weights. Fishman and Biryukov (1974) considered the problem of optimal glucose feed strategy for penicillin production. Ohno *et al.* (1976) used a method based on Greens' theorem for optimizing the produc-

Reproduced with permission of the copyright owner. Further reproduction prohibited without permission.

tion of lysine. Weigand (1981) calculated the optimal feeding strategy in a repeated fed-batch fermentation to maximize cell mass production.

2. Optimal State Feedback: Using an open-loop optimization scheme is appropriate in situations where the process model is accurately known and there are no external disturbances to the process. To account for unanticipated changes in the process or the environment, the use of optimal state feedback has been proposed in the literature in a number of specific applications. In this approach, the solution to the optimization problem is calculated off-line as a function of the states and implemented as a state feedback law. In this way, the process is "forced" to follow a path in state space which has been determined *a priori*. Modek and Lim (1987) used this approach to show that the closed-loop system was able to attenuate errors in initial conditions in a lysine fermentation. Chen and Huang (1981) derived the optimal initiator feeding policy as a function of the system states in a semi-batch isothermal solution polymerization process.

The derivation of optimal state feedback laws is available in the literature only for **specific** batch applications. There are no results available which provide conditions under which a state feedback exists or general formulae for the control law.

1.2 Scope and Objectives

The purpose of this thesis is to study the class of singular optimal control problems, where a performance index must be optimized at the final time of operation of a batch process. The specific objectives are listed below:

- To synthesize state feedback laws in the singular region of operation for end-point optimization of a batch reactor when the final time is fixed and there are no state constraints present.

Reproduced with permission of the copyright owner. Further reproduction prohibited without permission.

• To synthesize state feedback laws in the singular region of operation for end-point optimization of a batch reactor when the final time is free and there exists a state inequality constraint.

• To demonstrate how this general theory applies to specific batch chemical and biochemical reactors.

In chapter II, modeling issues in batch chemical processes are considered. The types of mathematical descriptions available for process optimization and control are outlined. In chapter III, a brief review of the optimal control formulation of the end-point optimization problem is given in the context of the classical Pontryagin Principle. This chapter addresses the key difficulties in using the classical optimization methods for end-point optimization in batch reactors and provides the motivation for synthesizing optimal state feedback laws. Then the main mission of this thesis, which is to derive for the first time state feedback laws for end-point optimization in batch reactors, is addressed. In chapter IV, optimal state feedback laws are derived which guarantee optimality at a fixed final time of the batch when there are no state constraints present. The mathematical framework of the derivation of the optimal state feedback lies within the differential geometric approach. In chapter V, these results are extended to include the case where the the final time is free and there exists a state inequality constraint. As illustrative examples of the application of the proposed methodology, several end-point optimization problems in a batch chemical and biochemical reactors are considered. In chapters IV and V, it is shown that under certain conditions the end-point optimization problem reduces to a problem of regulating a time-varying system. In chapter VI, a general theoretical framework for solving such regulation problems is addressed. In chapter VII, a case study of end-point optimization in a cephamycin C fermentation is considered

Reproduced with permission of the copyright owner. Further reproduction prohibited without permission.

where it is shown how the theory developed in this thesis is applied to achieve yield optimization of cephamycin C. Finally, in chapter VIII, the main results of the thesis are summarized and future directions are outlined.

Reproduced with permission of the copyright owner. Further reproduction prohibited without permission.

CHAPTER II

MODELING CONSIDERATIONS

The best model for a cat is another cat or, better, the cat itself

Norbert Wiener

2.1 Model Development

A mathematical model is a quantification of a physical process that enables *prediction* of process behavior. More precisely (Denn, 1986):

> *A mathematical model of a process is a system of equations whose solution, given specified input data, is representative of the response of the process to a corresponding set of inputs.*

Mathematical models are generated by a combination of equations from three methodologies. These are catagorized as follows:

• Fundamental: This methodology uses well-established physical, chemical or biological principles. Modeling chemical engineering systems always requires the application of conservation of mass and/or energy.

• Empirical: This methodology records the relationship between system inputs and outputs by "fitting" an equation to experimental data. It is usually necessary to

Reproduced with permission of the copyright owner. Further reproduction prohibited without permission.

make some *a priori* assumptions about the mathematical structure of the equations. For instance, one could use a cubic equation to relate density to temperature (see Kern, 1950)

• Hypothetical: This methodology involves making educated guesses due to lack of information about the system. For instance, one might guess that an unmeasured rate limiting enzyme is inhibited by the substrate and write the substrate and cell mass balance accordingly in a fermentation (see Dykstra *et al.*, 1987).

Using this approach a continuum of models can be developed, each appropriate for given objectives. In this thesis we consider only deterministic, continuous models which can be described by ordinary differential equations.

2.2 Model Reduction

A real system, placed in its real environment, represents a very complex situation. Processes such as biological processes could be characterized by a large number of individual reactions (of the order of a thousand reactions). A detailed mathematical model which accounts for each reaction of the system becomes too complex for practical applications such as optimization and control. A balance between physiological reality and simplicity calls for reduction in the complexity of the mathematical description to develop a tractable model that is of practical utility. For this reason, most complex chemical processes are described by simplified models by ignoring or lumping together some of the system dynamics.

Joshi and Palsson (1988) developed a reduced order growth model of an individual *E. coli* cell from a previously developed chemically structured complex single cell model. Through time-scale analysis they obtained a reduced order model with *constant* parameters from a high order model with constant parameters. However, in

Reproduced with permission of the copyright owner. Further reproduction prohibited without permission.

some cases, model reduction leads to *time varying* parameters. For instance, consider the following second order reaction in a batch reactor catalyzed by a catalyst E:

$$A \xrightarrow{E} B$$

The catalyst is subject to a first order decay. We can write a mathematical model for this process as follows:

$$\begin{aligned} \frac{dC_A}{dt} &= -k_A.a.C_A^2 \\ \frac{da}{dt} &= -k_E.a \end{aligned} \tag{2.1}$$

where a is the activity of the catalyst. Integrating the balance for a and substituting in the balance for species A, we obtain:

$$\frac{dC_A}{dt} = -k_A.(exp(-k_E t)).C_A^2 \tag{2.2}$$

Thus, the reduced model has a time-varying parameter $k_A.(exp(-k_E t))$.

Similarly, Chu (1987) considered the effect of temperature and pH on the parameters of a simple model for the production of cephalosporin C. The utilization of glucose was modeled as:

$$\frac{dS}{dt} = -\frac{1}{Y_s}\frac{\mu_s^m SX}{(K_s + S)} \tag{2.3}$$

The parameters μ_m^s, K_s and Y_s are functions of pH and temperature. Chu calculated optimal pH and temperature profiles to maximize the yield of cephalosporin C. When the fermentor is operated at this pH and temperature profile, the parameters μ_m^s, K_s and Y_s become time-varying.

Harmon *et al.* (1987) expressed the process dynamics of a fermentation by a linear time-varying parameter model. Similarly, Staniskis and Levisauskas (1984) described the production of α-amylase in a batch fermentation by a non-linear model with time-varying parameters.

Reproduced with permission of the copyright owner. Further reproduction prohibited without permission.

Thus, we observe that simple models developed for process optimization and control applications consist of a system of ordinary differential equations with constant or time-varying parameters. Furthermore, the model parameters and initial conditions could vary from batch to batch. For instance, in biological fermentations, minor changes in environmental conditions such as sterilization time, inoculum volume, and culture media can drastically change the specific growth rate and the specific product formation rate of the culture. Since the optimal depends on the model parameters and the initial conditions, it is necessary to develop an optimization strategy where the system states and the model parameters can be updated on-line.

2.3 Models with Affine Manipulated Input

In chemical engineering process models, the manipulated input is usually an affine function in the state model. Thus, throughout this thesis we will consider models of the following forms:

Time Invariant Models:

$$\dot{x} = f(x) + g(x)u \tag{2.4}$$

Time Varying Models:

$$\dot{x} = f(x,t) + g(x,t)u \tag{2.5}$$

where x is the vector of system states and u is a scalar manipulated input.

Cases where the manipulated input appears as a non-affine function in state model can be handled as follows. Consider the following model where the manipulated input appears as a non-affine function in state model.

$$\dot{x} = f(x,u,t) \tag{2.6}$$

Reproduced with permission of the copyright owner. Further reproduction prohibited without permission.

where x and f are vectors of dimension n. Define an auxiliary variable:

$$x_{n+1} = u \tag{2.7}$$

and define a new manipulated input v as:

$$v = \frac{dx_{n+1}}{dt} \tag{2.8}$$

Then the "prolonged" system is:

$$\frac{d}{dt}\begin{bmatrix} x \\ x_{n+1} \end{bmatrix} = \begin{bmatrix} f(x,t) \\ 0 \end{bmatrix} + \begin{bmatrix} 0 \\ 1 \end{bmatrix} v \tag{2.9}$$

which is a model of the form (2.5)

Reproduced with permission of the copyright owner. Further reproduction prohibited without permission.

2.4 Nomenclature

C_A = concentration of species A

K_s = kinetic parameter in equation (2.3)

S = glucose concentration

X = cell mass concentration

Y_s = yield coefficient

a = catalyst activity

f = vector function in dynamic model (2.4) or (2.5)

g = vector function in dynamic model (2.4) or (2.5)

k_A = kinetic parameter in equation (2.1)

k_E = kinetic parameter in equation (2.1)

t = time

u = scalar manipulated input

x = vector of system states

μ_s^m = kinetic parameter in equation (2.3)

Reproduced with permission of the copyright owner. Further reproduction prohibited without permission.

CHAPTER III

THE CLASSICAL OPTIMAL CONTROL PERSPECTIVE

For every complicated problem there is an answer that is short, simple and wrong.

H. L. Mencken

3.1 Introduction

In this chapter, a brief review of the classical optimal control methodology is presented. First, the end-point optimization problem is formulated using Pontryagin's Minimum Principle. The necessary conditions for optimality on the singular arc are reviewed for both fixed as well as free terminal times. Next, the necessary conditions for optimality on a constrained arc are presented. Finally, the difficulties in using the classical optimal control approach to end-point optimization problems in batch reactors is discussed.

3.2 Formulation of the End-Point Optimization Problem

End-point optimization problems for nonlinear systems can be mathematically formulated as follows:

Reproduced with permission of the copyright owner. Further reproduction prohibited without permission.

Minimize the performance index:

$$J = \phi(x(t_f), t_f) \tag{3.1}$$

subject to the dynamics

$$\begin{aligned} \dot{x} &= f(x,t) + g(x,t)u, \qquad 0 \leq t \leq t_f \\ & \qquad\qquad u_{min} \leq u \leq u_{max} \\ x(0) &= x_0 \end{aligned} \tag{3.2}$$

and the scalar state inequality constraint:

$$C(x,t) \leq 0 \tag{3.3}$$

where u is the (scalar) manipulated input bounded by u_{min} and u_{max}, x is the n-vector of states, t_f is the final time, $f(x,t)$ and $g(x,t)$ are smooth vector functions and ϕ is a smooth scalar function such that:

$$\begin{aligned} g(x,t) &\neq [0\ 0\ ...\ 0] \\ \frac{\partial \phi}{\partial x} &\neq [0\ 0\ ...\ 0] \end{aligned} \tag{3.4}$$

for all x. The part of the optimal solution where the state constraint is hit ($C(x,t) = 0$) is called the *constrained arc* or the *boundary arc*. The part of the solution where $C(x,t) < 0$ is called the *unconstrained arc* or the *interior arc*.

3.2.1 Necessary Conditions for Optimality on the Unconstrained Arc

By Pontryagin's Principle, the above minimization problem is equivalent to minimizing the Hamiltonian:

$$H(x, \lambda, u, t) = \lambda^T f(x,t) + \lambda^T g(x,t)u \tag{3.5}$$

where λ is the solution of

$$\begin{aligned} \dot{\lambda}^T &= -\lambda^T \left[\frac{\partial f}{\partial x}(x,t) + \frac{\partial g}{\partial x}(x,t)u \right] \\ \lambda(t_f) &= \frac{\partial \phi}{\partial x}(x(t_f), t_f) \end{aligned} \tag{3.6}$$

Reproduced with permission of the copyright owner. Further reproduction prohibited without permission.

Because the Hamiltonian is linear in the control, u, the optimal control problem is **singular**. The optimal trajectories $u(t)$ will correspond to either hitting an input constraint or to a singular extremal. By definition, a function $u(t)$ is called a singular extremal if it satisfies:

$$H_u(x, \lambda, u, t) = 0$$

and in addition

$$H_{uu}(x, \lambda, u, t) = 0$$

Methods for calculating singular extremals are available in the classical optimal control literature (see standards texts such as Bryson and Ho, 1975; Denn, 1969; Ray, 1981). In the above optimization problem,

$$H_u(x, \lambda, u, t) = \lambda^T g(x, t)$$

For a singular control $u(t)$ we will have:

$$\lambda^T g(x, t) = 0 \tag{3.7}$$

for all times; therefore its successive time derivatives are also zero. Thus, we have:

$$\begin{aligned} \frac{d}{dt}\left(\lambda^T g(x,t)\right) &= 0 \\ \frac{d^2}{dt^2}\left(\lambda^T g(x,t)\right) &= 0 \\ &\vdots \end{aligned} \tag{3.8}$$

This sequence of differentiations is performed until u appears explicitly. The resulting expression can then be solved for u in terms of x and λ.

Reproduced with permission of the copyright owner. Further reproduction prohibited without permission.

The function $\lambda^T g(x,t)$ is called the *switching function.* This function vanishes over the singular time interval. Outside the singular interval, the manipulated input, u, takes either its maximum value, u_{max}, or its minimum value, u_{min} depending on the sign of the switching function. When $\lambda^T g(x,t) < 0$, $u = u_{max}$ and when $\lambda^T g(x,t) > 0$, $u = u_{min}$. The time(s) at which the input switches from singular to non-singular interval and vice versa or the time(s) at which the input switches from minimum to maximum value or vice versa is called *switching time.*

Gabasov and Kirillova (1972) have reviewed the higher order necessary conditions for optimality. These conditions distinguish the optimal controls from non-optimal controls which satisfy the first order conditions. A second order necessary condition for optimality, called the generalized Legendre-Clebsch condition can be stated as follows:

$$(-1)^k \frac{\partial}{\partial u}\left[\left(\frac{d}{dt}\right)^{2k} H_u(x,\lambda,u,t)\right] \geq 0 \quad k = 0,1,2... \tag{3.9}$$

This condition was originally developed by Kelley, Kopp and Moyer (1966). Third order necessay conditions for optimality have also been developed for singular problems (Krener (1977), Lamnabhi-Lagarrigue and Stefani (1990)).

When the final time is free it has been shown (Bryson and Ho, 1975) that

$$\left(\frac{\partial \phi}{\partial t} + H\right)_{t=t_f} = 0 \tag{3.10}$$

If f, g, and ϕ are not explicit functions of time, H is constant (Bryson and Ho, 1975). Using (3.10), we obtain:

$$H = 0 \tag{3.11}$$

everywhere. Since, $\lambda^T g(x) = 0$ in the singular region, we have from equation (3.11):

$$\lambda^T f(x) = 0 \tag{3.12}$$

Reproduced with permission of the copyright owner. Further reproduction prohibited without permission.

in the singular region. This can be used as an extra first order necessary condition for optimality.

3.2.2 Necessary Conditions for Optimality on the Constrained Arc

On the constrained arc:

$$C(x,t) = 0 \tag{3.13}$$

The Hamiltonian H is defined as:

$$H = \lambda^T f(x,t) + \lambda^T g(x,t)u + \mu(t)C(x,t) \tag{3.14}$$

where

$$\mu(t) \geq 0 \tag{3.15}$$

and the adjoint states are defined as

$$\frac{d\lambda^T}{dt} = -\lambda^T \frac{\partial f(x,t)}{\partial x} - \lambda^T \frac{\partial g(x,t)}{\partial x} u - \mu(t) \left[\frac{\partial C(x,t)}{\partial x} \right] \tag{3.16}$$

On the constraint boundary, the time-varying parameter $\mu(t)$ is so chosen that

$$\frac{\partial H}{\partial u} = \lambda^T g(x,t) = 0 \tag{3.17}$$

Thus, the boundary arc is a *singular arc* in the sense of the minimum principle (Maurer, 1977).

3.3 Difficulties in Using the Classical Approach in End-Point Optimization

To calculate the optimal manipulated input profile, $u(t)$, it is necessary to solve *simultaneously* both the system states (equation 3.2) as well as the adjoint states (equations 3.6 and 3.16). However, the boundary conditions for the state and adjoint equations are split, i.e., the initial conditions of the state equations and the terminal

Reproduced with permission of the copyright owner. Further reproduction prohibited without permission.

conditions of the adjoint equations are known. Formulation of the end-point optimization problem in terms of Pontryagin's Principle is relatively straightforward; however the solution can rarely be analytically determined and numerical techniques must be used. Numerical methods such as gradient-based methods, multiple shooting methods, quazilinearization methods and differential dynamic programming methods have been used in the literature for specific optimization problems. Stutts (1983) reviewed the various numerical methods that have been proposed in the literature and concluded that each has shortcomings such as requiring intelligent initial guesses and slow convergence to local minima. Furthermore, all these methods are aimed at obtaining the optimal *open-loop* time profiles of the input function and therefore the optimal solution depends heavily upon the initial conditions and system parameters. This is a serious drawback in applying the classical methods to end-point optimization of batch reactors which can have large errors in initial conditions and batch-to-batch variations in model parameters. Furthermore, an open-loop implementation of an *a priori* determined input profile will not attenuate uncertainties and disturbances to the process.

Thus, it is observed that the classical approach to numerically solving the end-point optimization in batch reactors has many problems. These problems can be alleviated by developing a closed-loop optimization scheme. This approach would attenuate uncertainties and disturbances to the process and would be independent of initial conditions. Furthermore, this approach would provide a unidirectional algorithm for solving the optimal control problem which can be easily implemented *on-line*. Coupled with state and parameter estimation algorithms, such an approach would form the basis of an on-line adaptive optimization scheme.

Reproduced with permission of the copyright owner. Further reproduction prohibited without permission.

CHAPTER IV

STATE FEEDBACK LAWS FOR END-POINT OPTIMIZATION: FIXED FINAL TIME AND NO STATE CONSTRAINTS

Research is to see what everybody else sees, and to think what nobody else has thought.

Albert Szent-Gyorgyi

4.1 Introduction

In this chapter, the problem of synthesizing optimal state feedback laws is addressed for the case where the final time is fixed and there are no state constraints. The existence of a singular region as well as the nature of the state feedback laws (static or dynamic) are completely characterized in terms of the Lie bracket structure of the system dynamics. Explicit synthesis formulae for the state feedback laws are first obtained for time-invariant systems and then extended to time-varying systems. As illustrative examples of applications of the optimal state feedback laws, several end-point optimization problems in batch chemical and biochemical reactors are considered.

Reproduced with permission of the copyright owner. Further reproduction prohibited without permission.

4.2 End-Point Optimization of Time Invariant Systems

Consider the following end-point optimization problem:

Minimize the performance index

$$J = \phi(x(t_f)) \tag{4.1}$$

subject to the dynamics

$$\begin{aligned} \dot{x} &= f(x) + g(x)u \\ x(0) &= x_0 \quad 0 \leq t \leq t_f \end{aligned} \tag{4.2}$$

where u is the (scalar) manipulated input, x is the n-vector of states, t_f is the final time, ϕ is a non-constant scalar function of the system states and f and g are vector functions that depend on the system states. The final time, t_f is fixed and there are no state constraints.

It is seen from Chapter III that in the classical approach, the optimal control is determined by solving the algebraic equations which result by successively differentiating the switching function $H_u(x, \lambda, u)$ until the control, u, appears explicitly. This gives rise to the concept of order or degree of a singular problem, originally introduced by Kopp and Moyer (1965). Since then, problem-oriented definitions of order have been suggested (Kelley *et al.*, 1967; Robbins, 1967; McDanell and Powers, 1971) and the issue of defining the order of the singular control problem became a subject of controversy. Lewis (1980) surveys the various definitions of singular control order. The issue of defining the order of a singular control problem was resolved in the work of Krener (1977). In the same paper, Krener developed a higher-order minimum principle and elucidated the importance of Lie brackets in singular optimal control problems.

We first review the definition of Lie brackets of a nonlinear system:

Reproduced with permission of the copyright owner. Further reproduction prohibited without permission.

Given $f(x)$, $g(x)$ C^∞ vector fields on $\mathbb{R}^n$, the Lie bracket $[f,g](x)$ is a vector field defined by

$$[f,g](x) = \frac{\partial g(x)}{\partial x} f(x) - \frac{\partial f(x)}{\partial x} g(x)$$

where $\frac{\partial f(x)}{\partial x}$ and $\frac{\partial g(x)}{\partial x}$ are the Jacobians of dimension n x n. $[f,g]$ is also a C^∞ vector field on $\mathbb{R}^n$. One can define iterated Lie brackets $[f,[f,g]]$, $[f,[f,[f,g]]]$ etc. The following notation is standard

$$\begin{aligned} ad_f^0 g(x) &= g(x) \\ ad_f^1 g(x) &= [f,g](x) \\ ad_f^2 g(x) &= [f,[f,g]](x) \\ &\cdot \\ &\cdot \\ ad_f^k g(x) &= [f, ad_f^{k-1} g](x) \end{aligned}$$

The system theoretic significance of the Lie brackets can be illustrated by the following well-known result.

Proposition 4.1 (Hunt, 1982): The dynamic system (4.2) is locally controllable if the vector fields $g(x)$, $ad_f^1 g(x)$, ..., $ad_f^{n-1} g(x)$ are locally linearly independent for every x.

Throughout this section, we will make the standing assumption that $g(x)$, $ad_f^1 g(x)$, ..., $ad_f^{n-1} g(x)$ are linearly independent *almost everywhere in x* to guarantee local controllability of the system almost everywhere. This assumption is equivalent to:

$$det \left[g(x) \,|\, ad_f^1 g(x) \,|\, ... \,|\, ad_f^{n-1} g(x) \right] \not\equiv 0 \qquad (4.3)$$

Uncontrollable situations where some of these vector fields are linearly dependent for every x can be handled as will be illustrated in Examples 2 and 3.

Reproduced with permission of the copyright owner. Further reproduction prohibited without permission.

Definition 4.1: The system governed by equation (4.2) has a finite **degree of singularity s** *if*

$$[g, ad_f^\nu g](x) \in span\ \{g(x),\ ad_f^1 g(x),\ ...,\ ad_f^\nu g(x)\},\ for\ all\ \nu \leq s-1 \qquad (4.4)$$

$$[g, ad_f^s g](x) \notin span\ \{g(x),\ ad_f^1 g(x),\ ...,\ ad_f^s g(x)\} \qquad (4.5)$$

The system governed by equation (4.2) has an **infinite degree of singularity** ($s = \infty$) *if*

$$[g, ad_f^\nu g](x) \in span\ \{g(x),\ ad_f^1 g(x),\ ...,\ ad_f^\nu g(x)\},\ for\ all\ \nu \geq 0 \qquad (4.6)$$

Since $g(x)$, $ad_f^1 g(x)$, ..., $ad_f^{n-1} g(x)$ are assumed to be linearly independent, it follows from the definition that $1 \leq s \leq (n-2)$ or $s = \infty$.

Remark 4.1: It can be shown that this definition is completely equivalent to Krener's definition of degree of singularity (Krener, 1977) for the class of systems that have $g(x)$, $ad_f^1 g(x)$, ..., $ad_f^{n-1} g(x)$ linearly independent. Though the latter does not have this restriction, it is more difficult to use.

The following proposition is a rather straightforward consequence of known results (see Gabasov and Kirillova, 1972) when the above definition of s is used.

Proposition 4.2: Consider a system governed by equation (4.2) with finite degree of singularity s. Then s is odd and the first order necessary conditions for optimality

Reproduced with permission of the copyright owner. Further reproduction prohibited without permission.

for a singular extremal can be written as follows:

$$\begin{aligned}
\lambda^T g(x) &= 0 \\
\lambda^T ad_f^1 g(x) &= 0 \\
\lambda^T ad_f^2 g(x) &= 0 \\
&\cdot \\
&\cdot \\
&\cdot \\
\lambda^T ad_f^s g(x) &= 0 \\
\lambda^T ad_f^{s+1} g(x) + \lambda^T [g, ad_f^s g](x) u &= 0
\end{aligned} \tag{4.7}$$

where λ is the solution of (3.6). Furthermore, the second order necessary condition for optimality takes the form:

$$(-1)^{\frac{s+1}{2}} \lambda^T \left[g, ad_f^s g\right](x) \geq 0 \tag{4.8}$$

If (4.2) has an infinite degree of singularity, then the first order necessary conditions for optimality take the form $\lambda^T ad_f^\nu g(x) = 0$ for all $\nu \geq 0$.

4.3 Singular Extremal as a State Feedback Law Independent of the Adjoint States

The previous section provided a brief review of the geometric perspective of singular optimal control theory. It was seen in Proposition 4.2 that the first order and second order necessary conditions for optimality in the singular region can be put in a very concrete form in terms of the system Lie brackets. The key difficulty in using these necessary conditions arises from the presence of the adjoint states. To be able to calculate the optimal control input, $u(t)$, one must solve a two-point boundary value problem that involves forward-in-time integration of the state equations and backward-in-time integration of the adjoint equations. The analysis of the optimality

Reproduced with permission of the copyright owner. Further reproduction prohibited without permission.

conditions would be greatly facilitated if the adjoint states could be eliminated from the necessary conditions. This elimination problem was studied in a general (not necessarily singular) setting in the work of Rouff and Lamnabhi-Lagarrigue (1986).

In the present subsection we will address for the first time the problem of synthesizing state feedback laws to track singular trajectories, based on eliminating the adjoint states from the first-order necessary conditions for optimality. The case $s = \infty$ will be studied first; Theorem 4.1 will show that the problem of tracking singular extremals can be formulated as a standard regulator problem whenever a singular extremal exists. In Theorem 4.2, we will derive a static state feedback law that tracks the singular extremal when the degree of singularity is equal to $(n-2)$. Finally, in Theorem 4.3, we will derive a dynamic state feedback law that tracks the singular trajectories when the degree of singularity is less than $(n-2)$.

Theorem 4.1: Consider a system of the form of equation (4.2) with degree of singularity $s = \infty$ and a performance index of the form of equation (4.1).

(i) If $g(x)$, $ad_f^1 g(x)$, ..., $ad_f^{n-1} g(x)$ are linearly independent for **all x**, *then a singular extremal does not exist.*

(ii) If $g(x)$, $ad_f^1 g(x)$, ..., $ad_f^{n-1} g(x)$ are linearly independent almost everywhere, then the state trajectories corresponding to a singular extremal evolve on the surface $S(x) = 0$ where linear independence of $g(x)$, $ad_f^1 g(x)$, ..., $ad_f^{n-1} g(x)$ is lost:

$$S(x) = det\left[g(x) \,|\, ad_f^1 g(x) \,|\, \ldots \,|\, ad_f^{n-1} g(x)\right] = 0 \qquad (4.9)$$

Corollary 4.1: Controllable linear systems do not possess singular extremals.

Corollary 4.2: If the vector fields $g(x)$, $ad_f^1 g(x)$, ..., $ad_f^{n-1} g(x)$ are linearly indepen-

Reproduced with permission of the copyright owner. Further reproduction prohibited without permission.

dent for **all x** *and the set of vector fields*

$$\{g(x),\ ad_f^1 g(x),\ ...,\ ad_f^{n-2} g(x)\}$$

is involutive for **all x**, *i.e, the system is feedback linearizable in the Hunt-Su-Meyer sense (Hunt et al. (1983)), then such a system does not possess a singular extremal.*

Proof: From the involutivity assumption:

$$[g, ad_f^k g](x) = \sum_{j=0}^{n-2} \alpha_{jk}(x) ad_f^k g(x)$$

where $\alpha_{jk}(x)$ are scalar fields in x.

Hence $s > (n-2)$. But $s \leq (n-2)$ if finite. Thus $s = \infty$. Since the vector fields defined by $ad_f^k g(x)$ for $k = 0, 1, 2, ...(n-1)$ are linearly independent for all x, from Theorem 4.1 the system under consideration does not possess a singular extremal.

When a singular extremal does not exist, the optimal control is bang-bang in nature, that is, the optimal control corresponds to the maximum or the minimum value of the manipulated input. Since controllable linear systems and feedback linearizable nonlinear systems do not possess singular extremals, the existence of singular extremals is a manifestation of truly nonlinear behavior. Consequently, if it is known on physical grounds that a singular extremal exists for a given process, modeling such a process by a linear model or an involutive model is inappropriate for optimization purposes.

Another interesting conclusion from Theorem 4.1 is that optimality may correspond to loss of *state* controllability. In this case the optimal state trajectories must lie on the surface $S(x) = 0$ (equation (4.9))and the problem of synthesizing a state feedback to track the singular extremals reduces to a standard regulation problem for the output:

$$y = S(x) \tag{4.10}$$

Reproduced with permission of the copyright owner. Further reproduction prohibited without permission.

with zero set point. This regulation problem can be solved using standard techniques as long as $S(x)$ has a finite relative order. For instance, in the case of unity relative order ($\frac{\partial S(x)}{\partial x} g(x) \neq 0$)

$$u = -\frac{\frac{\partial S(x)}{\partial x}.f(x) + \beta S(x)}{\frac{\partial S(x)}{\partial x}.g(x)} \tag{4.11}$$

where β is an adjustable positive parameter, is an appropriate feedback law for the above regulation problem.

Theorem 4.2: For a system of the form of equation (4.2) and a performance index of the form of equation (4.1), the singular trajectories can be tracked by **static** *state feedback when* $s = n-2$. *The optimal state feedback law is given by:*

$$u = -\frac{det\left[g(x) \vdots ad_f^1 g(x) \vdots \ldots \vdots ad_f^{n-1} g(x)\right]}{det\left[g(x) \vdots ad_f^1 g(x) \vdots \ldots \vdots ad_f^{n-2} g(x) \vdots [g, ad_f^{n-2} g](x)\right]} \tag{4.12}$$

Theorem 4.3: For a system of the form of equation (4.2) and a performance index of the form of equation (4.1), the singular trajectories can be tracked by **dynamic** *state feedback when* $s \leq n-3$. *The optimal state feedback law is the solution of an* $(n-s-2)$*-th order ordinary differential equation of the form:*

$$\Phi(x, u, \frac{du}{dt}, \ldots, \frac{d^{n-s-2}u}{dt^{n-s-2}}) = 0$$

where Φ *is an algebraic function.*

Reproduced with permission of the copyright owner. Further reproduction prohibited without permission.

This is obtained by setting the determinant obtained from the following column vectors

$$
\begin{aligned}
&g(x)\\
&ad_f^1 g(x)\\
&\cdot\\
&\cdot\\
&\cdot\\
&ad_f^s g(x)\\
&ad_f^{s+1} g(x) + [g, ad_f^s g](x)u(t)\\
&ad_f^{s+2} g(x) + [g, ad_f^{s+1} g](x)u(t) + \left(I\frac{d}{dt} - \frac{\partial f(x)}{\partial x} - \frac{\partial g(x)}{\partial x}u(t)\right)\left([g, ad_f^s g](x)u(t)\right)\\
&\cdot\\
&\cdot\\
&\cdot\\
&ad_f^{n-1} g(x) + \sum_{k=0}^{n-s-2}\left(I\frac{d}{dt} - \frac{\partial f(x)}{\partial x} - \frac{\partial g(x)}{\partial x}u(t)\right)^k\left([g, ad_f^{n-k-2} g](x)u(t)\right)
\end{aligned}
\tag{4.13}
$$

equal to zero. In the above equations, I is the identity matrix and $\frac{d(.)}{dt}$ *is the total time derivative operator:* $\frac{d(.)}{dt} = [f(x) + g(x)u(t)]\frac{\partial(.)}{\partial x} + \frac{\partial(.)}{\partial t}$

4.4 End-Point Optimization for Time-Varying Systems

In the previous section, we derived state feedback laws for end-point optimization for processes which are described by time-invariant models. These feedback laws can be used directly for a large class of yield optimization problems in batch chemical reactors. However, as shown in Chapter II, there is a class of yield optimization problems which fall in the framework of end-point optimization formulated in this paper with the exception that the process models have time appear explicitly as a

Reproduced with permission of the copyright owner. Further reproduction prohibited without permission.

parameter or have parameters that vary with time. This motivates the extension of the results developed in the previous section to time-varying systems.

Consider the following optimization problem.

Minimize the performance index

$$J = \phi(x(t_f)) \tag{4.14}$$

subject to the dynamics

$$\begin{aligned} \dot{x} &= f(x,t) + g(x,t)u \\ x(0) &= x_0 \quad 0 \leq t \leq t_f \end{aligned} \tag{4.15}$$

where u is the (scalar) manipulated input, x is the n-vector of states, t_f is the final time, ϕ is a non-constant scalar function of the system states and f and g are vector functions that depend explicitly on the time variable, t.

The classical optimal control perspective presented in Chapter III is applicable to the above system. However, the recursive "ad" notation has to be modified to take into account the explicit time dependence of the system model on time.

We define modified Lie brackets of the time-varying system (4.15) as:

$$\begin{aligned} \overline{ad}_f^0 g(x,t) &= g(x,t) \\ \overline{ad}_f^1 g(x,t) &= [f,g](x,t) + \frac{\partial g(x,t)}{\partial t} \\ \overline{ad}_f^2 g(x,t) &= [f,\overline{ad}_f^1 g](x,t) + \frac{\partial \overline{ad}_f^1 g(x,t)}{\partial t} \\ &\vdots \\ \overline{ad}_f^k (g)(x,t) &= [f,\overline{ad}_f^{k-1} g](x,t) + \frac{\partial \overline{ad}_f^{k-1} g(x,t)}{\partial t} \end{aligned} \tag{4.16}$$

As in the case of time-invariant systems, we make the standing assumption that the vector fields $g(x,t)$, $\overline{ad}_f^1 g(x,t)$, ..., $\overline{ad}_f^{n-1} g(x,t)$ are linearly independent almost

Reproduced with permission of the copyright owner. Further reproduction prohibited without permission.

everywhere in x and t. This assumption is equivalent to:

$$det\ \left[g(x)\,|\,\overline{ad}_f^1 g(x,t)\,|\ldots|\,\overline{ad}_f^{n-1} g(x,t)\right] \not\equiv 0 \tag{4.17}$$

Definition 4.2: The system governed by equation (4.15) has a finite **degree of singularity s** *if*

$$[g, \overline{ad}_f^\nu g](x,t) \in span\ \{g(x,t),\ \overline{ad}_f^1 g(x,t),\ ...,\ \overline{ad}_f^\nu g(x,t)\},\ for\ all\ \nu \leq s-1 \tag{4.18}$$

$$[g, \overline{ad}_f^s g](x,t) \notin span\ \{g(x,t),\ \overline{ad}_f^1 g(x,t),\ ...,\ \overline{ad}_f^s g(x,t)\} \tag{4.19}$$

The system governed by equation (4.15) has an **infinite degree of singularity** $(s = \infty)$ *if*

$$[g, \overline{ad}_f^\nu g](x,t) \in span\ \{g(x,t),\ \overline{ad}_f^1 g(x,t),\ ...,\ \overline{ad}_f^\nu g(x,t)\},\ for\ all\ \nu \geq 0 \tag{4.20}$$

It follows immediately from the definition that $1 \leq s \leq (n-2)$ or $s = \infty$.

Using the definitions of the modified Lie brackets of the system and the degree of singularity, the first order necessary conditions on the singular region can be written as:

$$\begin{aligned}
\lambda^T g(x,t) &= 0 \\
\lambda^T \overline{ad}_f^1 g(x,t) &= 0 \\
\lambda^T \overline{ad}_f^2 g(x,t) &= 0 \\
&\cdot \\
&\cdot \\
&\cdot \\
\lambda^T \overline{ad}_f^s g(x,t) &= 0 \\
\lambda^T \overline{ad}_f^{s+1} g(x,t) + \lambda^T [g, \overline{ad}_f^s g](x,t) u &= 0
\end{aligned} \tag{4.21}$$

Furthermore, the second order necessary condition for optimality takes the form:

$$(-1)^{\frac{s+1}{2}} \lambda^T \left[g, \overline{ad}_f^s g\right](x,t) \geq 0$$

Reproduced with permission of the copyright owner. Further reproduction prohibited without permission.

The following theorems generalize the results of the previous section to time-varying systems. Theorem 4.4 refers to the case $s = \infty$ and Theorem 4.5 to the case of finite s.

Theorem 4.4: Consider a system of the form of equation (4.15) with degree of singularity $s = \infty$ and a performance index of the form of equation (4.14) .

(i) If $g(x,t)$, $\overline{ad}_f^1 g(x,t)$, ..., $\overline{ad}_f^{n-1} g(x,t)$ are linearly independent for **all x and t,** *then a singular extremal does not exist.*

(ii) If $g(x,t)$, $\overline{ad}_f^1 g(x,t)$, ..., $\overline{ad}_f^{n-1} g(x,t)$ are linearly independent almost everywhere, then the state trajectories corresponding to a singular extremal satisfy the following relationship:

$$\overline{S}(x,t) \equiv det\left[g(x,t) \vdots \overline{ad}_f^1 g(x,t) \vdots \ldots \vdots \overline{ad}_f^{n-1} g(x,t)\right] = 0 \qquad (4.22)$$

It can be easily shown on the lines of Corollary 4.1 that controllable linear time-varying systems do not possess singular extremals. Furthermore, it is observed from Theorem 4.4 that optimality may correspond to loss of *state* controllability. Whenever a singular extremal exists for a system with infinite degree of singularity, the problem of synthesizing a state feedback to track the singular trajectories reduces to a regulation problem for the time-varying output:

$$y = \overline{S}(x,t) \qquad (4.23)$$

with zero set point. The general problem of regulating a time-varying nonlinear system will be addressed in Chapter VI.

Theorem 4.5: Consider a system of the form of equation (4.15) and a performance index of the form of equation (4.14).

Reproduced with permission of the copyright owner. Further reproduction prohibited without permission.

(i) For s = n-2, the singular trajectories can be tracked by the following state feedback:

$$u = -\frac{det\left[g(x,t)\,|\,\overline{ad}_f^1 g(x,t)\,|\ldots|\,\overline{ad}_f^{n-1} g(x,t)\right]}{det\left[g(x,t)\,|\,\overline{ad}_f^1 g(x,t)\,|\ldots|\,\overline{ad}_f^{n-2} g(x,t)\,|\,[g,\overline{ad}_f^{n-2} g](x,t)\right]} \tag{4.24}$$

(ii) For s ≤ n-3, the singular trajectories can be tracked by a dynamic state feedback which is calculated by setting the determinant obtained from the following column vectors equal to zero.

$$\begin{array}{l}
g(x,t) \\
\overline{ad}_f^1 g(x,t) \\
\cdot \\
\cdot \\
\cdot \\
\overline{ad}_f^s g(x,t) \\
\overline{ad}_f^{s+1} g(x,t) + [g,\overline{ad}_f^s g](x,t)u(t) \\
\overline{ad}_f^{s+2} g(x,t) + [g,\overline{ad}_f^{s+1} g](x,t)u(t) + \\
\left(I\frac{d}{dt} - \frac{\partial f(x,t)}{\partial x} - \frac{\partial g(x,t)}{\partial x}u(t)\right)\left([g,\overline{ad}_f^s g](x,t)u(t)\right) \\
\cdot \\
\cdot \\
\cdot \\
\overline{ad}_f^{n-1} g(x,t) + \sum_{k=0}^{n-s-2}\left(I\frac{d}{dt} - \frac{\partial f(x,t)}{\partial x} - \frac{\partial g(x,t)}{\partial x}u(t)\right)^k\left([g,\overline{ad}_f^{n-k-2} g](x,t)u(t)\right)
\end{array} \tag{4.25}$$

If the time dependence of the system model is in terms of time-varying parameters, $f(x,k(t))$ and $g(x.k(t))$ where $k(t)$ is the vector of time-varying parameters, it is necessary to express the quantities $\overline{ad}_f^1 g$, $\overline{ad}_f^2 g$, ... in terms of the partials of f and g with respect to k and the time derivatives $\frac{dk}{dt}$, $\frac{d^2k}{dt^2}$, ..., to obtain concrete formulae

Reproduced with permission of the copyright owner. Further reproduction prohibited without permission.

for the state feedback law, This can be done in a very straightforward manner:

$$\begin{aligned}
\overline{ad}_f^1 g(x,t) &= [f,g](x,t) + \frac{\partial g(x,t)}{\partial t} \\
&= ad_f^1 g(x,t) + \frac{\partial g(x,t)}{\partial k}\frac{\partial k}{\partial t} \\
\overline{ad}_f^2 g(x,t) &= [f,\overline{ad}_f^1 g](x,t) + \frac{\partial \overline{ad}_f^1 g(x,t)}{\partial t} \\
&= ad_f^2 g(x,t) + \left([f,\frac{\partial g}{\partial k}](x,t) + \frac{\partial ad_f^1 g(x,t)}{\partial k} + \frac{\partial^2 g(x,t)}{\partial k^2}\cdot\frac{dk}{dt}\right)\frac{dk}{dt} + \\
&\quad \frac{\partial g(x,t)}{\partial k}\cdot\frac{d^2k}{dt^2} \\
&\quad . \\
&\quad . \\
&\quad .
\end{aligned} \tag{4.26}$$

In general, $\overline{ad}_f^j g(x,t)$ will be expressed as a function of x, $k(t)$, $\frac{dk}{dt}$, ..., $\frac{d^jk}{dt^j}$.

4.5 Implementation

The results obtained in the previous sections provide optimal feedback laws strictly in the singular region. In the non-singular region, the manipulated input takes the minimum or the maximum value. To determine what values (minimum or maximum) the manipulated input takes in the non-singular region as well as the switching times between the singular and non-singular regions, one has to integrate, off-line, the adjoint equations in addition to the state equations. The singular region corresponds to vanishing of the switching function $\lambda^T g$ whereas the non-singular regions correspond to non-zero values of the switching function. To determine whether the singular control is indeed optimal, one has to check the higher order necessary conditions as well.

To implement the optimal state feedback laws as a closed-loop scheme, the switching times between singular and non-singular regions are required. These switching times can be calculated analytically only for a restricted class of models. In most

Reproduced with permission of the copyright owner. Further reproduction prohibited without permission.

practical situations, these have to be computed numerically. There is no general theory in the literature for calculating the switching times between singular and non-singular extremals. In most numerical algorithms, one assumes a set of switching times, computes the singular and non-singular extremals and checks to see if the necessary conditions of optimality are satisfied. This procedure is carried out iteratively till a set of switching times are obtained for which the necessary conditions of optimality are satisfied.

From the off-line solution of the first order necessary conditions of optimality, the switching times and the values of the system states at the junctions between singular and non-singular regions are known. This information can be used to set up on-line criteria for the onset of the singular region in terms of the system states. For instance, Modek (1988) determined the onset of the singular interval in an ethanol fermentation by using an expression relating cell mass and substrate concentrations at the junction of the non-singular and singular regions. Alternatively, one can use the *a priori* calculated switching times determined from the off-line analysis. In this case a successful feedback implementation of the optimal feedback law depends on how sensitive the final performance index is to errors in the switching times. In example 3 it will be seen that the final performance index is not very sensitive to small errors in the switching time. When $s \leq n-3$ we also need initial conditions for the dynamic state feedback law. These initial conditions have to be set up in a similar fashion as the switching times.

If the model parameters are known *a priori*, the feedback laws derived in the previous sections can be used in conjunction with state estimators. Such an implementation can attenuate errors in the initial conditions and process disturbances. If some of the model parameters are not accurately known *a priori*, these need to be es-

Reproduced with permission of the copyright owner. Further reproduction prohibited without permission.

timated on-line. In this situation, a parameter estimation algorithm is also required. If the model parameters are time-varying and the functional form of these time-varying parameters is not known, the theory developed in the preceeding sections can be used as a basis for an adaptive optimal state feedback. In this approach, the optimal state feedback is coupled with a state and parameter estimation algorithm. The state and parameter estimation algorithm provides estimates of the system states and model parameters which are used to update the state feedback law periodically.

A variety of stochastic methods such as Extended Kalman Filtering (Jazwinski (1970)), and Prediction Error Identification (Ljung (1985)) as well as deterministic methods such as Nonlinear Least Squares, have been proposed in the literature to estimate the system states and parameters. These methods have been applied to a variety of batch systems for state and parameter estimation. For instance, Schuler and Papadopoulou (1986) developed a decoupled nonlinear estimator based on an Extended Kalman Filter for the real-time estimation of of the chain-length distribution and conversions in a batch polystyrene reactor. Ellis *et al.* (1988) applied a two time scale filtering technique to estimate the temperature, monomer conversion, initiator conversion, and the entire molecular weight distribution in a methyl methacrylate batch polymerization. Stephanopoulos and San (1984) demonstrated the use of Kalman filtering to estimate the specific growth rate and cell mass in a batch fermentation using on-line off-gas data.

4.6 Illustrative Examples

In this section, applications for the theory developed in the preceeding sections is illustrated through four simulation examples.

Reproduced with permission of the copyright owner. Further reproduction prohibited without permission.

4.6.1 Example 1: Linear System

We consider a yield optimization problem in a semi-batch chemical reactor where the following reactions are occuring:

$$A \rightarrow B$$

$$B \rightarrow C$$

$$A \rightarrow D$$

The species A is being fed to the reactor. All reactions follow first order kinetics. The unsteady state mass balance equations are given by:

$$\begin{aligned} \frac{d(C_A.V)}{dt} &= -k_B C_A.V - k_D C_A.V + s_F.u \\ \frac{d(C_B.V)}{dt} &= k_B C_A.V - k_C C_B.V \\ \frac{d(C_D.V)}{dt} &= k_D C_A.V \\ \frac{dV}{dt} &= u \end{aligned} \tag{4.27}$$

where the manipulated input, u, is the feed rate of species A. The objective is to operate the batch reactor so that the total amount of B is maximized at a prespecified final time t_f. Thus, the performance index to minimize is:

$$J = -C_B.V|_{t=t_f} \tag{4.28}$$

Define:

$$\begin{aligned} x_1 &= C_A.V \\ x_2 &= C_B.V \\ x_3 &= C_D.V \\ x_4 &= V \end{aligned} \tag{4.29}$$

The optimization problem can be stated as:

Minimize

$$J = -x_2(t_f) \tag{4.30}$$

Reproduced with permission of the copyright owner. Further reproduction prohibited without permission.

subject to

$$\frac{d}{dt}\begin{bmatrix} x_1 \\ x_2 \\ x_3 \\ x_4 \end{bmatrix} = \begin{bmatrix} -k_B x_1 - k_D x_1 \\ k_B x_1 - k_C x_2 \\ k_D x_1 \\ 0 \end{bmatrix} + \begin{bmatrix} s_F \\ 0 \\ 0 \\ 1 \end{bmatrix} u \tag{4.31}$$

The system model is of the form:

$$\dot{x} = f(x) + g(x)u \tag{4.32}$$

where:

$$x = \begin{bmatrix} x_1 \\ x_2 \\ x_3 \\ x_4 \end{bmatrix}$$

$$f(x) = \begin{bmatrix} -k_B x_1 - k_D x_1 \\ k_B x_1 - k_C x_2 \\ k_D x_1 \\ 0 \end{bmatrix}$$

$$g(x) = \begin{bmatrix} s_F \\ 0 \\ 0 \\ 1 \end{bmatrix}$$

It can be easily verified that the vector fields $g(x)$, $ad_f^1 g(x)$, $ad_f^2 g(x)$, $ad_f^3 g(x)$ are linearly independent constant vectors and so the system is controllable everywhere. We note from the vector fields $f(x)$ and $g(x)$ that the system under consideration is linear. Thus this system does not possess a singular extremal (Corollary 4.1) and

Reproduced with permission of the copyright owner. Further reproduction prohibited without permission.

therefore the optimal control is bang-bang in nature. The sign of $\lambda^T g(x) = s_F \lambda_1(t)$ determines if the maximum value or the minimum value of u should be used. It can be easily seen that:

$$\lambda_1(t) = \frac{k_B}{k_C - k_B - k_D}(exp(k_C[t - t_f]) - exp([k_B + k_D][t - t_f])) \qquad (4.33)$$

Figure 4.1 shows the time profile of $\lambda^T g(x)$ for the model parameters given in Table 4.1 and the initial conditions given in Table 4.2. Since $\lambda^T g(x)$ is always negative in this region, the optimal operation is to use the maximum feed rate u_{max} throughout the batch time. Figure 4.2 shows the time profile of species B when the maximum feed rate is used.

k_B	1.00 $1/hr$
k_C	0.50 $1/hr$
k_D	0.20 $1/hr$
s_F	10.00 kg/m^3
u_{max}	5.00 x 10^{-3} m^3/hr
t_f	5.00 hr

Table 4.1: Model Parameters

$C_A(0)$	1.0 kg/m^3
$C_B(0)$	0.0 kg/m^3
$C_D(0)$	0.0 kg/m^3
$V(0)$	1.0 x 10^{-3} m^3

Table 4.2: Initial Conditions

Reproduced with permission of the copyright owner. Further reproduction prohibited without permission.

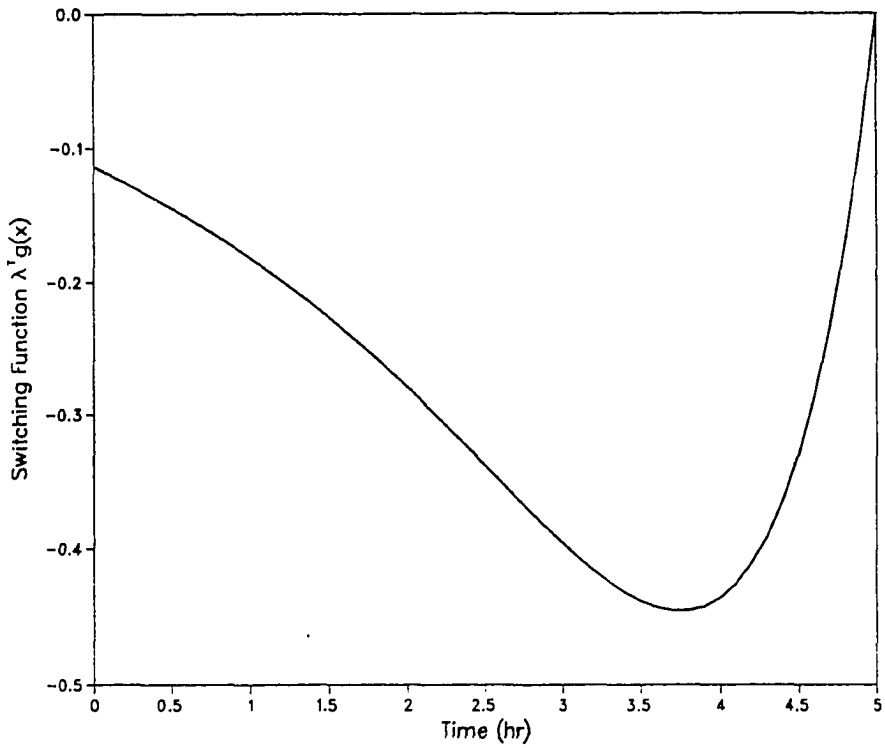

Figure 4.1: Profile of switching function $\lambda^T g(x)$ (example 1)

Reproduced with permission of the copyright owner. Further reproduction prohibited without permission.

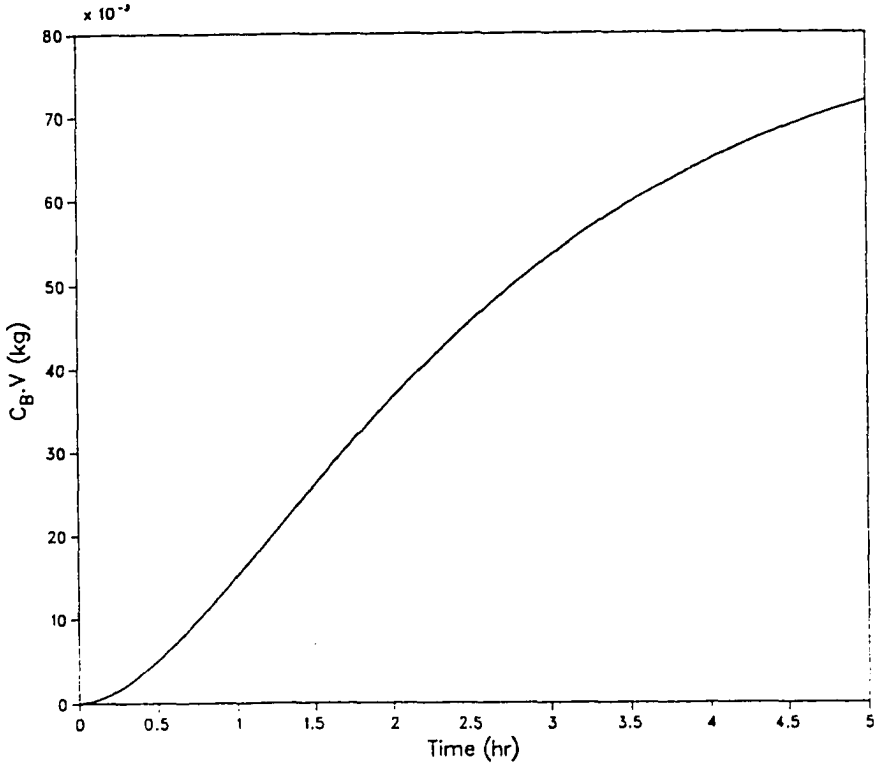

Figure 4.2: Optimal time profile of species B (example 1)

Reproduced with permission of the copyright owner. Further reproduction prohibited without permission.

4.6.2 Example 2: s = infinity

We consider a fed-batch fermentation for the production of Baker's Yeast (Menawat *et al*, 1987). The unsteady state material balances are as follows (See Nomenclature Section for explanation of symbols):

$$\begin{aligned} \frac{d(X.V)}{dt} &= \mu(S,t)X.V \\ \frac{d(S.V)}{dt} &= -\frac{\mu(S,t)X.V}{Y} + s_F u \\ \frac{dV}{dt} &= u \end{aligned} \tag{4.34}$$

The objective is to maximize the cell mass at a prespecified final time, t_f. Thus:

$$J = -X.V|_{t=t_f}$$

The manipulated variable, u, is the feedrate of the substrate. The specific growth rate, μ, is given by the Haldane-Monod function (Edwards, 1970)

$$\mu(S,t) = \frac{\mu_m(t).S}{K_1+S}\frac{K_2}{K_2+S} \tag{4.35}$$

The parameter $\mu_m(t)$ decreases with time due to degradation of intracellular enzymes and its time variation is shown in Figure 4.3. Condition (4.17) is violated everywhere for this system. In this situation, we need to do model reduction to eliminate the redundant state equations, so that condition (4.17) is satisfied almost everywhere in x. It can be easily shown that X, S, and V are algebraically related by:

$$\left(\frac{XV}{Y}+SV\right) - \left(\frac{X(0)V(0)}{Y}+S(0)V(0)\right) = s_F(V-V(0)) \tag{4.36}$$

Thus there are only two independent equations. Defining

$$\begin{aligned} x_1 &= XV \\ x_2 &= V \end{aligned} \tag{4.37}$$

Reproduced with permission of the copyright owner. Further reproduction prohibited without permission.

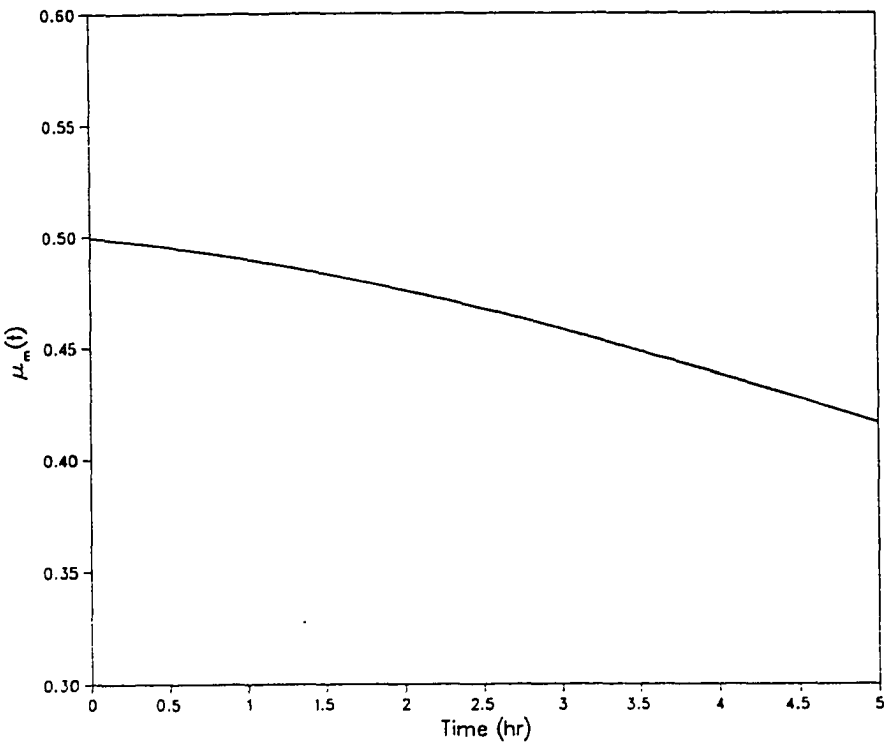

Figure 4.3: Profile of time-varying parameter $\mu_m(t)$ (example 2)

Reproduced with permission of the copyright owner. Further reproduction prohibited without permission.

and eliminating S from (4.36):

$$S = s_F - \frac{1}{Y}\left(\frac{x_1 - X(0)V(0)}{x_3}\right) + \left(\frac{S(0)V(0) - s_F V(0)}{x_3}\right) \tag{4.38}$$

the model can be put in the form:

$$\frac{d}{dt}\begin{bmatrix} x_1 \\ x_2 \end{bmatrix} = \begin{bmatrix} \hat{\mu}(x_1, x_2, t)x_1 \\ 0 \end{bmatrix} + \begin{bmatrix} 0 \\ 1 \end{bmatrix} u \tag{4.39}$$

where $\hat{\mu}$ is obtained by substituting S from (4.38) into the expression for μ (equation (4.35)). For this system:

$$x = \begin{bmatrix} x_1 \\ x_2 \end{bmatrix}, \; f(x,t) = \begin{bmatrix} \hat{\mu}(x_1, x_2, t)x_1 \\ 0 \end{bmatrix}, \; g(x,t) = \begin{bmatrix} 0 \\ 1 \end{bmatrix} \tag{4.40}$$

Since $n = 2$, we necessarily have $s = \infty$. It can be easily seen that the necessary condition

$$det\left[g(x,t) \vdots \overline{ad}_f^1 g(x,t)\right] = 0 \tag{4.41}$$

leads to

$$\frac{\partial \hat{\mu}}{\partial x_2} x_1 = 0 \tag{4.42}$$

In terms of the original variables (S and X), the above equation takes the form:

$$\frac{\partial \mu}{\partial S}(s_F - S)X = 0 \tag{4.43}$$

Since $S \neq s_F$, $X \neq 0$, this further simplifies to:

$$\frac{\partial \mu}{\partial S} = 0 \tag{4.44}$$

which from the kinetic expression (4.35) for μ leads to

$$S - \sqrt{K_1 K_2} = 0 \tag{4.45}$$

Thus, the problem of maximizing cell mass at the end of the batch time reduces to regulating the substrate concentration to $\sqrt{K_1 K_2}$. On intuitive grounds also, this

Reproduced with permission of the copyright owner. Further reproduction prohibited without permission.

K_1	0.5 kg/m^3
K_2	500.0 kg/m^3
s_F	25.0 kg/m^3
Y	0.5 kg/kg
t_f	5.0 hr

Table 4.3: Model Parameters

solution makes sense. To maximize biomass, the system must operate at that level of S that maximizes the specific growth rate μ.

We use the following state feedback law to regulate the substrate concentration to $\sqrt{K_1 K_2}$:

$$u = \frac{\frac{\mu(S,t)X}{Y} + (\sqrt{K_1 K_2} - S)}{\frac{s_F - S}{V}} \tag{4.46}$$

Since the reactor starts with a high substrate concentration, there will be an initial non-singular phase where no substrate is fed. The switch to the singular phase occurs when S reaches the value $\sqrt{K_1 K_2}$. Figures 4.4 and 4.5 show the optimal feeding profile, the optimal cell mass profile and the optimal substrate concentration profile for the system parameters in Table 4.3 and initial conditions designated Case A in Table 4.4. The first order necessary condition for optimality ($\lambda^T g(x) = 0$) was verified by integrating the adjoint equations backwards in time and is shown in Figure 4.6.

The robustness of the control law to errors in the kinetic parameters was tested. In the control law, the values of parameters K_1 and K_2 used were 10 % lower than those of the system parameters shown in Table 4.3. The results are summarized in Table 4.5. It is observed that the performance index is very close to that obtained in

Reproduced with permission of the copyright owner. Further reproduction prohibited without permission.

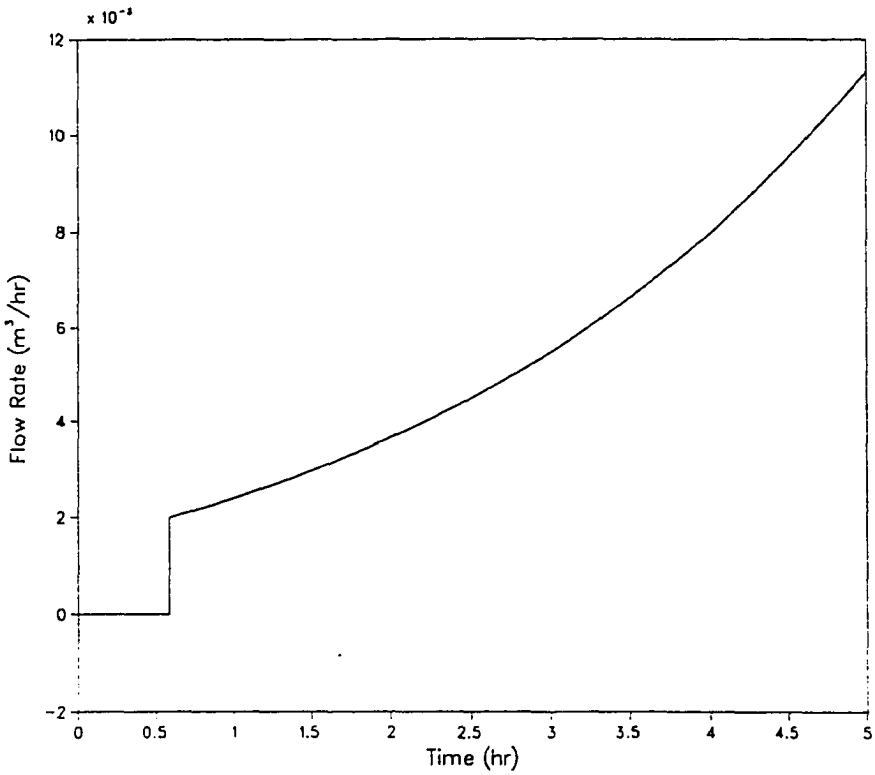

Figure 4.4: Optimal input profile (example 2)

Reproduced with permission of the copyright owner. Further reproduction prohibited without permission.

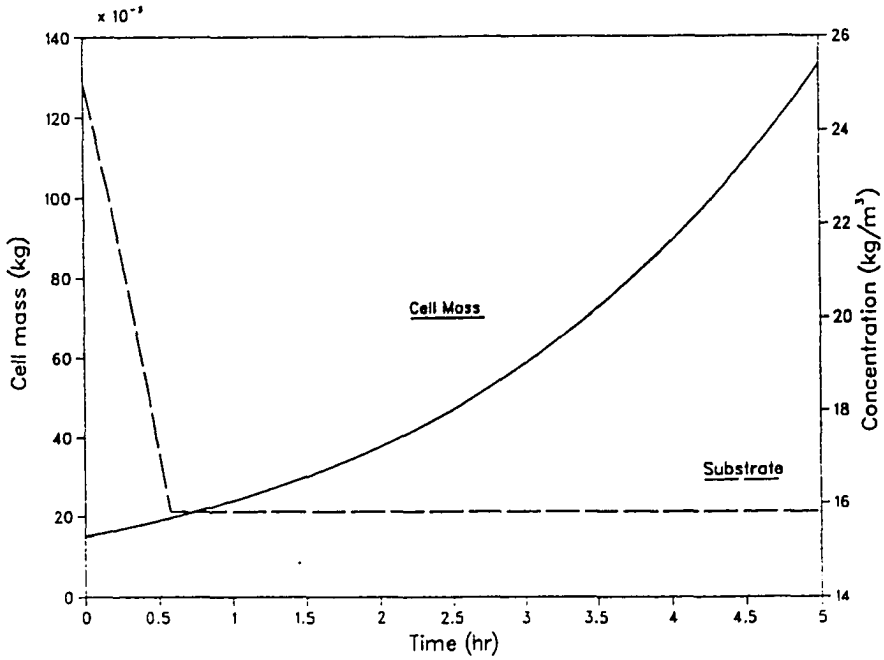

Figure 4.5: Optimal cell mass and substrate profiles (example 2)

Reproduced with permission of the copyright owner. Further reproduction prohibited without permission.

Case A	
$X(0)$	15.0 kg/m^3
$S(0)$	25.0 kg/m^3
$V(0)$	1.0 x 10^{-3} m^3
Case B	
$X(0)$	25.0 kg/m^3
$S(0)$	17.5 kg/m^3
$V(0)$	1.0 x 10^{-3} m^3

Table 4.4: Initial Conditions

the nominal case, where the true values of the parameters were used in the control law.

The sensitivity of the performance index of the control law with respect to errors in the initial conditions is also studied. Feedback implementation was compared to the conventional open-loop implementation. The input profile obtained for the initial conditions designated Case A in Table 4.4 was implemented in open loop to the system with initial conditions designated Case B in Table 4.4. This was compared to the case where the input profile was determined by the state feedback in closed loop. The condition $S = \sqrt{K_1 K_2}$ was used to calculate the switching time from the non-singular to singular region in the closed-loop implementation. The closed-loop scheme provides optimal performance since the switching time is calculated on-line and the substrate concentration is kept at the optimum level. The results are summarized in Table 4.6. It is observed that there is a reduction of about 3 % in the performance index of the open-loop scheme over the closed loop scheme.

Reproduced with permission of the copyright owner. Further reproduction prohibited without permission.

Parameters in Control Law	Parameters in Process	Performance Index
$K_1 = 0.5$, $K_2 = 500$	$K_1 = 0.5$, $K_2 = 500$	-132.993 x 10^{-3} kg
All other parameter	All other parameter	
values from Table 4.3	values from Table 4.3	
$K_1 = 0.45$, $K_2 = 450$	$K_1 = 0.5$, $K_2 = 500$	-132.932 x 10^{-3} kg
All other parameter	All other parameter	
values from Table 4.3	values from Table 4.3	

Table 4.5: Robustness Analysis

Open Loop Implementation
Initial Conditions: Case B in Table 4.4
Input Profile: Optimal solution for Case A
Performance Index at final time: -214.85 x 10^{-3} kg
Closed Loop Implementation
Initial Conditions: Case B in Table 4.4
Input Profile: State feedback law from equation (4.46)
Performance Index at final time: -221.84 x 10^{-3} kg

Table 4.6: Open Loop vs. Closed Loop Implementation

Reproduced with permission of the copyright owner. Further reproduction prohibited without permission.

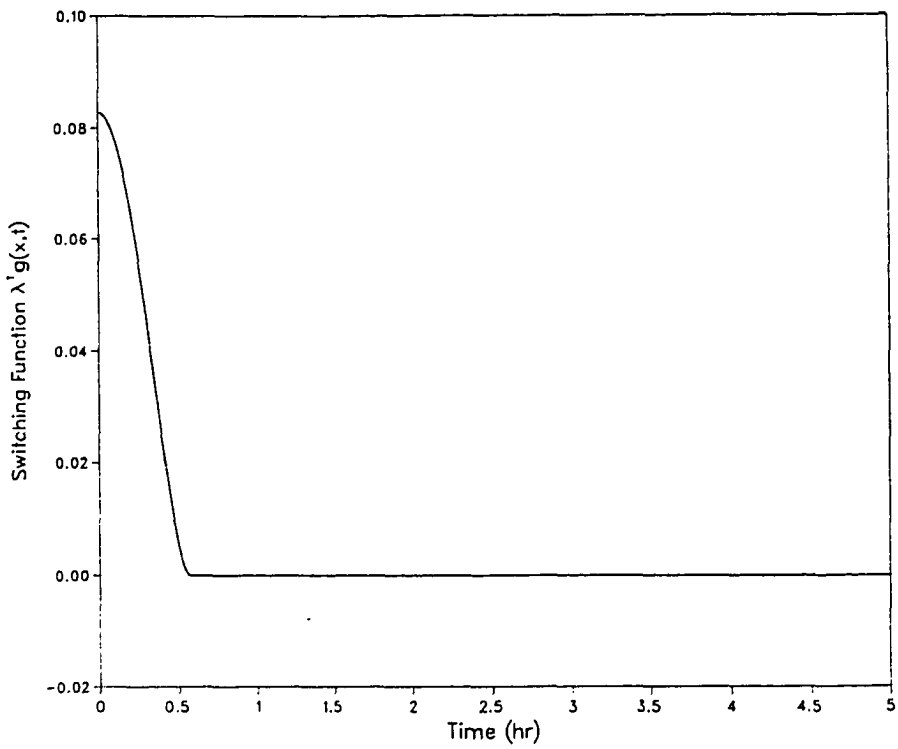

Figure 4.6: Profile of switching function $\lambda^T g(x,t)$ (example 2)

Reproduced with permission of the copyright owner. Further reproduction prohibited without permission.

4.6.3 Example 3: Static State Feedback

In this example, we consider a yield optimization problem in ethanol production of *S. cerevisiae* in a fed-batch fermentation. The unsteady state material balances are as follows (See Nomenclature Section for explanation of symbols):

$$\begin{aligned}
\frac{d(X.V)}{dt} &= \mu(S,P,t)X.V \\
\frac{d(S.V)}{dt} &= -\frac{\mu(S,P,t)X.V}{Y} + s_F u \\
\frac{d(P.V)}{dt} &= \epsilon(S,P,t)X.V \\
\frac{dV}{dt} &= u
\end{aligned} \tag{4.47}$$

where the manipulated input, u, is the feed rate of the substrate. The objective is to maximize the concentration of the product, ethanol, at a prespecified final time t_f. Thus

$$J = -P(t_f) \tag{4.48}$$

The following kinetic expressions for μ and ϵ derived by Aiba and co-workers (Aiba *et al.*, (1973)) are used.

$$\mu(S,P) = \frac{\mu_0(t)}{(1+P/K_P)}\frac{S}{(K_S+S)} \tag{4.49}$$

$$\epsilon(S,P) = \frac{\nu_0(t)}{(1+P/K_P^*)}\frac{S}{(K_S^*+S)} \tag{4.50}$$

The parameters μ_0 and ν_0 decrease with time due to degradation of intracellular enzymes and their time variation is shown in Figure 4.7.

Condition (4.17) is violated everywhere. As in Example 2, we do model reduction to eliminate the redundant state equation. It can be easily shown that X, S, and V

Reproduced with permission of the copyright owner. Further reproduction prohibited without permission.

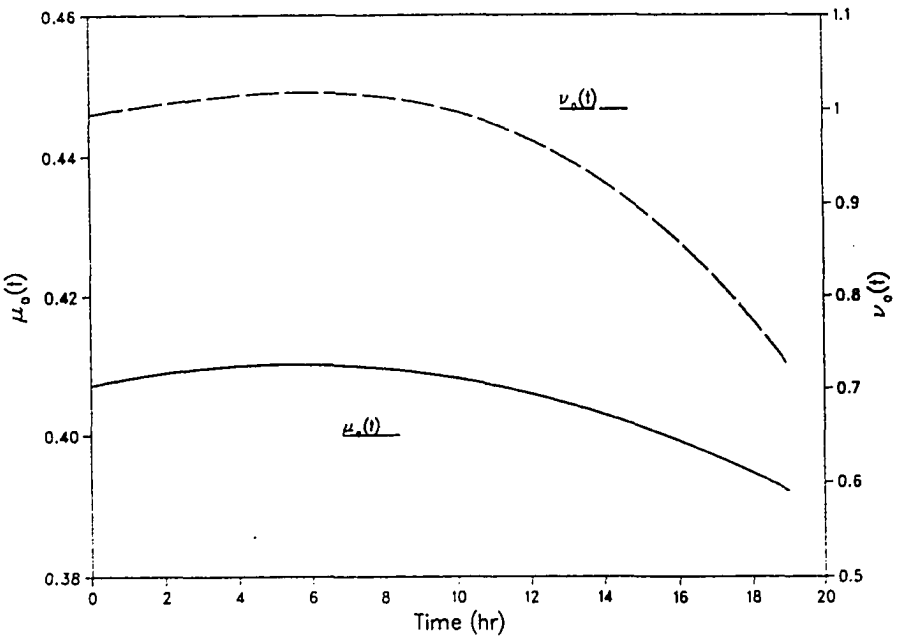

Figure 4.7: Profile of time-varying parameters $\mu_0(t)$ and $\nu_0(t)$ (example 3)

Reproduced with permission of the copyright owner. Further reproduction prohibited without permission.

are algebraically related by:

$$\left(\frac{XV}{Y}+SV\right)-\left(\frac{X(0)V(0)}{Y}+S(0)V(0)\right) = s_F(V-V(0)) \tag{4.51}$$

Thus there are only three independent equations. Defining

$$\begin{aligned} x_1 &= XV \\ x_2 &= PV \\ x_3 &= V \\ k(t) &= [\mu_0(t)\ \ \nu_0(t)]^T \end{aligned} \tag{4.52}$$

and eliminating the variable S from (4.51):

$$S = s_F - \frac{1}{Y}\left(\frac{x_1 - X(0)V(0)}{x_3}\right) + \left(\frac{S(0)V(0) - s_F V(0)}{x_3}\right) \tag{4.53}$$

the model can be put in the form:

$$\frac{d}{dt}\begin{bmatrix} x_1 \\ x_2 \\ x_3 \end{bmatrix} = \begin{bmatrix} \hat{\mu}(x_1,x_2,x_3,k(t))x_1 \\ \hat{\epsilon}(x_1,x_2,x_3,k(t))x_1 \\ 0 \end{bmatrix} + \begin{bmatrix} 0 \\ 0 \\ 1 \end{bmatrix} u \tag{4.54}$$

where $\hat{\mu}$ and $\hat{\epsilon}$ are obtained by substituting S from (4.53) and $P = \frac{x_2}{x_3}$ into the expressions for μ and ϵ. For this system:

$$x = \begin{bmatrix} x_1 \\ x_2 \\ x_3 \end{bmatrix},\ f(x,t) = \begin{bmatrix} \hat{\mu}(x_1,x_2,x_3,k(t))x_1 \\ \hat{\epsilon}(x_1,x_2,x_3,k(t))x_1 \\ 0 \end{bmatrix},\ g(x,t) = \begin{bmatrix} 0 \\ 0 \\ 1 \end{bmatrix} \tag{4.55}$$

It can easily be verified that now condition (4.17) is satisfied. Also, $n = 3$ and a straightforward calculation shows that $s = 1$ and so the state feedback that tracks the singular trajectories will be static. Using expressions (4.24) and (4.26) we obtain the following static state feedback law:

$$u = -\frac{det\left[g(x,t)\,|\,ad_f^1 g(x,t)\,|\,ad_f^2 g(x,t) + \dfrac{\partial ad_f^1 g(x,t)}{\partial k}\dfrac{dk}{dt}\right]}{det[g(x,t)\,|\,ad_f^1 g(x,t)\,|\,[g,ad_f^1 g](x,t)]} \tag{4.56}$$

Reproduced with permission of the copyright owner. Further reproduction prohibited without permission.

Since the fermentor starts with a high substrate concentration, there is an initial non-singular phase where no substrate is fed, followed by a singular phase which involves substrate feeding. In this region there is some accumulation of substrate. Substrate feeding leads to enhancement of product formation. However, the product also gets diluted due to increase in volume. Since these are competing effects, there will be a short non-singular phase at the end to use up the accumulated substrate. Thus, on intuitive grounds, we expect to have three phases - non-singular, singular, non-singular with two switching times to be calculated. The presence of the second non-singular region is further necessitated by the fact that the terminal conditions for the adjoint states, λ, are incompatible with the first order necessary condition on the singular region, $\lambda^T g(x,t) = 0$.

A two-dimensional search was performed numerically as described in Lim *et al.* (1986) to get initial estimates of the two switching times. These estimates were further refined till the first order condition $\lambda^T g(x,t) = 0$ was satisfied on the singular region. Figures 4.8 and 4.9 show the optimal feeding profile and the corresponding product profiles for the model parameters in Table 4.7 and the initial conditions designated Case A in Table 4.8. Figure 4.10 depicts the corresponding time profile of the switching function ($\lambda^T g(x,t)$) and the second order condition ($-\lambda^T [g, \overline{ad}_f^1 g](x,t)$). The switching function vanishes on the singular time interval and is positive everywhere else. The positivity of the switching function is consistent with $u(t)$ taking its minimal value ($u = 0$) in the non-singular intervals. Furthermore, the second order condition $-\lambda^T [g, \overline{ad}_f^1 g](x,t) \geq 0$ is satisfied in the singular region and so the singular extremal is indeed optimal.

The sensitivity of the performance index to errors in the first switching time was checked. In the non-singular regions u was set to 0. It was assumed that there was

Reproduced with permission of the copyright owner. Further reproduction prohibited without permission.

K_P	16.0 kg/m^3
K_S	0.22 kg/m^3
K_P^*	71.5 kg/m^3
K_S^*	0.44 kg/m^3
Y	0.1 kg/kg
s_F	150.0 kg/m^3
t_f	19.1 hr

Table 4.7: Model Parameters

Case A	
$X(0)$	1.0 kg/m^3
$S(0)$	150.0 kg/m^3
$P(0)$	0.0 kg/m^3
$V(0)$	10.0 x 10^{-3} m^3
Case B	
$X(0)$	0.9 kg/m^3
$S(0)$	165.0 kg/m^3
$P(0)$	0.0 kg/m^3
$V(0)$	10.0 x 10^{-3} m^3

Table 4.8: Initial Conditions

Reproduced with permission of the copyright owner. Further reproduction prohibited without permission.

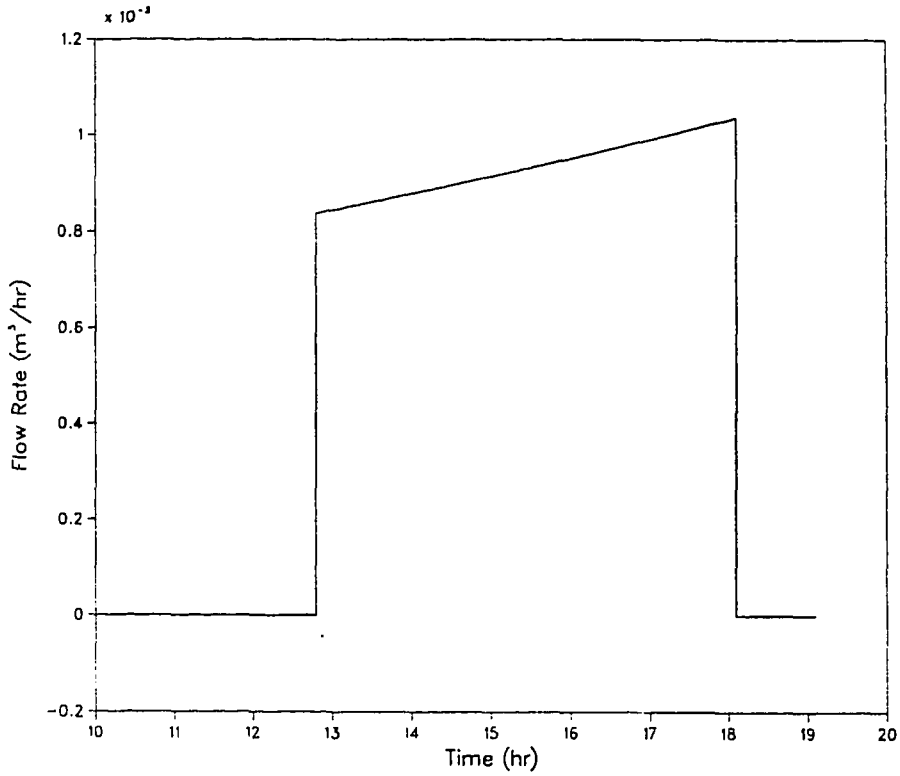

Figure 4.8: Optimal input profile (example 3)

Reproduced with permission of the copyright owner. Further reproduction prohibited without permission.

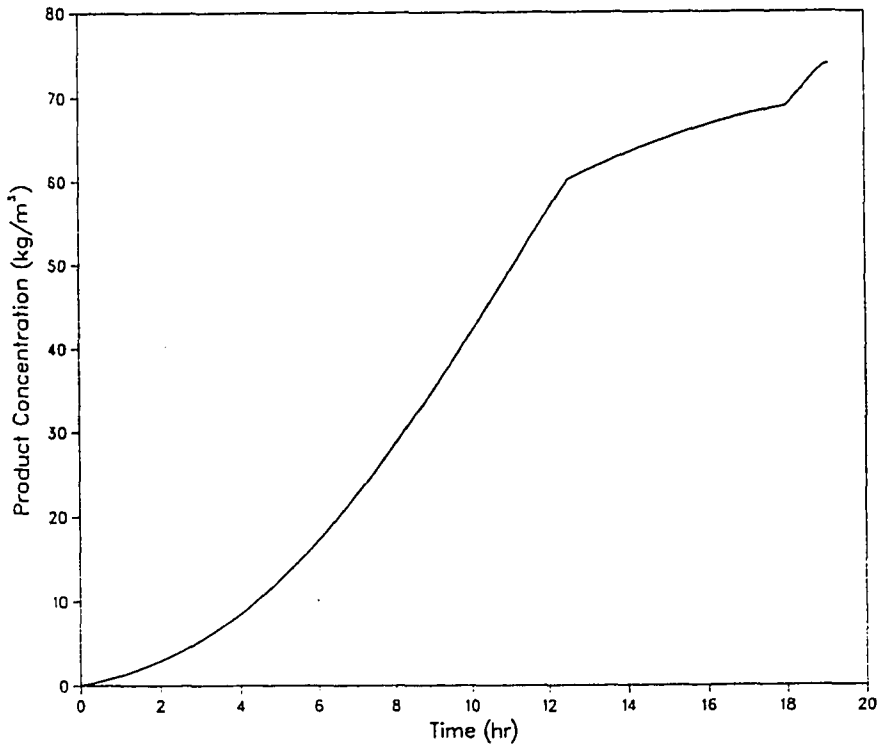

Figure 4.9: Optimal time profile of ethanol (example 3)

Reproduced with permission of the copyright owner. Further reproduction prohibited without permission.

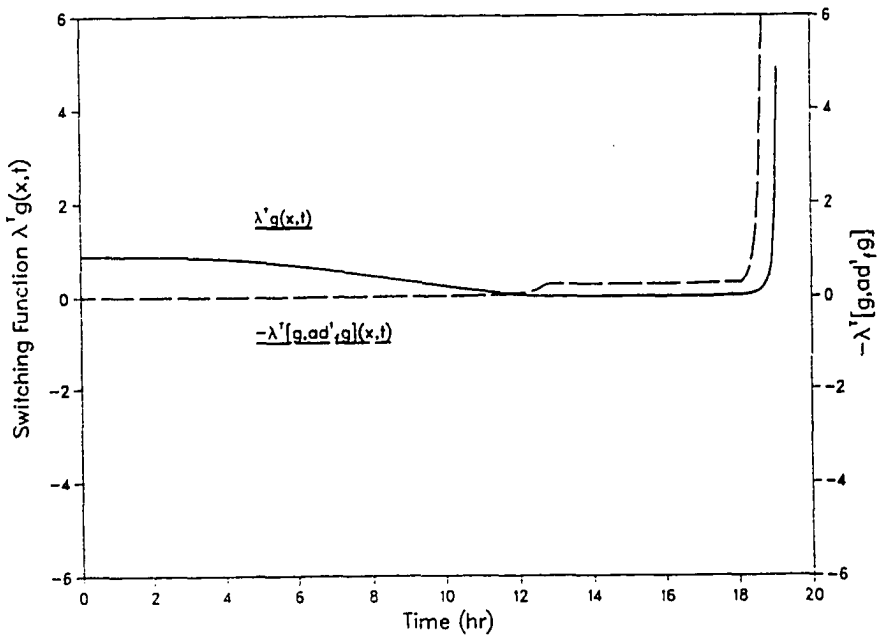

Figure 4.10: Profile of switching function $\lambda^T g(x,t)$ and second order condition $\lambda^T[g, \overline{ad}_f^1 g](x,t)$ (example 3)

Reproduced with permission of the copyright owner. Further reproduction prohibited without permission.

Assumed Switching Time (hr)	Performance Index (kg/m^3)
12.00	-73.607
12.25	-73.843
12.50	-73.850
12.75	-73.833
13.00	-73.749

Table 4.9: Sensitivity of error in switching time on performance index

an error in estimating the first switching time. Assuming various values of the first switching time, the feeding profile was calculated using the static state feedback law in the singular region. It is observed (Table 4.9) that the final performance index is quite robust to errors in the assumed switching time. A similar effect was observed for errors in the second switching time. From this study we conclude that the performance index is not very sensitive to errors in the switching times and so *a priori* estimates of the switching times can be used in closed-loop implementation. The sensitivity of yield optimization with respect to errors in the initial conditions was also studied. Feedback implementation was compared to the conventional open-loop implementation. The results are summarized in Table 4.10. It is observed that there is a reduction of about 10 % in the performance index when we implement the optimal input profile in an open-loop fashion. However, there is a 6.32 % improvement in the performance index over the open-loop scheme when the closed-loop scheme is used. Thus the closed-loop scheme is able to attenuate errors in the initial conditions.

Reproduced with permission of the copyright owner. Further reproduction prohibited without permission.

Optimal Solution for Case A:
Initial Conditions: Case A in Table 4.8
Switching Times: 12.5, 18 hrs
Ethanol Concentration at Final Time: 73.850 kg/m^3
Optimal Solution for Case B:
Initial Conditions: Case B in Table 4.8
Switching Times: 14.5, 17.5 hrs
Ethanol Concentration at Final Time: 79.660 kg/m^3
Open Loop Implementation:
Initial Conditions: Case B in Table 4.8
Switching Times: 12.5, 18 hrs (from Case A)
Input Profile: Optimal solution for Case A
Ethanol Concentration at Final Time: 73.408 kg/m^3
Closed Loop Implementation:
Initial Conditions: Case B in Table 4.8
Switching Times: 12.5, 18 hrs (from Case A)
Input Profile: State feedback law from equation (4.56)
Ethanol Concentration at Final Time: 78.049 kg/m^3

Table 4.10: Open-loop Vs. Closed-loop Implementation

Reproduced with permission of the copyright owner. Further reproduction prohibited without permission.

4.6.4 Example 4: Dynamic State Feedback

We consider a yield optimization problem in a semi-batch chemical reactor where the following reactions are occuring:

$$A \rightarrow B$$

$$B \rightarrow C$$

$$A \rightarrow D$$

The reaction from A to B follows the following kinetics:

$$-r = \frac{k_1 C_A.C_B}{k_2 + k_3 C_A + k_4 C_A^2} \tag{4.57}$$

All other reactions are first order reactions. The unsteady state mass balance equations are given by:

$$\begin{aligned}
\frac{d(C_A.V)}{dt} &= -\frac{k_1 C_A.C_B.V}{k_2 + k_3 C_A + k_4 C_A^2} - k_D C_A.V + s_F.u \\
\frac{d(C_B.V)}{dt} &= \frac{k_1 C_A.C_B.V}{k_2 + k_3 C_A + k_4 C_A^2} - k_C C_B.V \\
\frac{d(C_D.V)}{dt} &= k_D C_A.V \\
\frac{dV}{dt} &= u
\end{aligned} \tag{4.58}$$

The objective is to operate the reactor so that the total amount of B is maximized at a prespecified final time t_f. Thus, the performance index to minimize is:

$$J = -C_B.V|_{t=t_f} \tag{4.59}$$

Define:

$$\begin{aligned}
x_1 &= C_A.V \\
x_2 &= C_B.V \\
x_3 &= C_D.V \\
x_4 &= V
\end{aligned} \tag{4.60}$$

Reproduced with permission of the copyright owner. Further reproduction prohibited without permission.

The optimization problem can be stated as:

Minimize

$$J = -x_2(t_f) \tag{4.61}$$

subject to

$$\frac{d}{dt}\begin{bmatrix} x_1 \\ x_2 \\ x_3 \\ x_4 \end{bmatrix} = \begin{bmatrix} -\dfrac{k_1 x_1 x_2 x_4}{k_2 x_4^2 + k_3 x_1 x_4 + k_4 x_1^2} - k_D x_1 \\ \dfrac{k_1 x_1 x_2 x_4}{k_2 x_4^2 + k_3 x_1 x_4 + k_4 x_1^2} - k_C x_2 \\ k_D x_1 \\ 0 \end{bmatrix} + \begin{bmatrix} s_F \\ 0 \\ 0 \\ 1 \end{bmatrix} u \tag{4.62}$$

The system model is of the form:

$$\dot{x} = f(x) + g(x)u \tag{4.63}$$

where:

$$x = \begin{bmatrix} x_1 \\ x_2 \\ x_3 \\ x_4 \end{bmatrix}$$

$$f(x) = \begin{bmatrix} -\dfrac{k_1 x_1 x_2 x_4}{k_2 x_4^2 + k_3 x_1 x_4 + k_4 x_1^2} - k_D x_1 \\ \dfrac{k_1 x_1 x_2 x_4}{k_2 x_4^2 + k_3 x_1 x_4 + k_4 x_1^2} - k_C x_2 \\ k_D x_1 \\ 0 \end{bmatrix}$$

$$g(x) = \begin{bmatrix} s_F \\ 0 \\ 0 \\ 1 \end{bmatrix}$$

Reproduced with permission of the copyright owner. Further reproduction prohibited without permission.

It can be easily verified that the vector fields $g(x)$, $ad_f^1 g(x)$, $ad_f^2 g(x)$, $ad_f^3 g(x)$ are linearly independent and thus condition (4.9) is satisfied everywhere. For this system $n = 4$ and $s = 1$. Thus the optimal state feedback in the singular region will be dynamic. Substituting $n = 4$ and $s = 1$ in equation (4.13) we obtain a dynamic feedback law by setting the determinant of:

$$\begin{aligned} & g(x) \\ & ad_f^1 g(x) \\ & ad_f^2 g(x) + [g, ad_f^1 g](x)u \\ & ad_f^3 g(x) + \left([g, ad_f^2 g](x) + [f, [g, ad_f^1 g]](x) + [g, [g, ad_f^1 g](x)u\right) u + [g, ad_f^1 g](x)\frac{du}{dt} \end{aligned} \tag{4.64}$$

equal to zero. Since the reactor starts with a high concentration of A and the reaction rate is a decreasing function of A we expect that there will be an initial non-singular phase where no A is fed so that the concentration of A decreases, followed by a singular phase which involves feeding of species A. The terminal conditions of the adjoint states λ are compatible with the first order necessary condition on the singular region, $\lambda^T g(x) = 0$. Thus, intuitively we expect that there will be two phases - non-singular phase followed by a singular phase with one switching time to be calculated.

An initial estimate of the switching time was found by performing a one-dimensional numerical search as described by Lim *et al.* (1986). This estimate was further refined till the first order condition $\lambda^T g(x) = 0$ was satisfied on the singular region. Figures 4.11 and 4.12 show the optimal feeding profile and the optimal profile of species B for the system parameters in Table 4.11 and the initial conditions in Table 4.12. Figure 4.13 depicts the corresponding time profiles of the switching function ($\lambda^T g(x)$) and the second order condition ($-\lambda^T [g, ad_f^1 g](x)$). The switching function vanishes on the singular time interval and is positive everywhere else. The positivity of the switching

Reproduced with permission of the copyright owner. Further reproduction prohibited without permission.

function is consistent with $u(t)$ taking its minimum value ($u = 0$) in the non-singular interval. Furthermore, the second order condition $-\lambda^T[g, ad_f^1 g](x,t) \geq 0$ is satisfied in the singular region and so the singular extremal is indeed optimal.

Since the optimal state feedback is dynamic, we need the initial condition of u to implement the state feedback law. The effect of error in the initial conditon of u on the final performance index was studied. The results are shown in Table 4.13. It is observed that the final performance index is very robust to errors in the assumed initial condition for $u(t)$. From this study we conclude that the performance index is not sensitive at all to errors in the initial condition for $u(t)$ and so an *a priori* estimate of the initial condition for $u(t)$ can be used in closed-loop implementation.

The robustness of the dynamic state feedback law with respect to errors in the system parameter k_1 was tested. With the initial conditions for u and switching time from the nominal case, the dynamic feedback law was implemented using a 13.4 % higher k_1 than its true value. The results are summarized in Table 4.14. It is observed that the performance index is very close to that obtained in the nominal case.

Reproduced with permission of the copyright owner. Further reproduction prohibited without permission.

k_1	0.530 $m^3/kmoles/hr$
k_2	1.00
k_3	1.00 $m^3/kmoles$
k_4	1/22 $m^3/kmoles^2$
k_C	0.01 $1/hr$
k_D	0.01 $1/hr$
t_f	2.00 hr

Table 4.11: Model Parameters

$C_A(0)$	7.5 kg/m^3
$C_B(0)$	8.0 kg/m^3
$C_D(0)$	0.0 kg/m^3
$V(0)$	2.0 x 10^{-3} m^3

Table 4.12: Initial Conditions

Assumed Initial Condition of $u(t)$	Performance Index (kg)
0.00	-32.726 x 10^{-3}
0.25	-32.726 x 10^{-3}
0.50	-32.726 x 10^{-3}
0.75	-32.726 x 10^{-3}
1.00	-32.726 x 10^{-3}

Table 4.13: Sensitivity of error in initial condition of $u(t)$ on performance index

Reproduced with permission of the copyright owner. Further reproduction prohibited without permission.

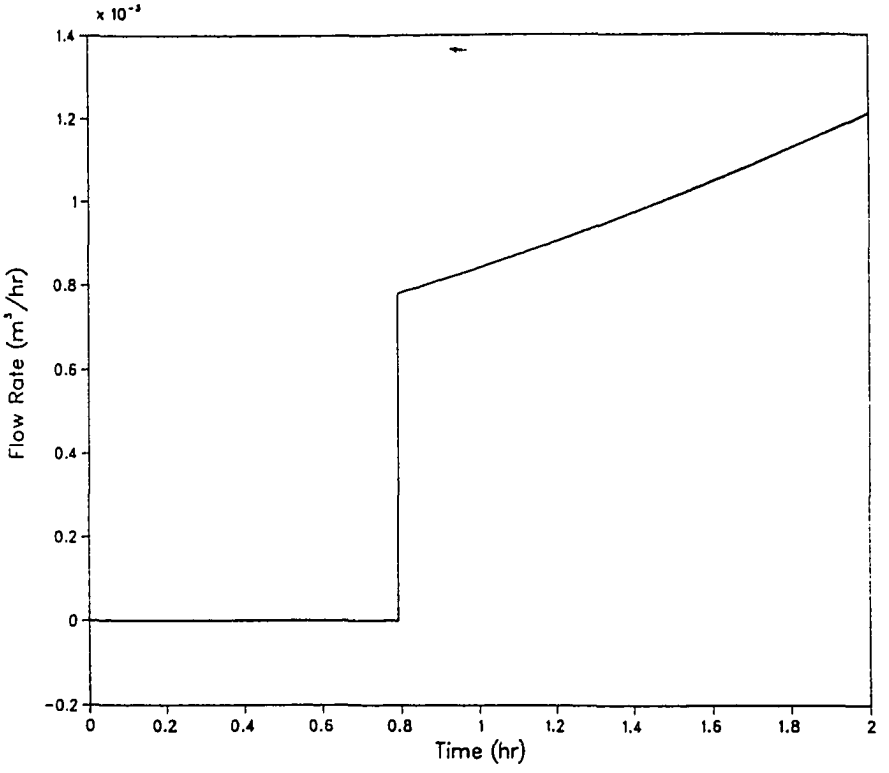

Figure 4.11: Optimal input profile (example 4)

Parameters in Control Law	Parameters in Process	Performance Index
$k_1 = 0.530$	$k_1 = 0.530$	-32.726 x 10^{-3} kg
All other parameter	All other parameter	
values from Table 4.11	values from Table 4.11	
$k_1 = 0.601$	$k_1 = 0.530$	-32.715 x 10^{-3} kg
All other parameter	All other parameter	
values from Table 4.11	values from Table 4.11	

Table 4.14: Robustness Analysis

Reproduced with permission of the copyright owner. Further reproduction prohibited without permission.

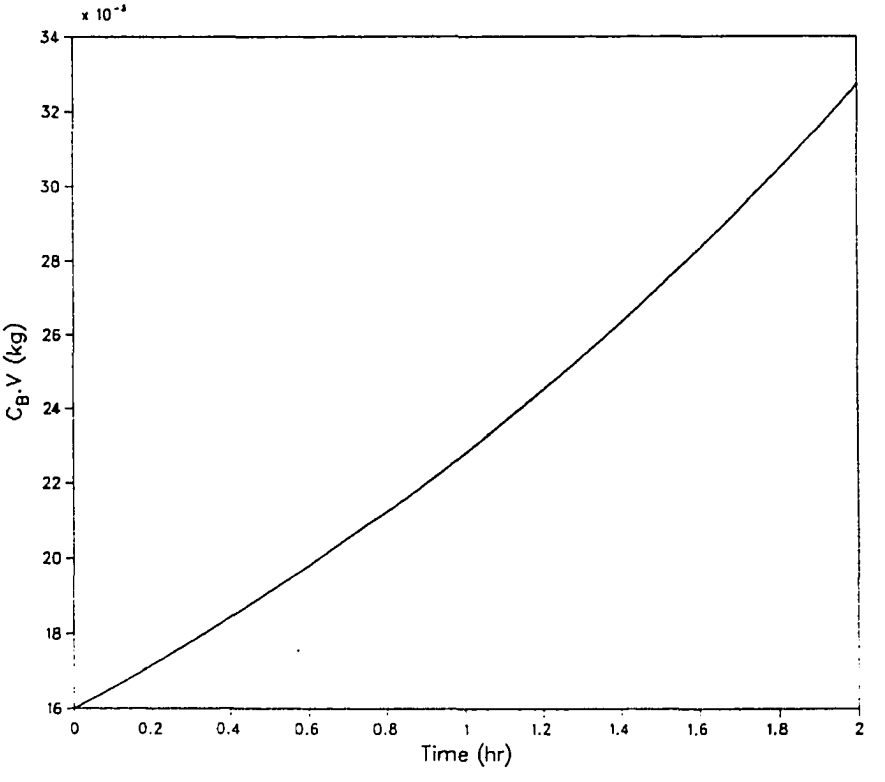

Figure 4.12: (Optimal time profile of species B example 4)

Reproduced with permission of the copyright owner. Further reproduction prohibited without permission.

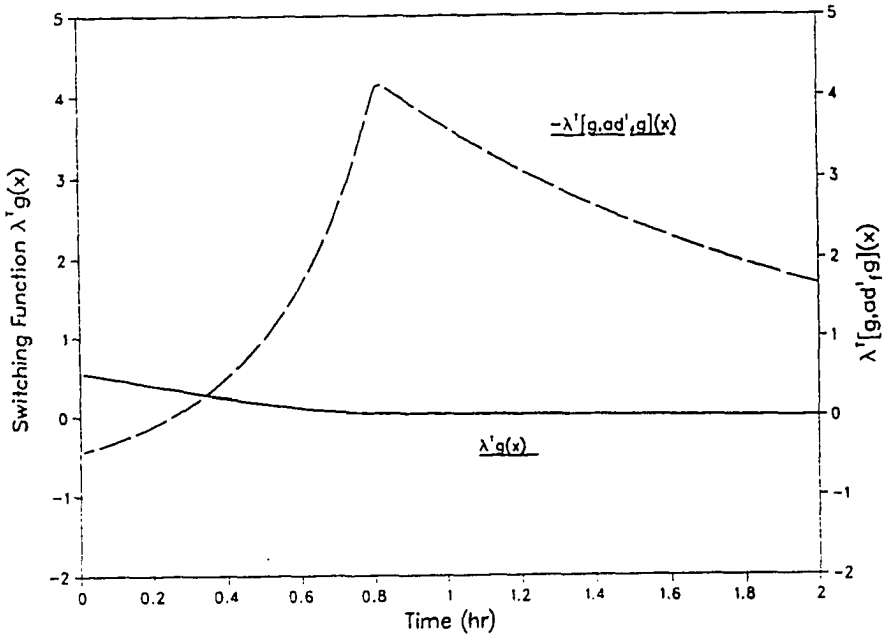

Figure 4.13: Profile of switching function $\lambda^T g(x)$ and second order condition $\lambda^T[g, ad_f^1 g](x)$ (example 4)

Reproduced with permission of the copyright owner. Further reproduction prohibited without permission.

4.7 Nomenclature

C_A = concentration of species A, kg/m^3

C_B = concentration of species B, kg/m^3

C_C = concentration of species C, kg/m^3

C_D = concentration of species D, kg/m^3

H = Hamiltonian

H_u = first derivative of Hamiltonian with respect to u

H_{uu} = second derivative of Hamiltonian with respect to u

I = identity matrix

J = performance index

K_1 = dissociation constant in expression (4.35) , kg/m^3

K_2 = inhibition constant in expression (4.35) , kg/m^3

k_B = kinetic rate constant of reaction $A \rightarrow B$, $1/hr$

K_S = kinetic parameter in rate expression (4.49) , kg/m^3

K_P = kinetic parameter in rate expression (4.49) , kg/m^3

K_S^* = kinetic parameter in rate expression (4.50) , kg/m^3

K_{P*} = kinetic parameter in rate expression (4.50) , kg/m^3

P = product concentration , kg/m^3

S = substrate concentration , kg/m^3

V = volume, m^3

X = cell mass concentration , kg/m^3

Y = yield coefficient

Reproduced with permission of the copyright owner. Further reproduction prohibited without permission.

det = determinant

f = vector function in dynamic model (4.2) or (4.15)

g = vector function in dynamic model (4.2) or (4.15)

k_1 = kinetic parameter in expression (4.57), $m^3/kg/hr$

k_2 = kinetic parameter in expression (4.57)

k_3 = kinetic parameter in expression (4.57), m^3/kg

k_4 = kinetic parameter in expression (4.57), m^3/kg^2

k_C = kinetic rate constant of reaction $B \rightarrow C$, $1/hr$

k_D = kinetic rate constant of reaction $A \rightarrow D$, $1/hr$

n = number of state equations (dimension of state vector x)

s = degree of singularity

s_F = concentration of feed, kg/m^3

t = time

t_f = final time, hr

u = manipulated input

x = vector of system states

y = output

Reproduced with permission of the copyright owner. Further reproduction prohibited without permission.

Greek Symbols

β = adjustable parameter in the feedback law (4.11)

ϵ = specific product formation rate, $1/hr$

λ = vector of adjoint states

μ = specific growth rate, $1/hr$

μ_m = kinetic parameter in rate expression (4.35), $m^3/kg/hr$

μ_0 = kinetic parameter in rate expression (4.49), $m^3/kg/hr$

ν_0 = kinetic parameter in rate expression (4.50), $m^3/kg/hr$

ϕ = scalar function expressing the performance index in terms of the system states

Reproduced with permission of the copyright owner. Further reproduction prohibited without permission.

CHAPTER V

STATE FEEDBACK LAWS FOR END-POINT OPTIMIZATION: FREE FINAL TIME AND A STATE INEQUALITY CONSTRAINT

In research the horizon recedes as we advance, and is no nearer at sixty than it was at twenty.

Mark Pattison

5.1 Introduction

In Chapter IV, feedback laws were derived for end-point optimization of the system when the final time was fixed and there were no state constraints. In this chapter we extend this methodology to include the case where the final time is free and there is a state inequality constraint to be satisfied.

State inequality constraints are usually physical constraints to the system. For example, in a semi-batch reactor one can feed only a finite amount of substrate due to a volume constraint on the reactor. Similarly, one may not want to operate a reactor beyond a certain maximum temperature for safety reasons. In a fed-batch bioreactor there could be constraints on the cell mass concentration (beyond which oxygen transfer is limited) or the substrate concentration (beyond which undesirable

Reproduced with permission of the copyright owner. Further reproduction prohibited without permission.

side reactions occur). Due to batch-to-batch variation in yield, the final time may not be fixed *a priori*. The reactor operation is stopped when the optimum yield is achieved. Thus, it is important to consider yield optimization problems with state inequality constraints and free terminal time. The purpose of this chapter is to develop state feedback laws for such optimization problems.

5.2 End Point Optimization of Time Invariant Systems

Consider the following end-point optimization problem:

Minimize the performance index:

$$J = \phi(x(t_f), t_f) \tag{5.1}$$

subject to the dynamics

$$\begin{aligned} \dot{x} &= f(x) + g(x)u, \quad 0 \leq t \leq t_f \\ & \qquad u_{min} \leq u \leq u_{max} \\ x(0) &= x_0 \end{aligned} \tag{5.2}$$

and the scalar state inequality constraint:

$$C(x) \leq 0 \tag{5.3}$$

In this formulation u is the scalar manipulated input bounded by u_{min} and u_{max}, x is the n-vector of states, t_f is the free final time, $f(x)$ and $g(x)$ are smooth vector functions and $\phi(x)$ is a smooth scalar function such that:

$$\begin{aligned} g(x) &\neq [0\ 0\ \ldots\ 0] \\ \frac{\partial \phi}{\partial x} &\neq [0\ 0\ \ldots\ 0] \end{aligned} \tag{5.4}$$

for all x.

Following the methodology developed in Chapter IV, we will first state the necessary conditons for optimality in terms of the system Lie brackets. By elimination

Reproduced with permission of the copyright owner. Further reproduction prohibited without permission.

of the adjoint states, we will derive optimal state feedback laws when the final time is free and there is a state inequality constraint.

Throughout this section, we will make the standing assumption that $g(x)$, $ad_f^1 g(x)$, ..., $ad_f^{n-1} g(x)$ are linearly independent *almost everywhere in* x to guarantee local controllability of the system almost everywhere. This assumption is equivalent to:

$$det \left[g(x) \,|\, ad_f^1 g(x) \,|\, ... \,|\, ad_f^{n-1} g(x) \right] \not\equiv 0 \tag{5.5}$$

5.2.1 Optimal State Feedback Laws on Unconstrained Arcs

As in Chapter IV we define the degree of singularity for the system represented by equation (5.2).

Definition 5.1 (Krener, 1977; Palanki et al., 1992):

The system governed by equation (5.2) has a finite **degree of singularity s** *if*

$$[g, ad_f^\nu g](x) \in span \{g(x), ad_f^1 g(x), ..., ad_f^\nu g(x)\}, \; for \; all \; \nu \leq s-1 \tag{5.6}$$

$$[g, ad_f^s g](x) \notin span \{g(x), ad_f^1 g(x), ..., ad_f^s g(x)\} \tag{5.7}$$

The system governed by equation (5.2) has an **infinite degree of singularity** ($s = \infty$) *if*

$$[g, ad_f^\nu g](x) \in span \{g(x), ad_f^1 g(x), ..., ad_f^\nu g(x)\}, \; for \; all \; \nu \geq 0 \tag{5.8}$$

Since $g(x)$, $ad_f^1 g(x)$, ..., $ad_f^{n-1} g(x)$ are assumed to be linearly independent, it follows from the definition that $1 \leq s \leq (n-2)$ or $s = \infty$.

The following proposition is a rather straightforward consequence of known results (see Gabasov and Kirillova, 1972).

Proposition 5.1: Consider a system governed by equation (5.2) with finite degree of

Reproduced with permission of the copyright owner. Further reproduction prohibited without permission.

singularity s. Then s is odd and the first order necessary conditions for optimality for a singular extremal can be written as follows:

$$\begin{aligned} &\lambda^T ad_f^k g(x) = 0 \qquad \leftarrow \qquad k = 0,1,2,....,s \\ &\lambda^T ad_f^{s+1} g(x) + \lambda^T [g, ad_f^s g](x)u = 0 \end{aligned} \tag{5.9}$$

Furthermore, the second order necessary condition for optimality in the singular region takes the form:

$$(-1)^{\frac{s+1}{2}} \lambda^T \left[g, ad_f^s g\right](x) \geq 0 \tag{5.10}$$

If (5.2) has an infinite degree of singularity, then the first order necessary conditions for optimality take the form $\lambda^T ad_f^\nu g(x) = 0$ for all $\nu \geq 0$.

If ϕ is independent of the final time t_f, then an additional necessary condition for optimality in the singular region is:

$$\lambda^T f(x) = 0 \tag{5.11}$$

Theorem 5.1: Consider a system of the form of equation (5.2) with degree of singularity $s = \infty$.

If $f(x)$ is linearly dependent on the vector fields $g(x)$, $ad_f^1 g(x)$, ..., $ad_f^{n-2} g(x)$ almost everywhere or the performance index depends explicitly on the free final time, then the state trajectories corresponding to a singular extremal evolve on the following surface:

$$S(x) = det\left[g(x) \,|\, ad_f^1 g(x) \,|\, ... \,|\, ad_f^{n-1} g(x)\right] = 0 \tag{5.12}$$

Theorem 5.2: Consider a system of the form of equation (5.2) with degree of singularity $s = n - 2$.

(i) If $f(x)$ is linearly independent of the vector fields $g(x)$, $ad_f^1 g(x)$, ..., $ad_f^{n-2} g(x)$ almost everywhere and the performance index does not depend explicitly on the free

Reproduced with permission of the copyright owner. Further reproduction prohibited without permission.

final time, then the state trajectories corresponding to a singular extremal evolve on the surface given by:

$$S(x) = det\left[f(x) \,|\, g(x) \,|\, ad_f^1 g(x) \,|\, ... \,|\, ad_f^{n-2} g(x)\right] = 0 \tag{5.13}$$

(ii) If $f(x)$ is linearly dependent on the vector fields $g(x)$, $ad_f^1 g(x)$, ..., $ad_f^{n-2} g(x)$ or the performance index depends explicitly on the free final time, then the optimal static state feedback is given by:

$$u = -\frac{det\left[g(x) \,|\, ad_f^1 g(x) \,|\, ... \,|\, ad_f^{n-1} g(x)\right]}{det\left[g(x) \,|\, ad_f^1 g(x) \,|\, ... \,|\, ad_f^{n-2} g(x) \,|\, [g, ad_f^{n-2} g](x)\right]} \tag{5.14}$$

Theorem 5.3: Consider a system of the form of equation (5.2) with degree of singularity $s = n - 3$.

(i) If $f(x)$ is linearly independent of the vector fields $g(x)$, $ad_f^1 g(x)$, ..., $ad_f^{n-2} g(x)$ and the performance index does not depend explicitly on the free final time, then the optimal static state feedback is given by:

$$u = -\frac{det\left[f(x) \,|\, g(x) \,|\, ad_f^1 g(x) \,|\, ... \,|\, ad_f^{n-2} g(x)\right]}{det\left[f(x) \,|\, g(x) \,|\, ad_f^1 g(x) \,|\, ... \,|\, ad_f^{n-3} g(x) \,|\, [g, ad_f^{n-3} g](x)\right]} \tag{5.15}$$

(ii) If $f(x)$ is linearly dependent on the vector fields $g(x)$, $ad_f^1 g(x)$, ..., $ad_f^{n-2} g(x)$ or the performance index depends explicitly on the free final time, then the optimal dynamic state feedback is given by:

$$\Phi(x, u, \frac{du}{dt}) = 0 \tag{5.16}$$

where Φ is an algebraic function. This is obtained by setting the determinant obtained

Reproduced with permission of the copyright owner. Further reproduction prohibited without permission.

from the following column vectors

$$
\begin{aligned}
&g(x)\\
&ad_f^1 g(x)\\
&\cdot\\
&\cdot\\
&\cdot\\
&ad_f^{n-3} g(x)\\
&ad_f^{n-2} g(x) + [g, ad_f^{n-3} g](x)u(t)\\
&ad_f^{n-1} g(x) + [g, ad_f^{n-2} g](x)u(t) + \left(I\frac{d}{dt} - \frac{\partial f(x)}{\partial x} - \frac{\partial g(x)}{\partial x}u(t)\right)\left([g, ad_f^{n-3} g](x)u(t)\right)
\end{aligned}
\tag{5.17}
$$

equal to zero.

In the above equations, I is the identity matrix and $\frac{d(.)}{dt}$ is the total time derivative operator: $\frac{d(.)}{dt} = [f(x) + g(x)u(t)]\frac{\partial(.)}{\partial x} + \frac{\partial(.)}{\partial t}$

Theorem 5.4: Consider a system of the form of equation (5.2) with degree of singularity $s \leq n-4$.

(i) If $f(x)$ *is linearly independent of the vector fields* $g(x)$, $ad_f^1 g(x)$, ..., $ad_f^{n-2} g(x)$ *and the performance index does not depend explicitly on the free final time, then the optimal dynamic state feedback is given by:*

$$\Phi(x, u, \frac{du}{dt}, ..., \frac{d^{n-s-3}u}{dt^{n-s-3}}) = 0$$

where Φ *is an algebraic function. This is obtained by setting the determinant obtained*

Reproduced with permission of the copyright owner. Further reproduction prohibited without permission.

from the following column vectors

$$
\begin{aligned}
&f(x)\\
&g(x)\\
&ad_f^1 g(x)\\
&\cdot\\
&\cdot\\
&\cdot\\
&ad_f^{s-1} g(x)\\
&ad_f^s g(x) + [g, ad_f^{s-1} g](x)u(t)\\
&ad_f^{s+1} g(x) + [g, ad_f^s g](x)u(t) + \left(I\frac{d}{dt} - \frac{\partial f(x)}{\partial x} - \frac{\partial g(x)}{\partial x}u(t)\right)\left([g, ad_f^{s-1} g](x)u(t)\right)\\
&\cdot\\
&\cdot\\
&\cdot\\
&ad_f^{n-2} g(x) + \sum_{k=0}^{n-s-3}\left(I\frac{d}{dt} - \frac{\partial f(x)}{\partial x} - \frac{\partial g(x)}{\partial x}u(t)\right)^k\left([g, ad_f^{n-k-3} g](x)u(t)\right)
\end{aligned}
\tag{5.18}
$$

equal to zero.

(ii) If $f(x)$ is linearly dependent on the vector fields $g(x)$, $ad_f^1 g(x)$, ..., $ad_f^{n-2} g(x)$ or the performance index depends explicitly on the free final time, then the optimal dynamic state feedback is given by:

$$\Phi(x, u, \frac{du}{dt}, ..., \frac{d^{n-s-2}u}{dt^{n-s-2}}) = 0$$

where Φ is an algebraic function. This is obtained by setting the determinant obtained

Reproduced with permission of the copyright owner. Further reproduction prohibited without permission.

from the following column vectors

$$
\begin{aligned}
&g(x)\\
&ad_f^1 g(x)\\
&\cdot\\
&\cdot\\
&\cdot\\
&ad_f^s g(x)\\
&ad_f^{s+1} g(x) + [g, ad_f^s g](x)u(t)\\
&ad_f^{s+2} g(x) + [g, ad_f^{s+1} g](x)u(t) + \left(I\frac{d}{dt} - \frac{\partial f(x)}{\partial x} - \frac{\partial g(x)}{\partial x}u(t)\right)\left([g, ad_f^s g](x)u(t)\right)\\
&\cdot\\
&\cdot\\
&\cdot\\
&ad_f^{n-1} g(x) + \sum_{k=0}^{n-s-2}\left(I\frac{d}{dt} - \frac{\partial f(x)}{\partial x} - \frac{\partial g(x)}{\partial x}u(t)\right)^k \left([g, ad_f^{n-k-2} g](x)u(t)\right)
\end{aligned}
\tag{5.19}
$$

equal to zero.

5.2.2 Optimal State Feedback Laws on Constrained Arcs

On the constrained arc, the optimization problem is reduced to the following regulation problem:

Regulate the output

$$y = C(x) \tag{5.20}$$

with zero set point subject to the dynamics:

$$\dot{x} = f(x) + g(x)u \tag{5.21}$$

Reproduced with permission of the copyright owner. Further reproduction prohibited without permission.

At the point where the system enters or leaves a constrained arc, a feasible *unconstrained arc* passing through this point must satisfy certain tangency conditions, namely, this arc must have zero values of the state variable constraint and all its time derivatives that *do not* involve the control variable (Speyer and Bryson, 1968). Thus, if the relative order of the system represented by equations (5.20) and (5.21) is r, then at the entry point, exit point and on the constrained arc, the following tangency conditions must be satisfied:

$$\begin{aligned} C(x) &= L_f^0 C(x) = 0 \\ \frac{dC(x)}{dt} &= L_f^1 C(x) = 0 \\ &\cdot \\ &\cdot \\ &\cdot \\ \frac{d^{r-1}C(x)}{dt^{r-1}} &= L_f^{r-1} C(x) = 0 \end{aligned} \tag{5.22}$$

If the system possesses a finite relative order, a state feedback for this regulation problem can be found by standard techniques. For instance (Kravaris and Chung, 1987) the state transformation:

$$u = \Psi(x,v) = \frac{v - \sum_{k=0}^{r} \beta_k L_f^k C(x)}{\beta_r L_g L_f^{r-1} C(x)} \tag{5.23}$$

transforms the system (5.21) into an input/output linear system of the form:

$$\sum_{k=0}^{r} \beta_k \frac{d^k y}{dt^k} = v \tag{5.24}$$

where β_0, β_1, ..., β_r are completely arbitrary. When the poles of the $v - y$ system are appropriately placed "far left" in the complex plane, one can use an external linear controller to force the system output $y(t)$ to zero.

Reproduced with permission of the copyright owner. Further reproduction prohibited without permission.

5.3 End-Point Optimization of Time Varying Systems

In the previous section we derived state feedback laws for end-point optimization of time *invariant* systems with free final time and a state inequality constraint. In this section, we extend these results to time-varying systems.

Consider the following optimization problem:

Minimize the performance index:

$$J = \phi(x(t_f), t_f) \tag{5.25}$$

subject to the dynamics

$$\begin{aligned} \dot{x} &= f(x,t) + g(x,t)u, \quad 0 \leq t \leq t_f \\ & \qquad\qquad u_{min} \leq u \leq u_{max} \\ x(0) &= x_0 \end{aligned} \tag{5.26}$$

and the scalar state inequality constraint:

$$C(x,t) \leq 0 \tag{5.27}$$

As in Chapter IV we make the standing assumption that expression 4.17 is satisfied and define the degree of singularity through equations 4.18, 4.19 and 4.20.

5.3.1 Optimal State Feedback Laws on Unconstrained Arcs

When the system under consideration is time varying, equation (5.11) is not valid as shown in Chapter III. Thus, the first order necessary conditons for optimality in the singular region are exactly the same as the case where the final time is fixed and the results are summarized below.

Theorem 5.5: Consider a system of the form of equation (5.26) with degree of singularity $s = \infty$ *and a performance index of the form of equation (5.25) . If*

Reproduced with permission of the copyright owner. Further reproduction prohibited without permission.

$g(x,t)$, $\overline{ad}_f^1 g(x,t)$, ..., $\overline{ad}_f^{n-1} g(x,t)$ are linearly independent almost everywhere, then the state trajectories corresponding to a singular extremal satisfy the following relationship:

$$\overline{S}(x,t) \equiv det\left[g(x,t) \vdots \overline{ad}_f^1 g(x,t) \vdots \ldots \vdots \overline{ad}_f^{n-1} g(x,t)\right] = 0 \tag{5.28}$$

Thus, the problem of synthesizing a state feedback to track the singular trajectories reduces to a regulation problem for the time-varying output:

$$y = \overline{S}(x,t) \tag{5.29}$$

with zero set point. The general problem of regulating a time-varying nonlinear system will be addressed in Chapter VI.

Theorem 5.5: Consider a system of the form of equation (5.26) and a performance index of the form of equation (5.25).

(i) For s = n-2, the singular trajectories can be tracked by the following state feedback:

$$u = -\frac{det\left[g(x,t) \vdots \overline{ad}_f^1 g(x,t) \vdots \ldots \vdots \overline{ad}_f^{n-1} g(x,t)\right]}{det\left[g(x,t) \vdots \overline{ad}_f^1 g(x,t) \vdots \ldots \vdots \overline{ad}_f^{n-2} g(x,t) \vdots [g, \overline{ad}_f^{n-2} g](x,t)\right]} \tag{5.30}$$

(ii) For $s \leq$ n-3, the singular trajectories can be tracked by a dynamic state feedback which is calculated by setting the determinant obtained from the following vectors

Reproduced with permission of the copyright owner. Further reproduction prohibited without permission.

equal to zero.

$$
\begin{aligned}
&g(x,t)\\
&\overline{ad}_f^1 g(x,t)\\
&\cdot\\
&\cdot\\
&\cdot\\
&\overline{ad}_f^s g(x,t)\\
&\overline{ad}_f^{s+1} g(x,t) + [g, \overline{ad}_f^s g](x,t)u(t)\\
&\overline{ad}_f^{s+2} g(x,t) + [g, \overline{ad}_f^{s+1} g](x,t)u(t) +\\
&\left(I\frac{d}{dt} - \frac{\partial f(x,t)}{\partial x} - \frac{\partial g(x,t)}{\partial x}u(t)\right)\left([g, \overline{ad}_f^s g](x,t)u(t)\right)\\
&\cdot\\
&\cdot\\
&\cdot\\
&\overline{ad}_f^{n-1} g(x,t) + \sum_{k=0}^{n-s-2}\left(I\frac{d}{dt} - \frac{\partial f(x,t)}{\partial x} - \frac{\partial g(x,t)}{\partial x}u(t)\right)^k\left([g, \overline{ad}_f^{n-k-2} g](x,t)u(t)\right)
\end{aligned}
\tag{5.31}
$$

5.3.2 Optimal State Feedback Laws on Constrained Arcs

On the constrained arc, the optimization problem is reduced to the following regulation problem:

Regulate the output

$$y = C(x,t) \tag{5.32}$$

with zero set point subject to the dynamics:

$$\dot{x} = f(x,t) + g(x,t)u \tag{5.33}$$

Reproduced with permission of the copyright owner. Further reproduction prohibited without permission.

The general problem of regulating a time-varying nonlinear system will be addressed in Chapter VI.

5.4 Implementation

In the previous section, state feedback laws have been derived for the unconstrained as well as the constrained regions. To implement the optimal state feedback laws as a closed-loop scheme, the sequence in which singular, non-singular and constrained arcs appear should be known *a priori*. Furthermore, the switching times between singular, non-singular and constrained arcs is required. The switch to a constrained arc from an unconstrained arc occurs when the system reaches the constraint boundary. The switch to a singular arc can be calculated analytically for a restricted class of systems (for example, for systems where a switching surface such as equations (5.12) and (5.13) can be calculated). In most practical situations, these have to be computed numerically as described in section 4.5. From the off-line solution of the first order necessary conditions of optimality, the switching times and the values of the system states at the junctions between singular and non-singular regions are known. This information can be used to set up on-line criteria for the onset of the singular region in terms of the system states (Modek, 1988). Alternatively, one can use the *a priori* calculated switching times determined from the off-line analysis. In this case a successful feedback implementation of the optimal feedback law depends on how sensitive the final performance index is to errors in the switching times. When the state feedback law is dynamic, we also need initial conditions for the dynamic state feedback law. These initial conditions have to be set up in a similar fashion as the switching times.

If the model parameters are *a priori* known, the feedback laws derived in the

Reproduced with permission of the copyright owner. Further reproduction prohibited without permission.

previous sections can be used in conjunction with state estimators. Such an implementation can attenuate errors in the initial conditions and process disturbances. If some of the model parameters are not accurately known *a priori*, these need to be estimated on-line. In this situation, a parameter estimation algorithm is also required.

Using equations (3.5) and (3.6), it can be shown that:

$$(H)_{t=t_f} = \left(\frac{\partial \phi}{\partial x}.f(x) + \frac{\partial \phi}{\partial x}.g(x)u\right) = \left(\frac{\partial \phi}{\partial x}\dot{x}\right)_{t=t_f}$$

Substituting the right hand side of the above equation in equation (3.10), we obtain:

$$\left(\frac{\partial \phi}{\partial t} + H\right)_{t=t_f} = \left(\frac{\partial \phi}{\partial t} + \frac{\partial \phi}{\partial x}\dot{x}\right)_{t=t_f} = \left(\frac{d\phi}{dt}\right)_{t=t_f} = 0 \qquad (5.34)$$

Thus, the stopping condition is obtained at the point where the performance index reaches its optimum value. This can be used for calculating the final time on-line.

5.5 Illustrative Examples

In this section, applications for the theory developed in the preceeding sections is illustrated through three simulation examples.

5.5.1 Example 1

The following exothermic reversible reaction is taking place in a batch reactor:

$$A \rightleftharpoons B$$

The forward reaction is second order with respect to the concentration of species A while the reverse reaction is first order with respect to the concentration of species B. It is desired to find the optimal temperature profile to minimize the following objective function.

$$J = -(C_B - \epsilon t_f) \qquad (5.35)$$

Reproduced with permission of the copyright owner. Further reproduction prohibited without permission.

There is a constraint on the maximum allowable reactor temperature:

$$T - T_{max} \leq 0 \tag{5.36}$$

The manipulated input is the cooling rate of the reactor. The mass and energy balance for this system are as follows:

$$\frac{d}{dt}\begin{bmatrix} C_A \\ T \end{bmatrix} = \begin{bmatrix} -k_1(T)C_A^2 + k_2(T)(C_{A0} - C_A) \\ \left(\frac{-\Delta H}{\rho C_p}\right)(k_1(T)C_A^2 - k_2(T)C_{A0} + k_2(T)C_A) \end{bmatrix} + \begin{bmatrix} 0 \\ \frac{T_c - T}{\rho C_p} \end{bmatrix} u \tag{5.37}$$

where

$$\begin{aligned} k_1 &= k_{10} exp\left[\frac{-E_1}{RT}\right] \\ k_2 &= k_{20} exp\left[\frac{-E_2}{RT}\right] \end{aligned} \tag{5.38}$$

This system is of the form (5.2) with

$$x = \begin{bmatrix} C_A \\ T \end{bmatrix}, \quad f(x) = \begin{bmatrix} -k_1(T)C_A^2 + k_2(T)(C_{A0} - C_A) \\ \left(\frac{-\Delta H}{\rho C_p}\right)(k_1(T)C_A^2 - k_2(T)C_{A0} + k_2(T)C_A) \end{bmatrix}$$

$$g(x) = \begin{bmatrix} 0 \\ \frac{T_c - T}{\rho C_p} \end{bmatrix}$$

It can be easily shown that $n = 2$, $s = \infty$ and $g(x)$ and $ad_f^1 g(x)$ are linearly independent almost everywhere in x.

Unconstrained Arc: Equation (5.35) depends explicitly on the final time and so equation (5.12) is valid in the singular region. Using equation (5.12), we obtain:

$$S(C_A, T) = det\left[g(x) \,|\, ad_f^1 g(x)\right] = E_1 k_1(T)C_A^2 + E_2 k_2(T)C_A - E_2 k_2(T)C_{A0} = 0 \tag{5.39}$$

Thus, the optimization problem reduces to regulating the function $S(C_A, T)$ to zero where the system states C_A and T are described by equation (3.37). We use the

Reproduced with permission of the copyright owner. Further reproduction prohibited without permission.

following nonlinear control law in the singular region:

$$u = -\frac{\frac{\partial S}{\partial C_A}.(-k_1 C_A^2 + k_2(C_{A0} - C_A)) + \frac{\partial S}{\partial T}.\left(\left(\frac{-\Delta H}{\rho C_p}\right)(k_1 C_A^2 - k_2 C_{A0} + k_2 C_A)\right) + S}{\frac{\partial S}{\partial T}.\left(\frac{T_c - T}{\rho C_p}\right)} \tag{5.40}$$

Constrained Arc: On the constraint boundary the control objective is to keep the system at $C(T) = T - T_{max} = 0$. For this system $r = 1$. We use the following nonlinear control law in the constrained region:

$$u = -\frac{\frac{\partial C}{\partial T}.\left(\left(\frac{-\Delta H}{\rho C_p}\right)(k_1 C_A^2 - k_2 C_{A0} + k_2 C_A)\right) + C}{\frac{\partial C}{\partial T}.\left(\frac{T_c - T}{\rho C_p}\right)} \tag{5.41}$$

Figure 5.1 shows the optimal temperature profile for the system parameters given in Table 5.1 and the initial conditions given in Table 5.2. Figure 5.2 shows the optimal cooling rate of the reactor. Since the reactant is cold at $t = 0$, there is an initial non-singular region where $u = 0$. Since the reaction is exothermic, the temperature rises till it hits the constraint T_{max} at time $t = t_b$. In the constraint boundary equation (5.41) is used. At $t = t_s$, the singular region is hit and equation (5.40) is used. Figure 5.3 shows the profile of the objective function with time. The final time is determined at the point when there is no further decrease in the objective function. The first order necessary condition for optimality was verified by integrating the adjoint equations backwards in time. Figure 5.4 shows the time profile of the first order condition $\lambda^T g(x)$ and it is observed that in the singular region $\lambda^T g(x) = 0$. Figure 5.5 shows the time profile of the Hamiltonian H and it is observed that indeed $\left(\frac{\partial \phi}{\partial t} + H\right)_{t=t_f} = 0$.

The constrained optimization problem was compared with the case where there is no state constraint present. Table 5.3 shows the results. As expected, the objective

Reproduced with permission of the copyright owner. Further reproduction prohibited without permission.

k_{10}	1.0 $m^3.kg^{-1}.s{-}1$
k_{20}	100.0 s
E_1	2 x 10^4 $Joules.Mole^{-1}.K^{-1}$
E_2	4 x 10^4 $Joules.Mole^{-1}.K^{-1}$
$-\Delta H$	5 x 10^4 $Joules.Mole^{-1}.K^{-1}$
ρC_p	1000.0 $Joules.m^{-3}.K^{-1}$
ϵ	1.5 x 10^{-5} $kg.s.m^{-3}$
T_c	15 ^oC
T_{max}	52 ^oC

Table 5.1: Model Parameters (example 1)

C_{A0}	1.0 kg/m^3
C_{B0}	0.0 kg/m^3
$T(0)$	25 ^oC

Table 5.2: Initial Conditions (example 1)

Reproduced with permission of the copyright owner. Further reproduction prohibited without permission.

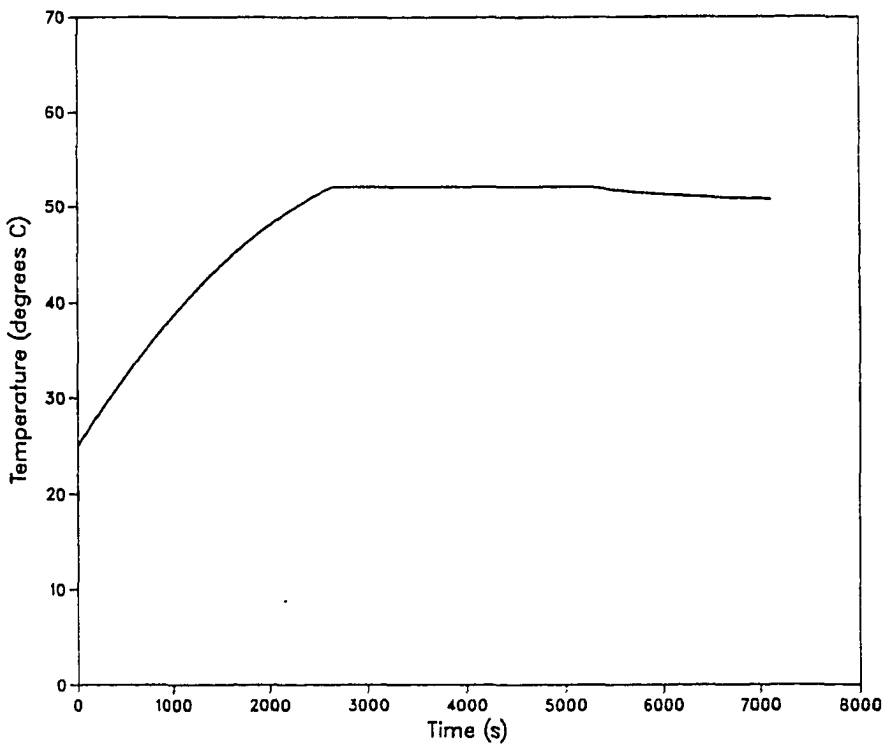

Figure 5.1: Optimal temperature profile (example 1)

Reproduced with permission of the copyright owner. Further reproduction prohibited without permission.

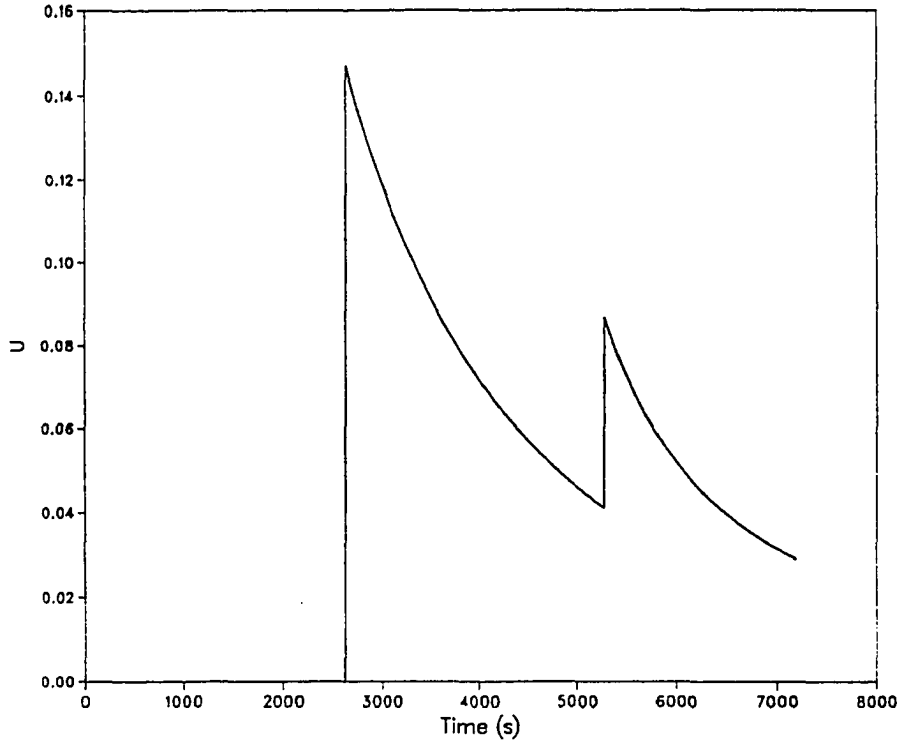

Figure 5.2: Optimal cooling rate profile (example 1)

Reproduced with permission of the copyright owner. Further reproduction prohibited without permission.

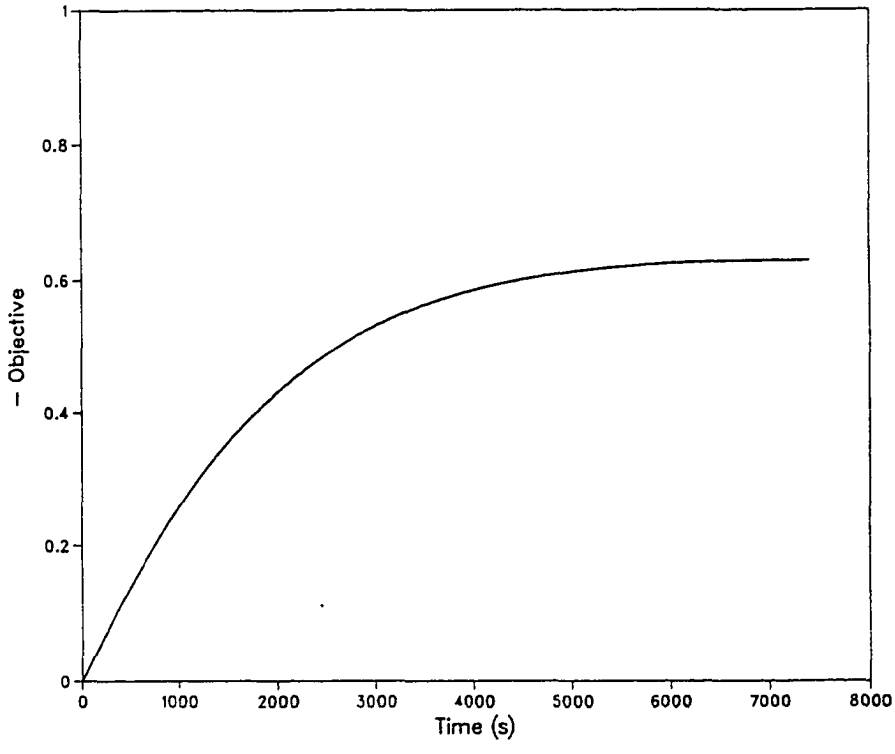

Figure 5.3: Profile of objective function (example 1)

Reproduced with permission of the copyright owner. Further reproduction prohibited without permission.

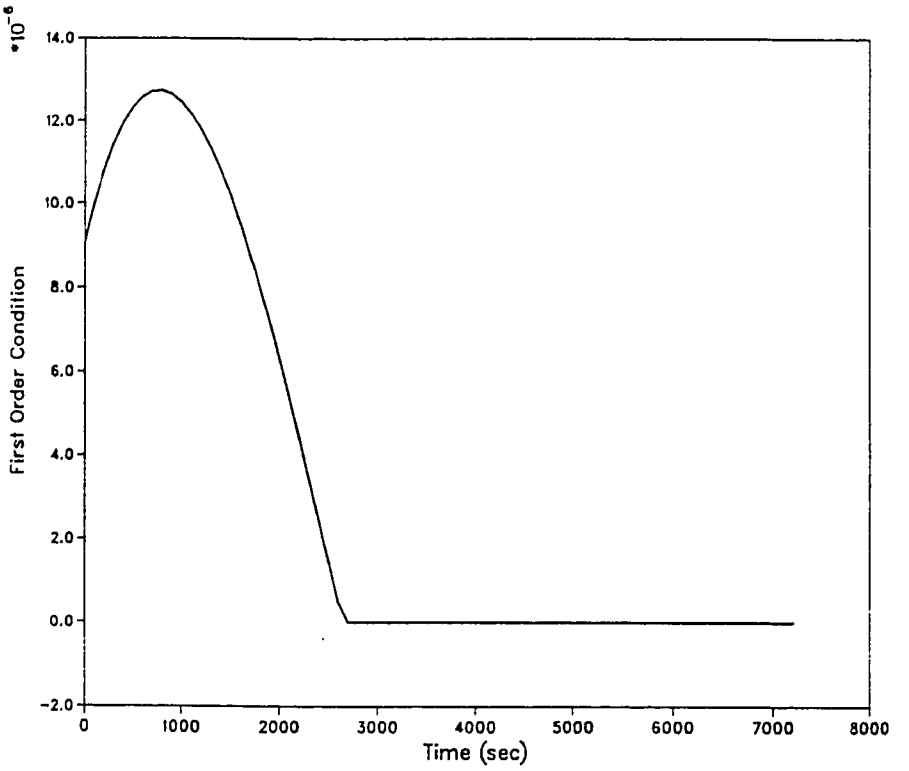

Figure 5.4: First order condition (example 1)

Reproduced with permission of the copyright owner. Further reproduction prohibited without permission.

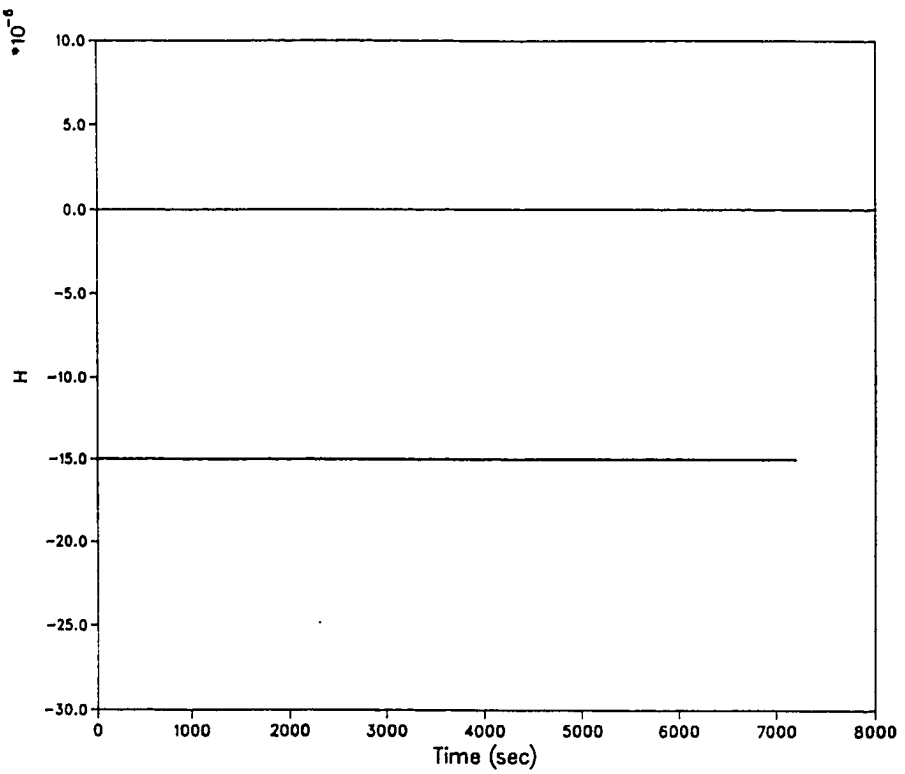

Figure 5.5: Hamiltonian (example 1)

Reproduced with permission of the copyright owner. Further reproduction prohibited without permission.

Constrained Optimization
Switching time to constrained arc: 2630 s
Switching time to singular arc: 5280 s
Final time: 7170 s
Objective function at final time: - 0.629 $kg.m^{-3}$
Unconstrained Optimization
Switching time to singular arc: 4630 s
Final time: 6750 s
Objective function at final time: - 0.629 $kg.m^{-3}$

Table 5.3: Constrained vs. Unconstrained Optimization (example 1)

function takes a longer time to reach its optimum value when the state constraint is present. The robustness of the control law to errors in the kinetic parameters was tested. In the control law, the values of the parameters k_{10} and k_{20} used were 10 % lower than those of the system parameters shown in Table 5.1. The results are summarized in Table 5.4. It is observed that the performance index is very close to that obtained in the nominal case, where the true values of the parameters were used in the control law.

Reproduced with permission of the copyright owner. Further reproduction prohibited without permission.

Parameters in Control Law	Parameters in Process	Performance Index
$k_{10} = 1.0,\ k_{20} = 100.0$	$k_{10} = 1.0,\ k_{20} = 100.0$	- 0.6296 $kg.m^{-3}$
All other parameter	All other parameter	
values from Table 5.1	values from Table 5.1	
$k_{10} = 0.9,\ k_{20} = 90.0$	$k_{10} = 1.0,\ k_{20} = 100.0$	- 0.6295 $kg.m^{-3}$
All other parameter	All other parameter	
values from Table 5.1	values from Table 5.1	

Table 5.4: Robustness Analysis (example 1)

5.5.2 Example 2

Consider the following lysine fermentation model proposed by Ohno *et al.* [1976]:

$$\frac{d}{dt}\begin{bmatrix} X.V \\ S.V \\ P.V \\ V \end{bmatrix} = \begin{bmatrix} \mu(S)X.V \\ -\frac{\mu}{Y}X.V \\ \pi(S)X.V \\ 0 \end{bmatrix} + \begin{bmatrix} 0 \\ s_F \\ 0 \\ 1 \end{bmatrix} u \tag{5.42}$$

where $\mu(S)$ and $\pi(S)$ have the following functionality:

$$\begin{aligned} \mu(S) &= \mu_m S \\ \pi(S) &= -k_1\mu_m^2 S^2 + k_2\mu_m S \end{aligned} \tag{5.43}$$

Furthermore, there is a scalar inequality constraint:

$$V - V_{max} \leq 0 \tag{5.44}$$

The objective function to be minimized at a free final time is:

$$J = -[(P.V) - \epsilon t]_{t=t_f} \tag{5.45}$$

Reproduced with permission of the copyright owner. Further reproduction prohibited without permission.

It can be easily shown that X, S, and V are algebraically related by:

$$\left(\frac{XV}{Y}+SV\right)-\left(\frac{X(0)V(0)}{Y}+S(0)V(0)\right) = s_F(V-V(0)) \tag{5.46}$$

Thus there are only three independent equations. Defining:

$$\begin{aligned} x_1 &= X.V \\ x_2 &= P.V \\ x_3 &= V \end{aligned} \tag{5.47}$$

and eliminating S from equation (5.46):

$$S = s_F - \frac{1}{Y}\left(\frac{x_1 - X(0)V(0)}{x_3}\right) + \left(\frac{S(0)V(0) - s_F V(0)}{x_3}\right) \tag{5.48}$$

the model can be put in the form:

$$\dot{x} = f(x) + g(x)u \tag{5.49}$$

where

$$x = \begin{bmatrix} x_1 \\ x_2 \\ x_3 \end{bmatrix}$$

$$f(x) = \begin{bmatrix} \hat{\mu}x_1 \\ \hat{\pi}x_1 \\ 0 \end{bmatrix}$$

$$g(x) = \begin{bmatrix} 0 \\ 0 \\ 1 \end{bmatrix} u$$

where $\hat{\mu}$ and $\hat{\pi}$ are obtained by substituting S from (5.48) into the expressions for μ and π (equation (5.43)) It can be easily shown that $n = 3$ and $s = 1$. From

Reproduced with permission of the copyright owner. Further reproduction prohibited without permission.

equation (5.14), the optimal static state feedback is given by:

$$u = -\frac{det\left[g(x) \vdots ad_f^1 g(x) \vdots ad_f^2 g(x)\right]}{det[g(x) \vdots ad_f^1 g(x) \vdots [g, ad_f^1 g](x)]} \tag{5.50}$$

Since the fermentor starts with a high substrate concentration, there is an initial non-singular phase where no substrate is fed, followed by a singular phase which involves substrate feeding. An initial estimate of the switching time to the singular region was found by performing a one-dimensional numerical search as described by Lim *et al.* (1986). This estimate was further refined till the first order condition $\lambda^T g(x) = 0$ was satisfied on the singular region. When the volume constraint is hit, $u = 0$. The final time, t_f, is determined when the objective function, ϕ reaches its optimum value. Figures 5.6 and 5.7 show the optimal input profile and the profile of the objective function for the model parameters in Table 5.5 and the initial conditions in Table 5.6. The various switching times and the objective function at the final time are shown in Table 5.7. Figures 5.8 and 5.9 show the time profile of the first order condition $\lambda^T g(x)$ and the second order condition $-\lambda^T [g, ad_f^1 g](x)$. It is observed that the switching function vanishes on the singular time interval and is positive in the initial non-singular region. The positivity of the switching function is consistent with $u(t)$ taking its minimum value ($u = 0$) in the non-singular interval. Furthermore, the second order condition $-\lambda^T [g, ad_f^1 g](x) \geq 0$ is satisfied in the singular region and so the singular extremal is indeed optimal. Figure 5.10 shows the time profile of the Hamiltonian H and it is observed that indeed $\left(\frac{\partial \phi}{\partial t} + H\right)_{t=t_f} = 0$.

The sensitivity of the performance index to errors in the switching time to the singular region was checked. Assuming various values of the switching time to the singular region, the feeding profile was calculated using the static state feedback law in the singular region. When the volume constraint was hit, u was set to zero. The final time, t_f, was determined when the objective function, ϕ reached its optimum

Reproduced with permission of the copyright owner. Further reproduction prohibited without permission.

μ_m	0.125 hr^{-1}
k_1	384.0 $(k\bar{g}\ product).(kg\ cells)^{-1}.hr$
k_2	134.0 $(kg\ product).(kg\ cells)^{-1}$
s_F	2.8 $kg.kg^{-1}$
Y	0.135 $(kg\ cell\ mass).(kg\ substrate)^{-1}$
ϵ	10.0 $kg.hr^{-1}$
V_{max}	20.0 x 10^{-3} m^3

Table 5.5: Model Parameters (example 2)

$X(0)$	0.1 $kg.m^{-3}$
$S(0)$	14.0 $kg.kg^{-1}$
$P(0)$	0.0 $kg.m^{-3}$
$V(0)$	5.0 x 10^{-3} m^{-3}

Table 5.6: Initial Conditions (example 2)

Switching time to singular arc: 8.85 h
Switching time to constrained arc: 26.00 h
Final time: 31.70 h
Objective function at final time: - 365.37 x 10^{-3} kg

Table 5.7: Constrained Optimization (example 2)

Reproduced with permission of the copyright owner. Further reproduction prohibited without permission.

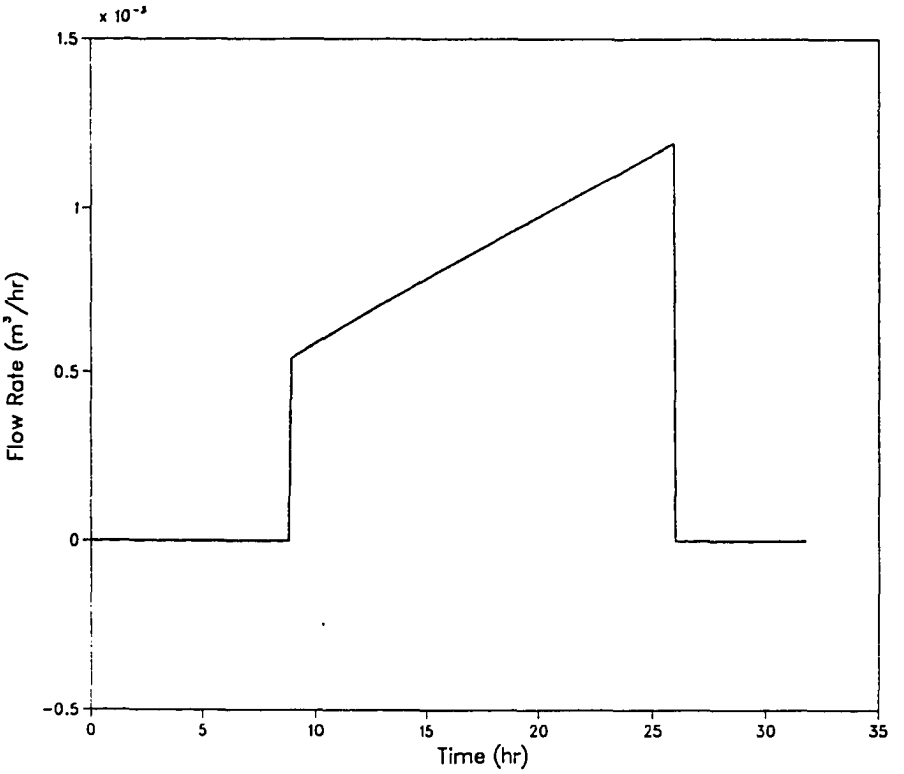

Figure 5.6: Optimal input profile (example 2)

Reproduced with permission of the copyright owner. Further reproduction prohibited without permission.

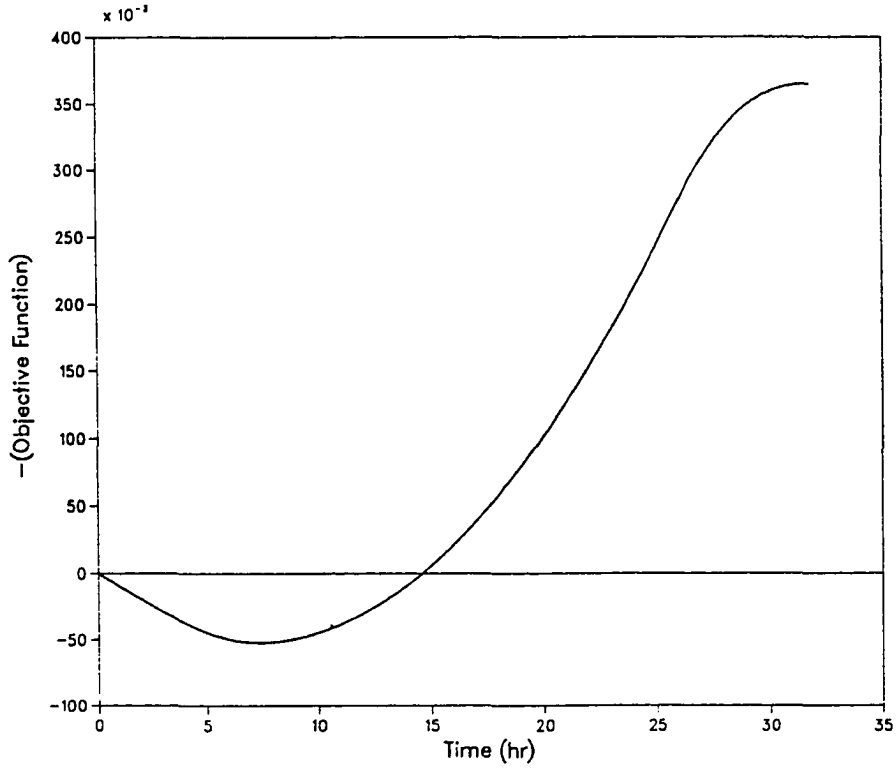

Figure 5.7: Profile of objective function (example 2)

Reproduced with permission of the copyright owner. Further reproduction prohibited without permission.

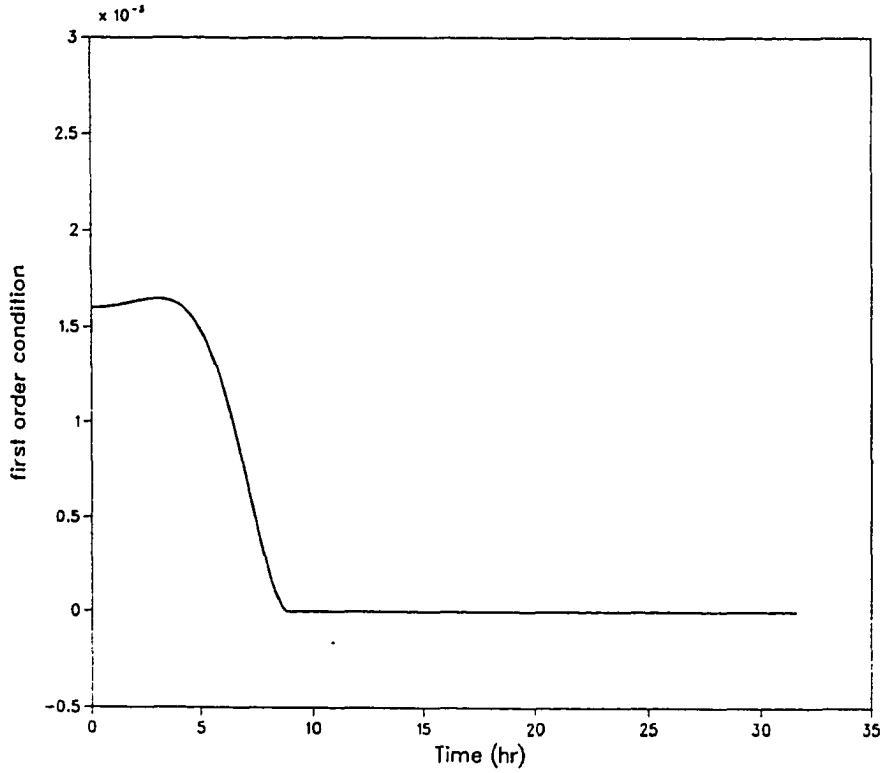

Figure 5.8: First order condition (example 2)

Reproduced with permission of the copyright owner. Further reproduction prohibited without permission.

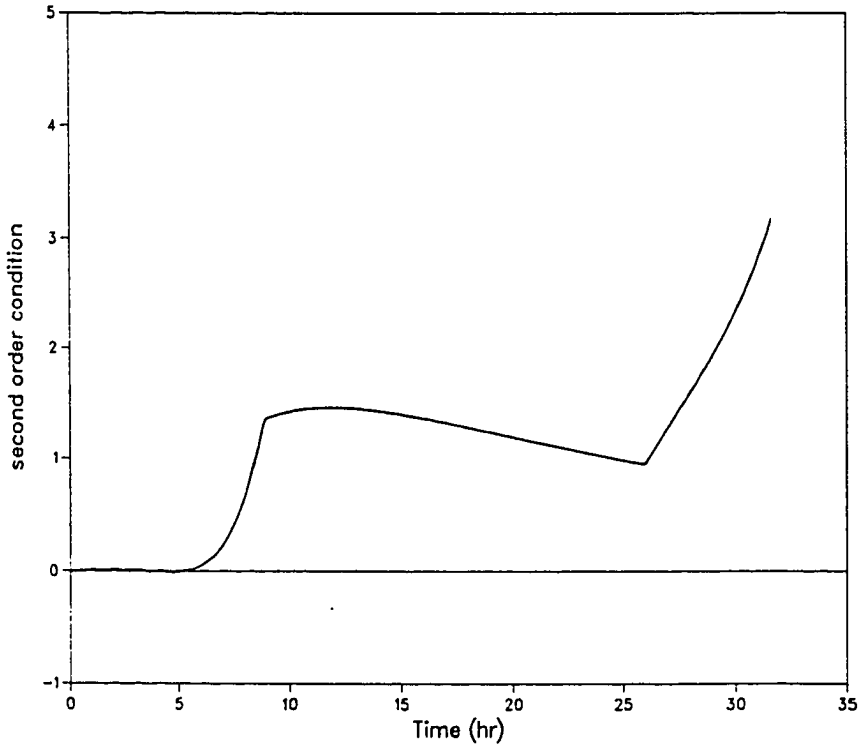

Figure 5.9: Second order condition (example 2)

Reproduced with permission of the copyright owner. Further reproduction prohibited without permission.

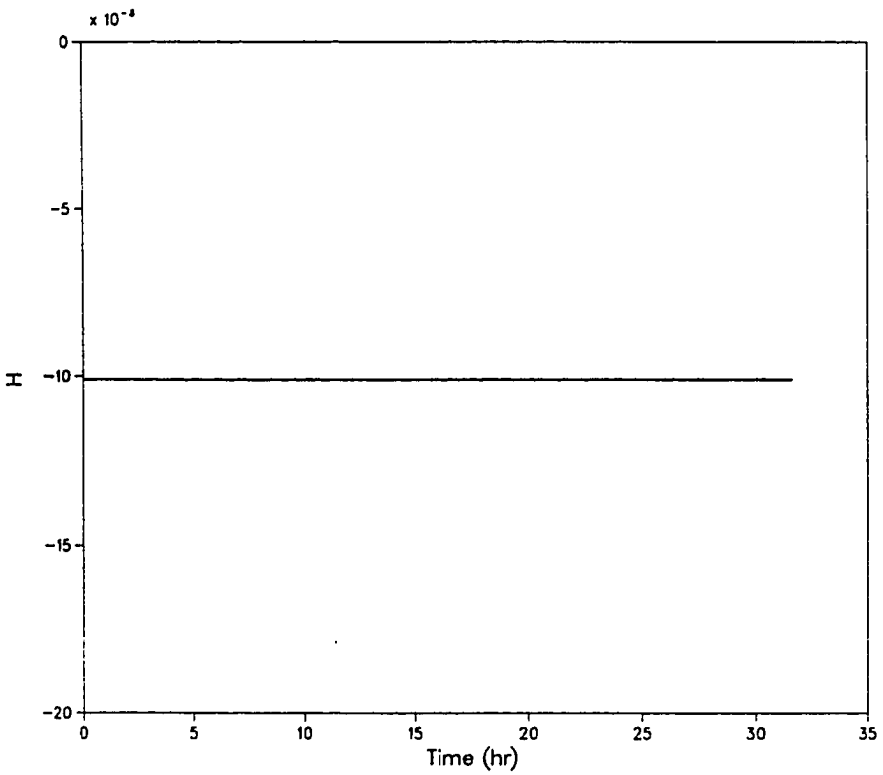

Figure 5.10: Hamiltonian (example 2)

Reproduced with permission of the copyright owner. Further reproduction prohibited without permission.

Assumed Switching Time (hr)	Performance Index (kg)	Final time (hr)
8.50	-364.244 x 10^{-3}	31.00
8.85	-365.379 x 10^{-3}	31.70
9.00	-365.370 x 10^{-3}	32.10
9.50	-364.356 x 10^{-3}	33.50

Table 5.8: Sensitivity of error in switching time on performance index

value. The results are shown in Table 5.8. It is observed that the final performance index is quite robust to errors in the assumed switching time. From this study we conclude that the performance index is not very sensitive to errors in the switching time and so an *a priori* estimate of the switching time can be used in closed-loop implementation.

5.5.3 Example 3

We consider a yield optimization problem in a semi-batch chemical reactor where the following reactions are occuring:

$$A \rightarrow B$$

$$B \rightarrow C$$

$$A \rightarrow D$$

The reaction from A to B follows the following kinetics:

$$-r = \frac{k_1 C_A . C_B}{k_2 + k_3 C_A + k_4 C_A^2} \tag{5.51}$$

Reproduced with permission of the copyright owner. Further reproduction prohibited without permission.

All other reactions are first order reactions. The unsteady state mass balance equations are given by:

$$\begin{aligned}
\frac{d(C_A.V)}{dt} &= -\frac{k_1 C_A.C_B.V}{k_2 + k_3 C_A + k_4 C_A^2} - k_D C_A.V + C_{AF}.u \\
\frac{d(C_B.V)}{dt} &= \frac{k_1 C_A.C_B.V}{k_2 + k_3 C_A + k_4 C_A^2} - k_C C_B.V \\
\frac{d(C_D.V)}{dt} &= k_D C_A.V \\
\frac{dV}{dt} &= u
\end{aligned} \tag{5.52}$$

Furthermore, there is a scalar inequality constraint:

$$V - V_{max} \leq 0 \tag{5.53}$$

We will consider two different objective functions.

Case I: (Objective function independent of the final time)

The objective function to be minimized at a free final time is:

$$J = -C_B.V|_{t=t_f} \tag{5.54}$$

Case II: (Objective function dependent on the final time)

The objective function to be minimized at a free final time is:

$$J = -[C_B.V - \epsilon t_f] \tag{5.55}$$

Define:

$$\begin{aligned}
x_1 &= C_A.V \\
x_2 &= C_B.V \\
x_3 &= C_D.V \\
x_4 &= V
\end{aligned} \tag{5.56}$$

Reproduced with permission of the copyright owner. Further reproduction prohibited without permission.

The model can be put in the form:

$$\frac{d}{dt}\begin{bmatrix} x_1 \\ x_2 \\ x_3 \\ x_4 \end{bmatrix} = \begin{bmatrix} -\dfrac{k_1 x_1 x_2 x_4}{k_2 x_4^2 + k_3 x_1 x_4 + k_4 x_1^2} - k_D x_1 \\ \dfrac{k_1 x_1 x_2 x_4}{k_2 x_4^2 + k_3 x_1 x_4 + k_4 x_1^2} - k_C x_2 \\ k_D x_1 \\ 0 \end{bmatrix} + \begin{bmatrix} C_{AF} \\ 0 \\ 0 \\ 1 \end{bmatrix} u \qquad (5.57)$$

The system model is of the form:

$$\dot{x} = f(x) + g(x)u \qquad (5.58)$$

where:

$$x = \begin{bmatrix} x_1 \\ x_2 \\ x_3 \\ x_4 \end{bmatrix}$$

$$f(x) = \begin{bmatrix} -\dfrac{k_1 x_1 x_2 x_4}{k_2 x_4^2 + k_3 x_1 x_4 + k_4 x_1^2} - k_D x_1 \\ \dfrac{k_1 x_1 x_2 x_4}{k_2 x_4^2 + k_3 x_1 x_4 + k_4 x_1^2} - k_C x_2 \\ k_D x_1 \\ 0 \end{bmatrix}$$

$$g(x) = \begin{bmatrix} C_{AF} \\ 0 \\ 0 \\ 1 \end{bmatrix}$$

It can be easily shown that for this system $n = 4$ and $s = 1$.

Solution for Case I:

It is observed that ϕ, f, g are independent of t. Furthermore, $f(x)$, $g(x)$, $ad_f^1 g(x)$,

Reproduced with permission of the copyright owner. Further reproduction prohibited without permission.

and $ad_f^2 g(x)$ are linearly independent. Thus, from equation (5.15), the optimal static state feedback is given by:

$$u = - \frac{det\left[f(x) \,|\, g(x) \,|\, ad_f^1 g(x) \,|\, ad_f^2 g(x)\right]}{det[f(x) \,|\, g(x) \,|\, ad_f^1 g(x) \,|\, [g, ad_f^1 g](x)]} \tag{5.59}$$

Since the reactor starts with a high concentration of A and the reaction rate is a decreasing function of A we expect that there will be an initial non-singular phase where no A is fed so that the concentration of A decreases, followed by a singular phase which involves feeding of species A. An initial estimate of the switching time was found by performing a one dimensional numerical search as described by Lim *et al.* (1986). This estimate was further refined till the first order condition $\lambda^T g(x) = 0$ was satisfied on the singular region. When the volume constraint is hit, $u = 0$. The final time, t_f, is determined when the objective function, ϕ reaches its optimum value.

Figures 5.11 and 5.12 show the optimal input profile and the profile of the objective function for the system parameters in Table 5.9 and the initial conditions in Table 5.10. The various switching times and the objective function at the final time are shown in Table Table 5.11. Figures 5.13 and 5.14 depict the corresponding time profiles of the switching function ($\lambda^T g(x)$) and the second order condition ($-\lambda^T [g, ad_f^1 g](x)$). The switching function vanishes on the singular time interval and is positive everywhere else. The positivity of the switching function is consistent with $u(t)$ taking its minimum value ($u = 0$) in the non-singular interval. Furthermore, the second order condition $-\lambda^T [g, ad_f^1 g](x,t) \geq 0$ is satisfied in the singular region and so the singular extremal is indeed optimal. The final time, t_f, is determined when the objective function, ϕ reaches its optimum value. Figure 5.15 shows the time profile of the Hamiltonian H. It is observed that $H = 0$ everywhere.

The robustness of the dynamic state feedback law with respect to errors in the

Reproduced with permission of the copyright owner. Further reproduction prohibited without permission.

k_1	0.530 $m^3/kmoles/hr$
k_2	1.00
k_3	1.00 $m^3/kmoles$
k_4	1/22 $m^3/kmoles^2$
k_C	0.01 $1/hr$
k_D	0.01 $1/hr$
ϵ	2.0

Table 5.9: Model Parameters (example 3)

$C_A(0)$	7.5 kg/m^3
$C_B(0)$	8.0 kg/m^3
$C_D(0)$	0.0 kg/m^3
$V(0)$	2.0 x 10^{-3} m^3

Table 5.10: Initial Conditions (example 3)

Switching time to singular arc: 0.793 h
Switching time to constrained arc: 1.86 h
Final time: 3.39 h
Objective function at final time: -44.810 x 10^{-3} kg

Table 5.11: Constrained Optimization (example 3, Case I)

Reproduced with permission of the copyright owner. Further reproduction prohibited without permission.

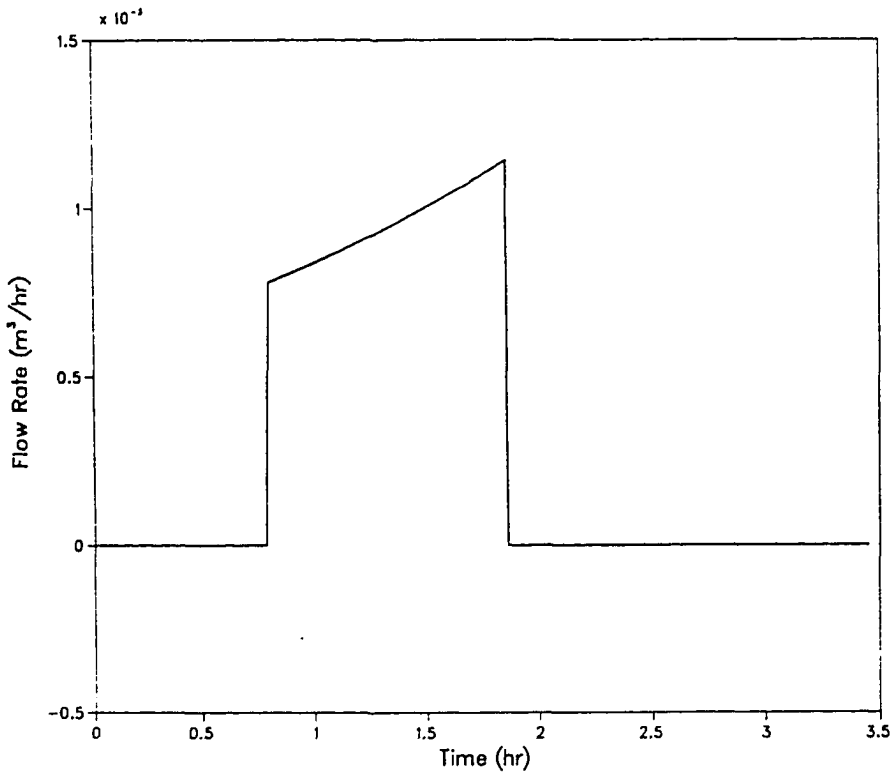

Figure 5.11: Optimal input profile (example 3, Case I)

Reproduced with permission of the copyright owner. Further reproduction prohibited without permission.

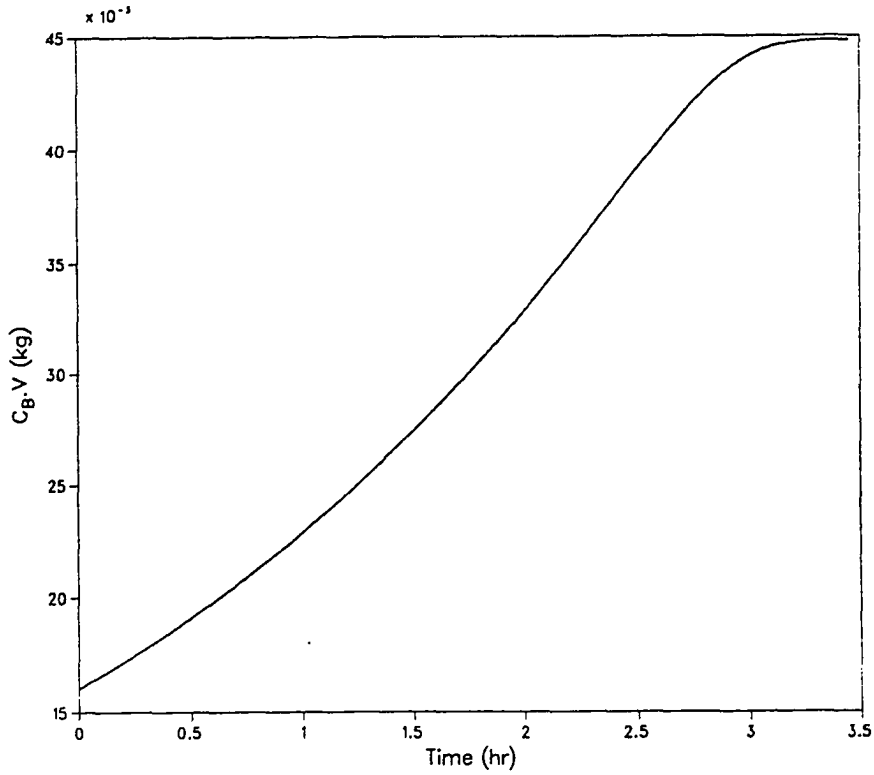

Figure 5.12: Profile of objective function (example 3, Case I)

Reproduced with permission of the copyright owner. Further reproduction prohibited without permission.

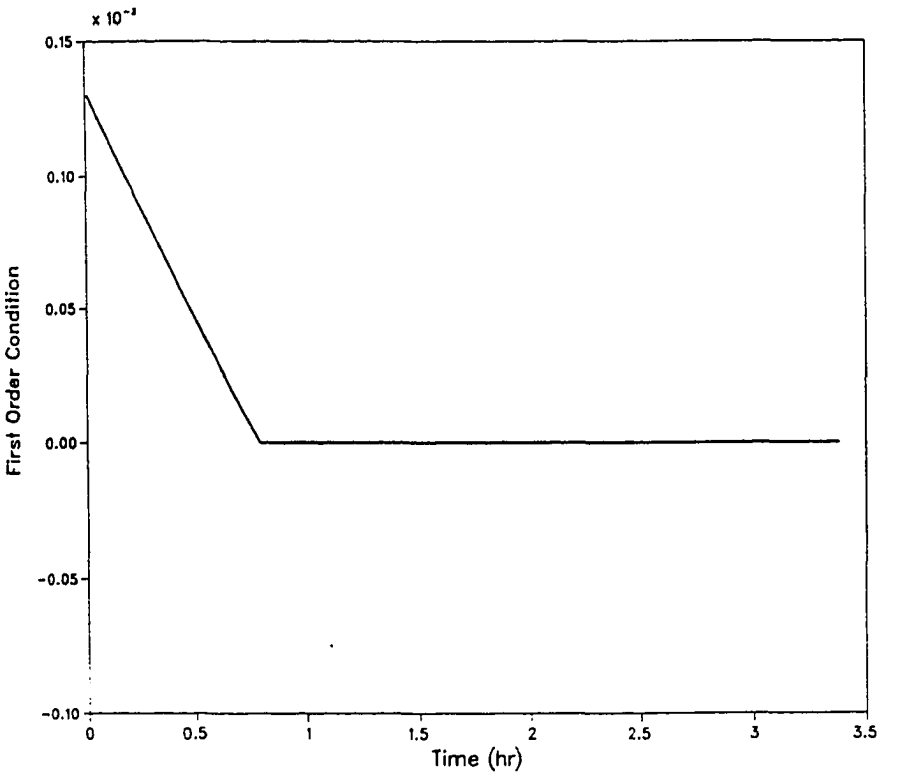

Figure 5.13: First order condition (example 3, Case I)

Reproduced with permission of the copyright owner. Further reproduction prohibited without permission.

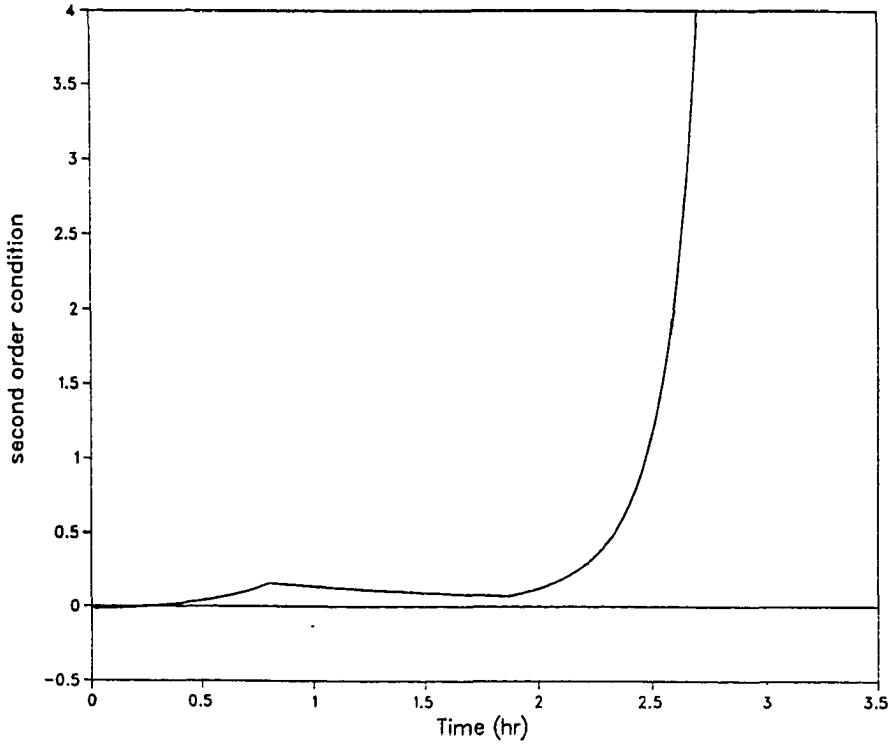

Figure 5.14: Second order condition (example 3, Case I)

Reproduced with permission of the copyright owner. Further reproduction prohibited without permission.

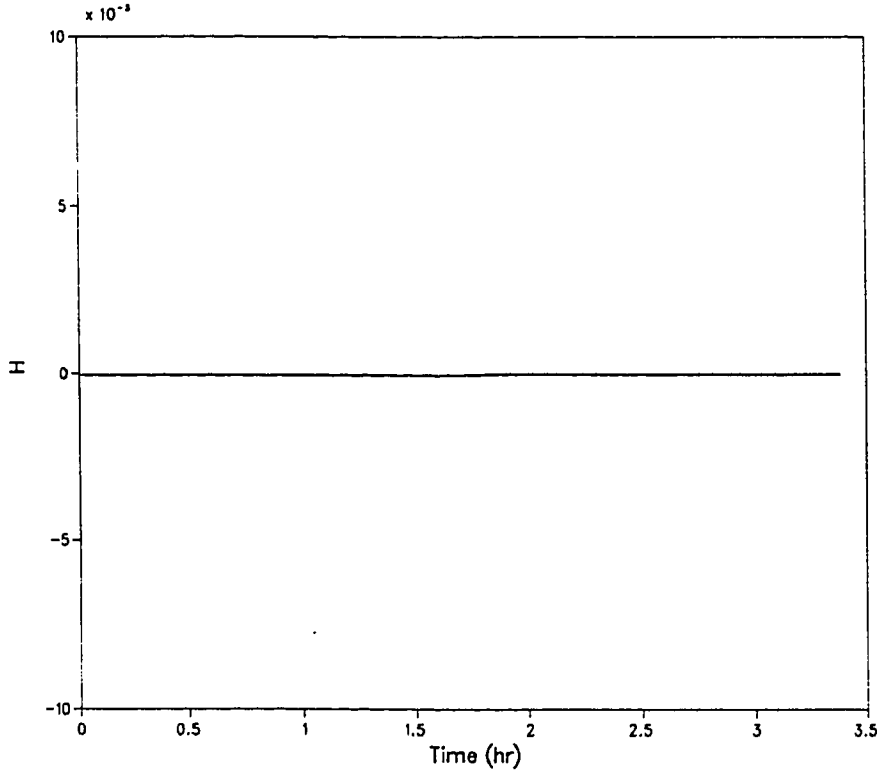

Figure 5.15: Hamiltonian (example 3, Case I)

Reproduced with permission of the copyright owner. Further reproduction prohibited without permission.

Parameters in Control Law	Parameters in Process	Performance Index
$k_1 = 0.530$	$k_1 = 0.530$	-44.810 x 10^{-3} kg
All other parameter	All other parameter	
values from Table 5.9	values from Table 5.9	
$k_1 = 0.600$	$k_1 = 0.530$	-44.718 x 10^{-3} kg
All other parameter	All other parameter	
values from Table 5.9	values from Table 5.9	

Table 5.12: Robustness Analysis

system parameter k_1 was tested. With the switching time from the nominal case, the static feedback law was implemented using a 13.4 % higher k_1 than its true value. The results are summarized in Table 5.12. It is observed that the performance index is very close to that obtained in the nominal case.

The sensitivity of the performance index to errors in the switching time to the singular region was checked. Assuming various values of the switching time to the singular region, the feeding profile was calculated using the static state feedback law in the singular region. When the volume constraint was hit, u was set to zero. The final time, t_f, was determined when the objective function, ϕ reached its optimum value. The results are shown in Table 5.13. It is observed that the final performance index is quite robust to errors in the assumed switching time. From this study we conclude that the performance index is not very sensitive to errors in the switching time and so an *a priori* estimate of the switching time can be used in closed-loop implementation.

Solution for Case II:

Reproduced with permission of the copyright owner. Further reproduction prohibited without permission.

Assumed Switching Time (hr)	Performance Index (kg)	Final Time (hr)
0.75	-44.676 x 10^{-3}	3.31
0.791	-44.810 x 10^{-3}	3.39
0.85	-44.760 x 10^{-3}	3.39
0.90	-44.720 x 10^{-3}	3.39

Table 5.13: Sensitivity of error in initial condition of $u(t)$ on performance index

It can be easily verified that the vector fields $g(x)$, $ad_f^1 g(x)$, $ad_f^2 g(x)$, $ad_f^3 g(x)$ are linearly independent. Thus the optimal state feedback in the singular region will be dynamic. Substituting $n = 4$ and $s = 1$ in equation (5.17) we obtain a dynamic feedback law by setting the determinant of:

$$\begin{aligned} & g(x) \\ & ad_f^1 g(x) \\ & ad_f^2 g(x) + [g, ad_f^1 g](x)u \\ & ad_f^3 g(x) + \left([g, ad_f^2 g](x) + [f, [g, ad_f^1 g]](x) + [g, [g, ad_f^1 g](x)u\right) u + [g, ad_f^1 g](x)\frac{du}{dt} \end{aligned} \tag{5.60}$$

equal to zero.

Figures 5.16 and 5.17 show the optimal input profile and the profile of the objective function for the system parameters in Table 5.9 and the initial conditions in Table 5.10. The various switching times and the objective function at the final time are shown in Table 5.14. Figures 5.18 and 5.19 depict the corresponding time profiles of the switching function ($\lambda^T g(x)$) and the second order condition ($-\lambda^T [g, ad_f^1 g](x)$). The switching function vanishes on the singular time interval and is positive everywhere else. The positivity of the switching function is consistent with $u(t)$ taking its minimum value ($u = 0$) in the non-singular interval. Furthermore, the second

Reproduced with permission of the copyright owner. Further reproduction prohibited without permission.

Switching time to singular arc:0.793 h
Switching time to constrained arc:1.86 h
Final time: 3.19 h
Objective function at final time: -38.3 x 10^{-3} kg

Table 5.14: Constrained Optimization (example 3, Case II)

Assumed Initial Condition of $u(t)$	Performance Index (kg)
0.60	-38.3 x 10^{-3}
0.75	-38.3 x 10^{-3}
0.90	-38.3 x 10^{-3}

Table 5.15: Sensitivity of error in initial condition of $u(t)$ on performance index

order condition $-\lambda^T[g, ad_f^1 g](x,t) \geq 0$ is satisfied in the singular region and so the singular extremal is indeed optimal. The final time, t_f, is determined when the objective function, ϕ reaches its optimum value. Figure 5.20 shows the time profile of the Hamiltonian H. It is observed that indeed $\left(\frac{\partial \phi}{\partial t} + H\right)_{t=t_f} = 0$.

Since the optimal state feedback is dynamic, we need the initial condition of u to implement the state feedback law. The effect of error in the initial conditon of u on the final performance index was studied. The results are shown in Table 5.15. It is observed that the final performance index is very robust to errors in the assumed initial condition for $u(t)$. From this study we conclude that the performance index is not sensitive at all to errors in the initial condition for $u(t)$ and so an *a priori* estimate of the initial condition for $u(t)$ can be used in closed-loop implementation.

The robustness of the dynamic state feedback law with respect to errors in the

Reproduced with permission of the copyright owner. Further reproduction prohibited without permission.

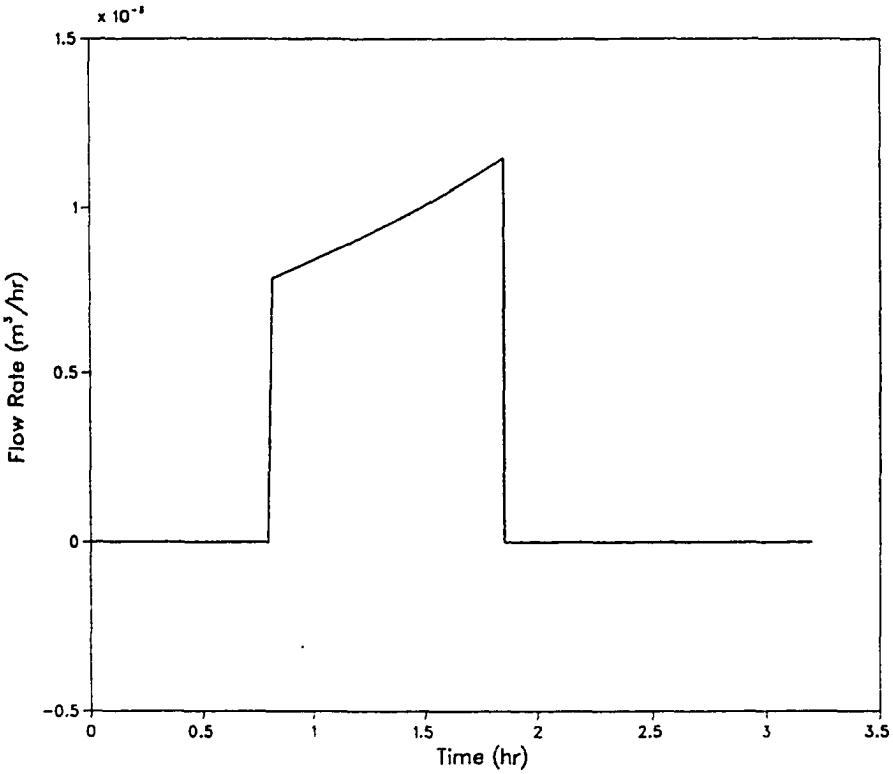

Figure 5.16: Optimal input profile (example 3, Case II)

Reproduced with permission of the copyright owner. Further reproduction prohibited without permission.

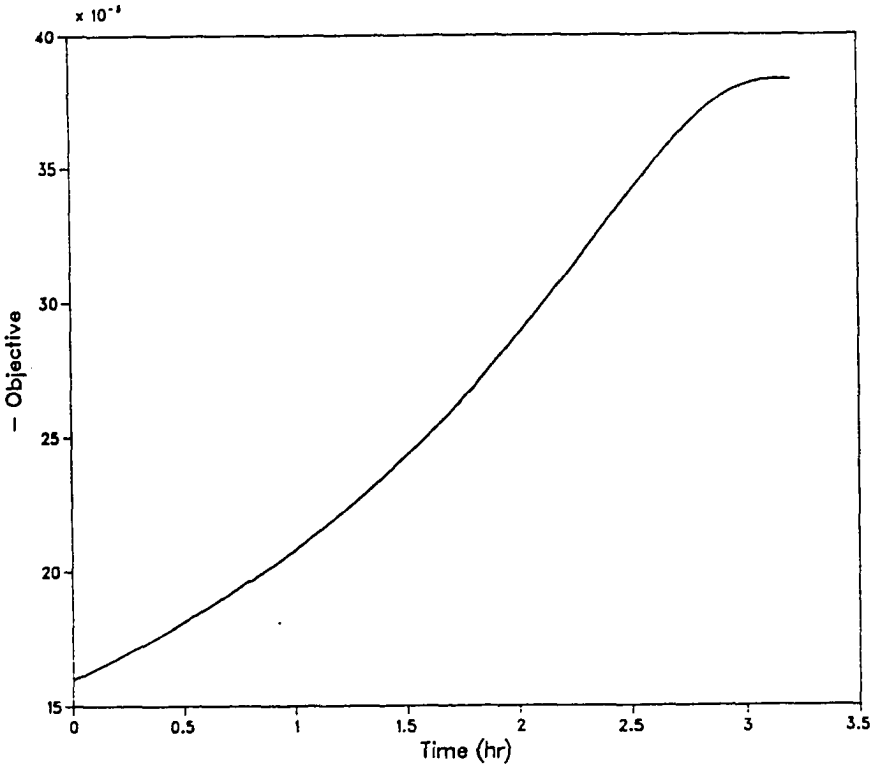

Figure 5.17: Profile of objective function (example 3, Case II)

Reproduced with permission of the copyright owner. Further reproduction prohibited without permission.

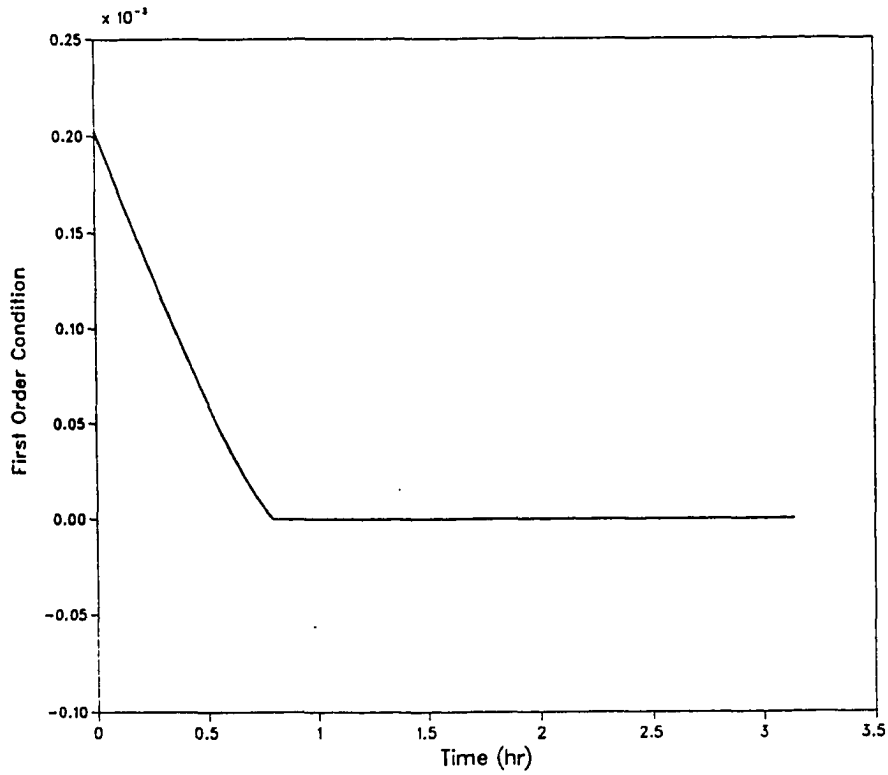

Figure 5.18: First order condition (example 3, Case II)

Reproduced with permission of the copyright owner. Further reproduction prohibited without permission.

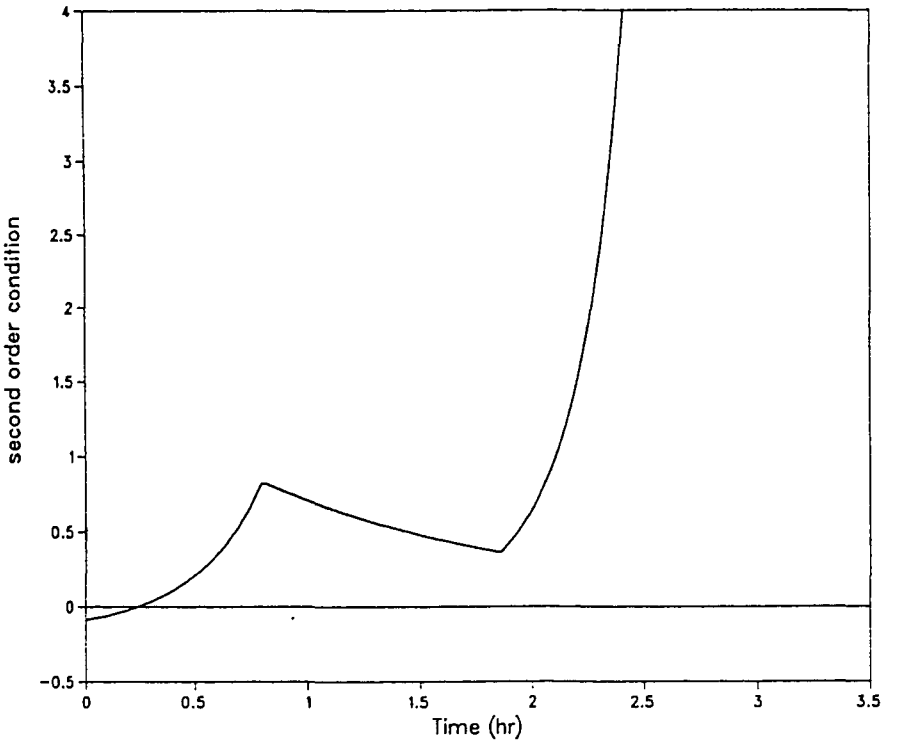

Figure 5.19: Second order condition (example 3, Case II)

Reproduced with permission of the copyright owner. Further reproduction prohibited without permission.

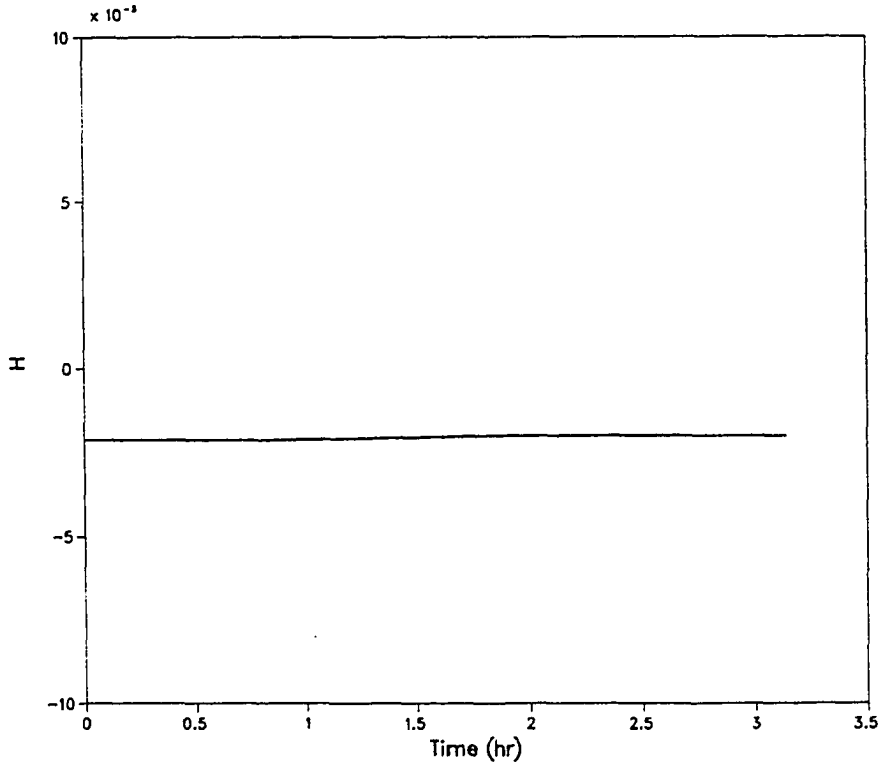

Figure 5.20: Hamiltonian (example 3, Case II)

Reproduced with permission of the copyright owner. Further reproduction prohibited without permission.

Parameters in Control Law	Parameters in Process	Performance Index
$k_1 = 0.530$ All other parameter values from Table 5.9	$k_1 = 0.530$ All other parameter values from Table 5.9	-38.3 x 10^{-3} kg
$k_1 = 0.56$ All other parameter values from Table 5.9	$k_1 = 0.530$ All other parameter values from Table 5.9	-38.3 x 10^{-3} kg
$k_1 = 0.59$ All other parameter values from Table 5.9	$k_1 = 0.530$ All other parameter values from Table 5.9	-38.3 x 10^{-3} kg

Table 5.16: Robustness Analysis

system parameter k_1 was tested. The results are summarized in Table 5.16. It is observed that the performance index is very close to that obtained in the nominal case.

Reproduced with permission of the copyright owner. Further reproduction prohibited without permission.

5.6 Nomenclature

C_A = concentration of species A, kg/m^3

C_B = concentration of species B, kg/m^3

C_C = concentration of species C, kg/m^3

C_D = concentration of species D, kg/m^3

C_p = specific heat

E_1, E_2 = activation energies, $Joules/mole/K$

H = Hamiltonian

H_u = first derivative of Hamiltonian with respect to u

H_{uu} = second derivative of Hamiltonian with respect to u

I = identity matrix

J = performance index

P = product concentration , kg/m^3

S = substrate concentration , kg/m^3

T = temperature , K

V = volume, m^3

X = cell mass concentration , kg/m^3

Y = yield coefficient, *kg cell mass/kg substrate*

Reproduced with permission of the copyright owner. Further reproduction prohibited without permission.

det = determinant

f = vector function in dynamic model

g = vector function in dynamic model

k_1 = kinetic rate constant

k_2 = kinetic rate constant

k_3 = kinetic rate constant

k_4 = kinetic rate constant

k_B = kinetic rate constant of reaction $A \rightarrow B$, $1/hr$

k_C = kinetic rate constant of reaction $B \rightarrow C$, $1/hr$

k_D = kinetic rate constant of reaction $A \rightarrow D$, $1/hr$

n = number of state equations (dimension of state vector x)

s = degree of singularity

s_F = concentration of feed, kg/m^3

t = time

t_f = final time, hr

u = manipulated input

x = vector of system states

y = output

Reproduced with permission of the copyright owner. Further reproduction prohibited without permission.

Greek Symbols

β = adjustable parameter

λ = vector of adjoint-states

μ = specific growth rate, $1/hr$

μ_m = kinetic parameter in rate expression (47), $1/hr$

ϕ = scalar function expressing the performance index in terms of the system states

ρ = density, kg/m^3

Reproduced with permission of the copyright owner. Further reproduction prohibited without permission.

CHAPTER VI

REGULATION OF TIME-VARYING SYSTEMS

The difficulties of the slopes we have overcome.

Now we have to face the difficulties of the valleys.

Bertold Brecht

6.1 Introduction

In chapters IV and V it was shown that under certain conditions, end-point optimization of a time-varying system was equivalent to *regulation* of a time-varying system. This chapter deals with the general problem of synthesizing nonlinear feedback laws for regulation of time-varying systems.

Recently, there have been major developments in the nonlinear systems theory literature using techniques from differential geometry (see Isidori, 1989). Some of the most important results in the area include solutions of problems of invertibility (Hirschorn, 1979a,b), exact state-space linearization (Jakubesyk and Respondek, 1980; Su, 1982; Hunt *et al.*, 1983 a, b; and input/output linearization (Claude *et al.*, 1983; Isidori and Ruberti, 1984; Kravaris and Chung 1987). These developments have been motivated by the geometric approach of linear systems theory (Wonham, 1979). There has been considerable effort to design controllers so that the closed-loop

Reproduced with permission of the copyright owner. Further reproduction prohibited without permission.

response is exactly linear in a global sense. For instance, Kravaris and Chung (1987) provided explicit formulae that made the input/output behavior of the closed loop system exactly linear in the case of *time-invariant* single-input-single-output (SISO) systems. They further showed that once such a state feedback law is applied to a nonlinear process, one can use an external linear controller for set point tracking and rejection of disturbances. Daoutidis and Kravaris (1992) synthesized dynamic output feedback controllers for minimum-phase nonlinear *time-invariant* processes.

In this chapter this methodology is extended to time-varying single-input-single output (SISO) systems. SISO systems of the following type are considered:

$$\begin{aligned} \dot{x} &= f(x,t) + g(x,t)u \\ y &= h(x,t) \end{aligned} \tag{6.1}$$

where f and g are C^∞ vector fields in $\mathbb{R}^n$ x $\mathbb{R}$, h is a C^∞ scalar field on $\mathbb{R}^n$ x $\mathbb{R}$, and $u \in \mathbb{R}$. Note that the regulation problems posed in chapters IV and V can be described by equation 6.1.

First, modified Lie derivatives are defined to account for the explicit time dependence of the system model on time. The relative order of the time-varying system is defined. Zero dynamics in time-varying systems are calculated to characterize system stability. State feedback laws are synthesized which provide a linear time-invariant input-output response. Internal stability results under state feedback are provided. Then, a dynamic output feedback controller for the time-varying system is synthesized and it is shown under what conditions the system possesses internal stablility. Finally the proposed methodology is illustrated through a simulation example.

Reproduced with permission of the copyright owner. Further reproduction prohibited without permission.

6.2 Mathematical Preliminaries

Differential geometry provides the necessary nonlinear analysis tools for nonlinear controller synthesis. The so-called *Lie algebra* is a nonlinear analog of matrix algebra and provides a compact way of representing a sequence of additions, multiplications and differentiations. Kravaris and Chung (1987) derived a static state feedback law for time invariant systems using the standard Lie derivative notation. However, this notation is inadequate for time-varying systems and modifications need to be made to this notation to explicitly account for the time variability of the model.

Modified Lie derivatives are defined as as follows:

$$\begin{aligned}
\overline{L}_f^0 h(x,t) &= h(x,t) \\
\overline{L}_f^1 h(x,t) &= < dh, f > (x,t) + \frac{\partial h}{\partial t}(x,t) \\
\overline{L}_f^2 h(x,t) &= < d\overline{L}_f^1 h, f > (x,t) + \frac{\partial}{\partial t}\overline{L}_f^1 h(x,t) \\
\overline{L}_f^3 h(x,t) &= < d\overline{L}_f^2 h, f > (x,t) + \frac{\partial}{\partial t}\overline{L}_f^2 h(x,t) \qquad (6.2) \\
&\cdot \\
&\cdot \\
\overline{L}_f^k h(x,t) &= < d\overline{L}_f^{k-1} h, f > (x,t) + \frac{\partial}{\partial t}\overline{L}_f^{k-1} h(x,t)
\end{aligned}$$

6.2.1 Relative Order

Definition 6.1: For a system of the form (6.1), the **relative order** of the output y with respect to the manipulated input u is the smallest integer r for which

$$L_g \overline{L}_f^{r-1} h(x,t) \neq 0 \qquad (6.3)$$

for *all* $t \in [t_o, \infty]$. If such an integer does not exist, we say that the system has an infinite relative order. Successive differentiations of the output with respect to time

Reproduced with permission of the copyright owner. Further reproduction prohibited without permission.

yield the following expressions:

$$\begin{aligned} y &= h(x,t) \\ \frac{dy}{dt} &= \overline{L}_f^1 h(x,t) \\ \frac{d^2y}{dt^2} &= \overline{L}_f^2 h(x,t) \\ &\cdot \\ &\cdot \\ \frac{d^{r-1}y}{dt^{r-1}} &= \overline{L}_f^{r-1} h(x,t) \\ \frac{d^ry}{dt^r} &= \overline{L}_f^r h(x,t) + (L_g \overline{L}_f^{r-1} h(x,t))u \end{aligned} \tag{6.4}$$

The reason for modifying the standard Lie derivative notation is obvious from the above expressions; successive differentiation of the output with respect to time upto the $(r-1)$th time derivative results in the generation of successive modified Lie derivatives of the system. Furthermore, it is clear that the relative order of the time-varying system is the smallest time derivative of the output with respect to time which depends explicitly on the input.

6.3 Zero Dynamics

In this section, we compute the zero dynamics of the time-varying system. These will be used later on to study the stability of the closed-loop system under input/output linearizing state feedback. Before the zero dynamics of the time-varying nonlinear system are computed, it is first necessary to provide a notion of linear independence for time-varying vector fields and scalar fields.

Reproduced with permission of the copyright owner. Further reproduction prohibited without permission.

6.3.1 Linear Independence of Vector Fields

A set of vectors $v_1(x,t), v_2(x,t), ..., v_n(x,t)$ *are linearly dependent at a point* (x_0, t_0) *if we can find a set of non-zero parameters* α_1, α_2, ..., α_n *such that:*

$$\alpha_1 v_1(x_0,t_0) + \alpha_2 v_2(x_0,t_0) + ... + \alpha_n v_n(x_0,t_0) = 0 \qquad (6.5)$$

If $\alpha_1 = \alpha_2 = ... = \alpha_n = 0$ *is the only set of parameters for which equation (6.5) is satisfied, then the set of vectors* $v_1(x,t), v_2(x,t), ..., v_n(x,t)$ *are linearly* **independent** *at a point* (x_0, t_0). This definition of linear independence at a point can be extended to an entire region in the (x,t) space.

Consider a region R_0 *in the* (x,t) *space. If we can find a set of non-zero parameters* $\alpha_1(x_i,t_i)$, $\alpha_2(x_i,t_i)$, ..., $\alpha_n(x_i,t_i)$ *for every point* (x_i,t_i) *in the region* R_0 *such that:*

$$\alpha_1(x_i,t_i)v_1(x_i,t_i) + \alpha_2(x_i,t_i)v_2(x_i,t_i) + ... + \alpha_n(x_i,t_i)v_n(x_i,t_i) = 0 \qquad (6.6)$$

then the set of vectors $v_1(x,t), v_2(x,t), ..., v_n(x,t)$ are linearly dependent in the region R_0. *If* $\alpha_1(x_i,t_i) = \alpha_2(x_i,t_i) = ... = \alpha_n(x_i,t_i) = 0$ *is the only set of parameters for which equation (6.6) is satisfied, then the set of vectors* $v_1(x,t), v_2(x,t), ..., v_n(x,t)$ *are linearly* **independent.**

Reproduced with permission of the copyright owner. Further reproduction prohibited without permission.

6.3.2 Invertible Transformations

Consider the time-varying coordinate transformation from $\mathbb{R}^n$ x $\mathbb{R}$ to $\mathbb{R}^n$ x $\mathbb{R}$ of the form:

$$\begin{aligned}
\dot{\zeta}_1 &= \theta_1(t, x_1, x_2, ..., x_n) \\
\dot{\zeta}_2 &= \theta_2(t, x_1, x_2, ..., x_n) \\
&\cdot \\
&\cdot \\
&\cdot \\
\dot{\zeta}_n &= \theta_n(t, x_1, x_2, ..., x_n)
\end{aligned} \tag{6.7}$$

where θ_1, θ_2, ..., θ_n are scalar fields on $\mathbb{R}^n$ x $\mathbb{R}$.

Proposition 6.1: The transformation (6.7) is invertible if and only if the row vectors of the jacobian matrix

$$\begin{bmatrix}
\frac{\partial\theta_1}{\partial x_1} & \frac{\partial\theta_1}{\partial x_2} & \cdots & \frac{\partial\theta_1}{\partial x_n} \\
\frac{\partial\theta_2}{\partial x_1} & \frac{\partial\theta_2}{\partial x_2} & \cdots & \frac{\partial\theta_2}{\partial x_n} \\
\cdot & \cdot & & \cdot \\
\cdot & \cdot & & \cdot \\
\cdot & \cdot & & \cdot \\
\frac{\partial\theta_n}{\partial x_1} & \frac{\partial\theta_n}{\partial x_2} & \cdots & \frac{\partial\theta_n}{\partial x_n}
\end{bmatrix} \tag{6.8}$$

are linearly independent.

Proof: Define $x_0 = t$ and consider the "prolonged" vectors:

$$\begin{aligned}
\zeta &= [\zeta_0\ \zeta_1\ ...\ \zeta_n]^T \\
\theta &= [\theta_0\ \theta_1 ...\ \theta_n]^T \\
X &= [x_0\ x_1\ ...\ x_n]^T
\end{aligned} \tag{6.9}$$

Reproduced with permission of the copyright owner. Further reproduction prohibited without permission.

where $\zeta_0 = \theta_0 = x_0$. Then, using (6.9) , we can represent (6.7) and $\zeta_0 = \theta_0$ in compact form as:

$$\underline{\zeta} = \underline{\theta}(X) \tag{6.10}$$

Using the inverse function theorem, the above transformation is invertible if and only if:

$$det\left[\frac{\partial\theta(X)}{\partial X}\right] \equiv det\begin{bmatrix} 1 & 0 & & 0 \\ \frac{\partial\theta_1}{\partial x_0} & \frac{\partial\theta_1}{\partial x_1} & \cdots & \frac{\partial\theta_1}{\partial x_n} \\ \frac{\partial\theta_2}{\partial x_0} & \frac{\partial\theta_2}{\partial x_1} & \cdots & \frac{\partial\theta_2}{\partial x_n} \\ . & . & \cdots & . \\ . & . & \cdots & . \\ . & . & \cdots & . \\ \frac{\partial\theta_n}{\partial x_0} & \frac{\partial\theta_n}{\partial x_1} & & \frac{\partial\theta_n}{\partial x_n} \end{bmatrix} \neq 0 \tag{6.11}$$

This implies that the row vectors of (6.8) are linearly independent.

6.3.3 Linear Independence of Scalar Fields

With the above definitions of linear independence of vector fields and invertible transformations of time-varying systems, we define linear independence of scalar fields.

A set of scalar functions $s_1(x,t), s_2(x,t), ..., s_n(x,t)$ are linearly independent in the

Reproduced with permission of the copyright owner. Further reproduction prohibited without permission.

region R_0 if the row vectors of

$$\begin{bmatrix} \frac{\partial s_1}{\partial x_1} & \frac{\partial s_1}{\partial x_2} & \cdots & \frac{\partial s_1}{\partial x_n} \\ \frac{\partial s_2}{\partial x_1} & \frac{\partial s_2}{\partial x_2} & \cdots & \frac{\partial s_2}{\partial x_n} \\ \vdots & \vdots & \cdots & \vdots \\ \frac{\partial s_n}{\partial x_1} & \frac{\partial s_n}{\partial x_2} & \cdots & \frac{\partial s_n}{\partial x_n} \end{bmatrix}$$

are linearly independent.

Thus, a set of linearly independent scalar fields form an invertible transformation.

Lemma 6.1: Consider the system represented by equation (6.1) with relative order r. The scalar fields $h(x,t)$, $\overline{L}_f^1 h(x,t)$, $\overline{L}_f^2 h(x,t)$, ..., $\overline{L}_f^{r-1} h(x,t)$ are linearly independent.

Proof: Define $x_0 = t$ and define the following "prolonged" vectors

$$\begin{aligned} X &= [x_0 \,\vdots\, x]^T \\ F(X) &= [1 \,\vdots\, f(x,x_0)]^T \\ G(X) &= [0 \,\vdots\, g(x,x_0)]^T \end{aligned} \tag{6.12}$$

and the "prolonged" scalar

$$H(X) = h(x,x_0) \tag{6.13}$$

Then, the "prolonged" system can be written as:

$$\begin{aligned} \dot{X} &= F(X) + G(X)u \\ y &= H(X) \end{aligned} \tag{6.14}$$

Reproduced with permission of the copyright owner. Further reproduction prohibited without permission.

It can be easily seen that:

$$\begin{aligned} H(X) &= h(x,t) \\ L_F^1 H(X) &= \overline{L}_f^1 h(x,t) \\ L_F^2 H(X) &= \overline{L}_f^2 h(x,t) \\ &\cdot \\ &\cdot \\ &\cdot \\ L_F^{r-1} H(X) &= \overline{L}_f^{r-1} h(x,t) \end{aligned} \tag{6.15}$$

and the relative order of the prolonged system is the same as the relative order of the original system.

It can be easily shown (Isidori, 1989) that given ϕ, a real valued function and f and g vector fields, all defined in $\mathbb{R}^{n+1}$, for any choice of s, k, $r > 0$

$$< dL_f^s \phi(x), ad_f^{k+r} g(x) > = \sum_{i=0}^{r} (-1)^i \binom{r}{i} L_f^{r-i} < dL_f^{s+i} \phi(x), ad_f^k g(x) > \tag{6.16}$$

Using the above expression and the definition of relative order, we have for all i, j such that $i + j \leq r - 2$

$$< dL_F^j H(X), ad_F^j G(X) > = 0 \tag{6.17}$$

and for all i, j such that $i + j = r - 1$

$$< dL_F^j H(X), ad_F^j G(X) > = (-1)^{r-1-j} L_G L_F^{r-1} H(X) \neq 0 \tag{6.18}$$

Reproduced with permission of the copyright owner. Further reproduction prohibited without permission.

The above conditons, all together show that the matrix

$$\begin{bmatrix} dH(X) \\ dL_F^1 H(X) \\ \cdot \\ \cdot \\ \cdot \\ dL_F^{r-1} H(X) \end{bmatrix} \cdot \left[G(X)\ ad_F^1 G(X) \ldots ad_F^{r-1} G(X) \right] =$$

$$\begin{bmatrix} 0 & . & . & . & < dH(X), ad_F^{r-1} G(X) > \\ 0 & . & . & . & * \\ . & . & . & . & * \\ . & . & . & . & * \\ . & . & . & . & * \\ < dL_F^{r-1} H(X), G(X) > & * & * & * & * \end{bmatrix} \tag{6.19}$$

has rank r and thus the row vectors $dH(X)$, $dL_F^1 H(X)$, ..., $dL_F^{r-1} H(X)$ are linearly independent in $\mathbb{R}^{n+1}$. Using (6.15), we conclude that the scalar fields $h(x,t)$, $\overline{L}_f^1 h(x,t)$, $\overline{L}_f^2 h(x,t)$, ..., $\overline{L}_f^{r-1} h(x,t)$ are linearly independent in $\mathbb{R}^n$x$\mathbb{R}$.

An immediate consequence of Lemma 6.1 is that the $(r-1)$xn matrix

$$\begin{bmatrix} \frac{\partial h}{\partial x_1} & & & \frac{\partial h}{\partial x_n} \\ \frac{\partial \overline{L}_f h}{\partial x_1} & . & . & \frac{\partial \overline{L}_f h}{\partial x_n} \\ . & . & . & . \\ . & . & . & . \\ . & . & . & . \\ \frac{\partial \overline{L}_f^{r-2} h}{\partial x_1} & . & . & \frac{\partial \overline{L}_f^{r-2} h}{\partial x_n} \end{bmatrix} \tag{6.20}$$

has rank $(r-1)$.

Reproduced with permission of the copyright owner. Further reproduction prohibited without permission.

We can always rotate the indices of the state variables x_1 to x_n such that:

$$\begin{bmatrix} \frac{\partial h}{\partial x_{n-r+1}} & \cdots & \frac{\partial h}{\partial x_{n-1}} \\ \frac{\partial \overline{L}_f h}{\partial x_{n-r+1}} & \cdots & \frac{\partial \overline{L}_f h}{\partial x_{n-1}} \\ \vdots & \cdots & \vdots \\ \frac{\partial \overline{L}_f^{r-2} h}{\partial x_{n-r+1}} & \cdots & \frac{\partial \overline{L}_f^{r-2} h}{\partial x_{n-1}} \end{bmatrix} \neq 0 \qquad (6.21)$$

Also, by rotation, we can assure that the nth component of the vector $g(x,t)$ is non-zero.

The problem of calculating the inverse of *linear* time-varying systems has been studied in the literature and the applicability of a system inverse either implicitly or explicitly to numerous control problems has been demonstrated. Fruend (1971) derived a full order process inverse for a linear time-varying system. Silverman (1968) showed that a reduced order process inverse of order $(n-r)$ could be constructed by a time-varying coordinate transformation for a linear time-varying system. However, this method involves considerable matrix manipulations (Bell and Tsang, 1990). Byrnes and Isidori (1985) derived an invertible coordinate transformation for time *invariant* nonlinear systems which provides a minimal order realization of the inverse of the nonlinear system. This result can be easily extended to time-varying systems as shown by the theorem below. Note that in this case the coordinate transformation is time-varying. The existance of a finite relative order for *all* $t \in [t_0, \infty]$ ensures that the coordinate transformation is well behaved.

Theorem 6.1: Consider the system represented by equation (6.1) with relative order r. If r is strictly less than n, it is always possible to find (n-r) functions $t_1(x,t)$,

Reproduced with permission of the copyright owner. Further reproduction prohibited without permission.

$t_2(x,t)$, ..., $t_{n-r}(x,t)$ *such that the mapping*

$$\zeta = T(x,t) = \begin{bmatrix} t_1(x,t) \\ . \\ . \\ . \\ t_{n-r}(x,t) \\ h(x,t) \\ \overline{L}_f^1 h(x,t) \\ . \\ . \\ . \\ \overline{L}_f^{r-2} h(x,t) \\ \overline{L}_f^{r-1} h(x,t) \end{bmatrix} \tag{6.22}$$

has a jacobian matrix which is nonsingular and therefore qualifies as an invertible coordinate transformation. Furthermore, it is always possible to choose $t_1(x,t)$, $t_2(x,t)$, ..., $t_{n-r}(x,t)$ *such that:*

$$L_g t_i(x,t) = 0 \text{ for all } 1 \leq i \leq (n-r) \text{ and for all } x \tag{6.23}$$

Proof: Consider the vector g. We can find functions t_1, t_2, ..., t_{n-1} in (x,t) such that:

$$\begin{aligned} \frac{\partial t_1}{\partial x_1} g_1 + \frac{\partial t_1}{\partial x_2} g_2 + \ldots + \frac{\partial t_1}{\partial x_n} g_n &= 0 \\ \frac{\partial t_2}{\partial x_1} g_1 + \frac{\partial t_2}{\partial x_2} g_2 + \ldots + \frac{\partial t_2}{\partial x_n} g_n &= 0 \\ &\vdots \\ \frac{\partial t_{n-1}}{\partial x_1} g_1 + \frac{\partial t_{n-1}}{\partial x_2} g_2 + \ldots + \frac{\partial t_{n-1}}{\partial x_n} g_n &= 0 \end{aligned} \tag{6.24}$$

Reproduced with permission of the copyright owner. Further reproduction prohibited without permission.

To prove that

$$dim\left(span\{dt_1, dt_2, ..., dt_{n-1}\} + span\{dh, d\overline{L}_f^1 h, ..., d\overline{L}_f^{r-1} h\}\right) = n \qquad (6.25)$$

We prove this by contradiction. Suppose that

$$dim\left(span\{dt_1, dt_2, ..., dt_{n-1}\} + span\{dh, d\overline{L}_f^1 h, ..., d\overline{L}_f^{r-1} h\}\right) < n \qquad (6.26)$$

Then, there exists a real function $\gamma(x,t)$ such that:

$$\left(span\{dt_1, dt_2, ..., dt_{n-1}\} + span\{dh, d\overline{L}_f^1 h, ..., d\overline{L}_f^{r-1} h\}\right).\gamma(x,t) = 0 \qquad (6.27)$$

This imples that

$$(span\{dt_1, dt_2, ..., dt_{n-1}\}).\gamma(x,t) = 0 \qquad (6.28)$$

$$\left(span\{dh, d\overline{L}_f^1 h, ..., d\overline{L}_f^{r-1} h\}\right).\gamma(x,t) = 0 \qquad (6.29)$$

From equations (6.24) and (6.28), we get:

$$\gamma(x,t) = span\{g\} \qquad (6.30)$$

Substituting in equation (6.29), we get:

$$\begin{aligned} \frac{\partial h}{\partial x_1} g_1 + \frac{\partial h}{\partial x_2} g_2 + ... + \frac{\partial h}{\partial x_n} g_n &= 0 \\ \frac{\partial \overline{L}_f^1 h}{\partial x_1} g_1 + \frac{\partial \overline{L}_f^1 h}{\partial x_2} g_2 + ... + \frac{\partial \overline{L}_f^1 h}{\partial x_n} g_n &= 0 \\ &\vdots \\ \frac{\partial \overline{L}_f^{r-1} h}{\partial x_1} g_1 + \frac{\partial \overline{L}_f^{r-1} h}{\partial x_2} g_2 + ... + \frac{\partial \overline{L}_f^{r-1} h}{\partial x_n} g_n &= 0 \end{aligned} \qquad (6.31)$$

In other words:

$$< d\overline{L}_f^{r-1} h, g > = 0 \qquad (6.32)$$

Reproduced with permission of the copyright owner. Further reproduction prohibited without permission.

This is a contradiction by definition of relative order. Thus, equation (6.25) is true.

Since $\{dh, \overline{L_f}^{-1}h, ..., \overline{L_f}^{-1}h\}$ has dimension r, we can choose $(n-r)$ vectors $\{t_1, t_2, ..., t_{n-r}\}$ such that the vectors $\{t_1, t_2, ..., t_{n-r}, dh, \overline{L_f}^{-1}h, ..., \overline{L_f}^{-1}h\}$ are linearly independent and thus qualify as an invertible transformation.

Under the coordinate transformation (6.22), we obtain the following form:

$$\begin{aligned}
\dot{\zeta}_1 &= F_1(\zeta, t) \\
&\cdot \\
&\cdot \\
&\cdot \\
\dot{\zeta}_{n-r} &= F_{n-r}(\zeta, t) \\
\dot{\zeta}_{n-r+1} &= \zeta_{n-r+2} \\
&\cdot \\
&\cdot \\
&\cdot \\
\dot{\zeta}_{n-1} &= \zeta_n \\
\dot{\zeta}_n &= \Phi(\zeta, t) + G(\zeta, t)u \\
y &= \zeta_{n-r+1}
\end{aligned} \tag{6.33}$$

where

$$\begin{aligned}
F_i &= < dt_i, f > + \frac{\partial t_i}{\partial t} \; i = 1, 2, ..., n-r \\
\Phi &= \overline{L_f}(x, t) \\
G &= L_g \overline{L_f}^{-1}(x, t)
\end{aligned}$$

Corollary 6.1: Consider a system of the form (6.1) with relative order r which has

Reproduced with permission of the copyright owner. Further reproduction prohibited without permission.

been transformed into the form (6.33). Then the dynamic system:

$$\begin{aligned}
\dot{z}_1 &= F_1\left(t, z_1, ..., z_{n-r}, y, \frac{dy}{dt}, \frac{d^2y}{dt^2}, ..., \frac{d^{r-1}y}{dt^{r-1}}\right) \\
\dot{z}_2 &= F_2\left(t, z_1, ..., z_{n-r}, y, \frac{dy}{dt}, \frac{d^2y}{dt^2}, ..., \frac{d^{r-1}y}{dt^{r-1}}\right) \\
&\cdot \\
&\cdot \\
&\cdot \\
\dot{z}_{n-r} &= F_{n-r}\left(t, z_1, ..., z_{n-r}, y, \frac{dy}{dt}, \frac{d^2y}{dt^2}, ..., \frac{d^{r-1}y}{dt^{r-1}}\right) \\
u &= \frac{\frac{d^ry}{dt^r} - \Phi\left(t, z_1, ..., z_{n-r}, y, \frac{dy}{dt}, \frac{d^2y}{dt^2}, ..., \frac{d^{r-1}y}{dt^{r-1}}\right)}{G\left(t, z_1, ..., z_{n-r}, y, \frac{dy}{dt}, \frac{d^2y}{dt^2}, ..., \frac{d^{r-1}y}{dt^{r-1}}\right)}
\end{aligned} \tag{6.34}$$

is a minimal order realization of the inverse of the nonlinear system (6.1).

The notion of forced and unforced dynamics are determined by considering the first $n - r$ equations of the above normal form.

Forced Zero Dynamics: The forced zero dynamics of the system (6.1) are given by:

$$\begin{aligned}
\dot{z}_1 &= F_1(t, z_1, ..., z_{n-r}, U_1, ..., U_r) \\
\dot{z}_2 &= F_2(t, z_1, ..., z_{n-r}, U_1, ..., U_r) \\
&\cdot \\
&\cdot \\
&\cdot \\
\dot{z}_{n-r} &= F_{n-r}(t, z_1, ..., z_{n-r}, U_1, ..., U_r)
\end{aligned} \tag{6.35}$$

Unforced Zero Dynamics: The unforced zero dynamics of the system (6.1) are given

Reproduced with permission of the copyright owner. Further reproduction prohibited without permission.

by:

$$\begin{aligned}
\dot{z}_1 &= F_1(t, z_1, ..., z_{n-r}, 0, ..., 0) \\
\dot{z}_2 &= F_2(t, z_1, ..., z_{n-r}, 0, ..., 0) \\
&\cdot \\
&\cdot \\
&\cdot \\
\dot{z}_{n-r} &= F_{n-r}(t, z_1, ..., z_{n-r}, 0, ..., 0)
\end{aligned} \tag{6.36}$$

6.4 State Feedback

Consider a nonlinear time-varying system of the form:

$$\begin{aligned}
\dot{x} &= f(x,t) + g(x,t)u \\
y &= h(x,t)
\end{aligned} \tag{6.37}$$

which is minimum phase and has finite relative order, r. It is desirable to find a state feedback of the form:

$$u = \lambda(x,t) + \mu(x,t)v \tag{6.38}$$

where v is an external input, so that the closed-loop system:

$$\begin{aligned}
\dot{x} &= [f(x,t) + g(x,t)\lambda(x,t)] + [g(x,t)\mu(x,t)]v \\
y &= h(x,t)
\end{aligned} \tag{6.39}$$

(i) is time invariant

(ii) has linear input/output dynamics.

The result is summarized in the following theorem:

Theorem 6.2: The state feedback law:

$$u = \frac{v - \sum_{k=0}^{r} \beta_k \overline{L}_f^k h(x,t)}{\beta_r L_g \overline{L}_f^{r-1} h(x,t)} \tag{6.40}$$

Reproduced with permission of the copyright owner. Further reproduction prohibited without permission.

induces linear, time invariant closed-loop input/output dynamics described by:

$$\sum_{k=0}^{r} \beta_k \frac{d^k y}{dt^k} = v \tag{6.41}$$

Proof: The proof is an immediate consequence of the definition of relative order.

6.4.1 Linear Controller Design with State Feedback

We saw in the previous section that under the state feedback law, equation (6.40), the *time-varying nonlinear* system (6.1) is transformed into a *time-invariant linear* input-output system (6.41). Note that the parameters β_0, β_1, ..., β_r are completely arbitrary, which means that the $v - y$ system can have arbitrarily placed poles and, therefore, prespecified bounded-input/bounded-output (BIBO) stability characteristics. An external controller with integral action such as a PI controller

$$v = K_c \left[(y_d - y) + \frac{1}{\tau_I} \int_0^t (y_d - y) \right] \tag{6.42}$$

can then be used for offsetless tracking of the desired trajectory $y_d(t)$. The resulting structure is called the *globally linearizing control (GLC) structure.* Thus the design procedure using the GLC structure is extremely simple and can be summarized as follows:

1. Compute the linearizing state feedback, equation (6.40) from the system model.

2. Select β_0, β_1, β_2, .., β_r so that the poles of the transformed system are stable and "fast"..

3. Tune a PI controller (or any appropriate linear controller) for the linear time-invariant $v - y$ system.

Reproduced with permission of the copyright owner. Further reproduction prohibited without permission.

6.4.2 Internal Stability

Theorem 6.3: Consider the system (6.1) under the state feedback (6.40) and assume that β_0, β_1, β_2, .., β_r have been chosen such that the roots of the polynomial $\beta_r s^r + ... + \beta_1 s + \beta_0$ are in the open left-half plane. The unforced closed loop system will be internally stable in the large if the zero dynamics of the open-loop system are stable.

Proof: Under the state feedback transformation (6.40), the system (6.1) is transformed into the following form:

$$\begin{aligned}
\dot{\zeta}_1 &= F_1(\zeta, t) \\
&\cdot \\
&\cdot \\
&\cdot \\
\dot{\zeta}_{n-r} &= F_{n-r}(\zeta, t) \\
\dot{\zeta}_{n-r+1} &= \zeta_{n-r+2} \\
&\cdot \\
&\cdot \\
&\cdot \\
\dot{\zeta}_{n-1} &= \zeta_n \\
\dot{\zeta}_n &= -\frac{\beta_0}{\beta_r}\zeta_{n-r+1} - ... - \frac{\beta_{r-1}}{\beta_r}\zeta_n \\
y &= \zeta_{n-r+1}
\end{aligned} \tag{6.43}$$

Since the roots of the polynomial $\beta_r s^r + ... + \beta_1 s + \beta_0$ are in the open left-half plane, it is clear that the modes ζ_{n-r+1} to ζ_n will be stable. Thus, closed-loop stability will depend on the forced zero dynamics of the open-loop system. The closed-loop system will be internally uniformly asymptotically stable if the forced dynamics are stable in the the sense that for any set of initial conditions $\zeta(0)$ and any exponentially

Reproduced with permission of the copyright owner. Further reproduction prohibited without permission.

decaying inputs $U_1, U_2, ..., U_r$:

$$\lim_{t\to\infty} \zeta_i(t) = 0 \quad i = 1, 2, ..., n-r \tag{6.44}$$

Under an appropriate choice of β_i, the output y and its successive time derivatives will get arbitrarily close to zero in finite time. Thus, for practical purposes the internal stability will depend on the stability characteristics of the unforced zero dynamics of the open-loop system.

Local stability results can be obtained by examining the stability of the linearized system. We first review the definition of linearization of a time-varying system. Consider the nonlinear time-varying system:

$$\dot{z} = F(t, z) \tag{6.45}$$

Suppose $F(t, 0) = 0 \ t \geq 0$ and $F(t, .)$ is continuously differentiable. Define

$$A(t) = \left[\frac{\partial F(t,z)}{\partial z}\right]_{z=0} \tag{6.46}$$

and

$$F^*(t, z) = F(t, z) - A(t)z \tag{6.47}$$

If the following relation holds:

$$\lim_{||z||\to 0} \sup_{t\geq 0} \frac{||F^*(t,z)||}{||z||} = 0 \tag{6.48}$$

then the system

$$\dot{z} = A(t)z \tag{6.49}$$

is the *linearized* system of the nonlinear system (6.45) around the equilibrium point 0 (Vidyasagar, 1978).

If a linearized system for the time-varying nonlinear system exists, then local stability results can be obtained using Lyapunov's indirect method which states

Reproduced with permission of the copyright owner. Further reproduction prohibited without permission.

(Vidyasagar, 1978):

If the equilibrium point 0 of the linearized system (6.49) is uniformly asymptotically stable over $[0, \infty]$, *then the equilibrium point of the nonlinear system (6.45) is also uniformly asymptotically stable.*

Consider the system represented by (6.43) with an equilibrium point at 0. Assuming that relation (6.48) holds, the linearized system can be represented as:

$$\dot{\zeta} = A(t)\zeta \tag{6.50}$$

where

$$A(t) = \left[\begin{array}{cccccccc} \frac{\partial F_1}{\partial \zeta_1} & \frac{\partial F_1}{\partial \zeta_2} & & & & & & \frac{\partial F_1}{\partial \zeta_n} \\ \frac{\partial F_2}{\partial \zeta_1} & \frac{\partial F_2}{\partial \zeta_2} & & & & & & \frac{\partial F_2}{\partial \zeta_n} \\ . & . & . & . & . & . & . & . \\ . & . & . & . & . & . & . & . \\ . & . & . & . & . & . & . & . \\ \frac{\partial F_{n-r}}{\partial \zeta_1} & \frac{\partial F_{n-r}}{\partial \zeta_2} & & & & & & \frac{\partial F_{n-r}}{\partial \zeta_n} \\ 0 & 0 & . & 0 & 1 & . & . & 0 \\ 0 & 0 & . & 0 & 0 & . & . & 0 \\ . & . & . & . & . & . & . & . \\ . & . & . & . & . & . & . & . \\ . & . & . & . & . & . & . & 1 \\ 0 & . & . & -\frac{\beta_0}{\beta_r} & -\frac{\beta_1}{\beta_r} & . & . & -\frac{\beta_{r-1}}{\beta_r} \end{array}\right]_{\zeta = 0} \tag{6.51}$$

Case I: The matrix A is time invariant. Then, the system (6.50) is asymptotically stable around 0 if the eigenvalues of the matrix A are negative. It can be easily shown that the eigenvalues of the matrix A are the roots of the polynomial

$$\beta_0 s^r + ... + \beta_1 s + \beta_0 \tag{6.52}$$

Reproduced with permission of the copyright owner. Further reproduction prohibited without permission.

and the eigenvalues of the sub-matrix:

$$A^* = \left[\begin{array}{cccccc} \frac{\partial F_1}{\partial \zeta_1} & \frac{\partial F_1}{\partial \zeta_2} & & & & \frac{\partial F_1}{\partial \zeta_{n-r}} \\ \frac{\partial F_2}{\partial \zeta_1} & \frac{\partial F_2}{\partial \zeta_2} & & & & \frac{\partial F_2}{\partial \zeta_{n-r}} \\ . & . & & & & . \\ . & . & & & & . \\ . & . & & & & . \\ \frac{\partial F_{n-r}}{\partial \zeta_1} & \frac{\partial F_{n-r}}{\partial \zeta_2} & & & & \frac{\partial F_{n-r}}{\partial \zeta_{n-r}} \end{array} \right]_{\zeta = 0} \tag{6.53}$$

But the sub-matrix (6.53) represents the linearized zero dynamics of the open-loop system. Thus, if the parameters β_0, β_1, ..., β_r are so chosen that the roots of the polynomial (6.52) are negative, then the closed loop system is locally stable if the zero dynamics of the open-loop system are locally stable.

Case II: The matrix A is time-varying. The general solution of 6.50 is given by:

$$\zeta(t) = \Phi(t, t_0)\zeta(t_0) \tag{6.54}$$

where $\Phi(.,.)$ is the state transition matrix associated with $A(.)$.

Theorem 6.4 (Vidyasagar, 1978): The equilibrium point 0 of 6.50 is uniformly asymptotically stable over $[0, \infty]$ *if and only if*

$$\begin{aligned} &\sup_{t_0 \geq 0} \sup_{t \geq t_0} ||\Phi(t, t_0)||_i < \infty \\ &||\Phi(t, t_0)||_i \longrightarrow 0 \text{ as } t \longrightarrow \infty, \text{ uniformly in } t_0 \end{aligned} \tag{6.55}$$

In this case it is clear that if relation (6.55) is satisfied for the time-varying subsystem (6.53), this does not guarantee that the relation (6.52) will hold for the system (6.50). In other words, if the linearized zero dynamics of the open-loop system are locally stable, this does *not* guarantee that the equilibrium point of matrix A is stable. In this case, one has to check for the stability of the entire system represented by (6.50)

Reproduced with permission of the copyright owner. Further reproduction prohibited without permission.

6.5 Output Feedback Controller Synthesis via GLC

In many practical situations, on-line measurements of all the states are not available. In a typical situation, only the output is measured on-line and this motivates the problem of synthesizing nonlinear output feedback control laws for accurate tracking of set-points and effective rejection of disturbances. This synthesis problem can be conveniently tackled within the GLC framework, if the input/output linearizing feedback is combined with an appropriate state observer.

Theorem 6.5: Consider a nonlinear system of the form (6.1), with relative order r. Then, the dynamic system:

$$\begin{aligned} \dot{\zeta} &= A^*\zeta + b^*(y_{sp} - y) \\ \dot{w} &= f(w,t) + g(w,t)\frac{C^*\zeta + \frac{\beta_r}{\gamma_r}(y_{sp} - y) - \sum_{k=0}^{r}\beta_k \overline{L}_f^k h(w,t)}{\beta_r L_g \overline{L}_f^{r-1} h(w,t)} \\ u &= \frac{C^*\zeta + \frac{\beta_r}{\gamma_r}(y_{sp} - y) - \sum_{k=0}^{r}\beta_k \overline{L}_f^k h(w,t)}{\beta_r L_g \overline{L}_f^{r-1} h(w,t)} \end{aligned} \tag{6.56}$$

where

$$A^* = \begin{bmatrix} 0 & 1 & 0 & \cdots & 0 \\ 0 & 0 & 1 & \cdots & 0 \\ \vdots & \vdots & \vdots & \cdots & \vdots \\ 0 & \frac{\gamma_1}{\gamma_r} & -\frac{\gamma_2}{\gamma_r} & \cdots & -\frac{\gamma_{r-1}}{\gamma_r} \end{bmatrix} \tag{6.57}$$

Reproduced with permission of the copyright owner. Further reproduction prohibited without permission.

$$b^* = \begin{bmatrix} 0 \\ 0 \\ . \\ . \\ . \\ -\frac{1}{\gamma_r} \end{bmatrix} \tag{6.58}$$

$$C^* = \left[\beta_0 \,\vdots\, (\beta_1 - \beta_r\frac{\gamma_1}{\gamma_r}) \,\vdots\, ... \,\vdots\, (\beta_{r-1} - \beta_r\frac{\gamma_{r-1}}{\gamma_r})\right] \tag{6.59}$$

represents the $(n+r)^{th}$ *order state space realization of a dynamic output feedback controller which induces the closed-loop input/output behavior:*

$$y + \sum_{k=1}^{r}\gamma_k\frac{d^k y}{dt^k} = y_{sp} \tag{6.60}$$

Proof: Define the auxiliary variable

$$v = C^*\zeta + \frac{\beta_r}{\gamma_r}(y_{sp} - y) \tag{6.61}$$

Then, it can be easily verified that the system

$$\begin{aligned} \zeta^* &= A^*\zeta + b^*(y_{sp} - y) \\ v &= C^*\zeta + \frac{\beta_r}{\gamma_r}(y_{sp} - y) \end{aligned} \tag{6.62}$$

represents a minimal state-space realization of

$$\sum_{k=1}^{r}\gamma_k\frac{d^k v}{dt^k} = \sum_{k=0}^{r}\beta_k\frac{d^k}{dt^k}(y_{sp} - y) \tag{6.63}$$

with input, the error $(y_{sp} - y)$ and the output, the auxiliary variable v, which can be interpreted as a choice of the linear controller in the GLC structure. The other

Reproduced with permission of the copyright owner. Further reproduction prohibited without permission.

component of the controller becomes:

$$\begin{aligned} \dot{w} &= f(w,t) + g(w,t)\frac{v - \sum_{k=0}^{r}\beta_k \overline{L}_f^k h(w,t)}{\beta_r L_g \overline{L}_f^{r-1} h(w,t)} \\ u &= \frac{v - \sum_{k=0}^{r}\beta_k \overline{L}_f^k h(w,t)}{\beta_r L_g \overline{L}_f^{r-1} h(w,t)} \end{aligned} \tag{6.64}$$

which is the input-output linearizing state feedback law with the states reconstructed through an open-loop observer. When $w(0) = x(0)$, it easily follows that $w(t) = x(t)$. Then (6.64) induces exactly the behavior:

$$\sum_{k=0}^{r}\beta_k \frac{d^k y}{dt^k} = v \tag{6.65}$$

Combining (6.41) and (6.64), we easily obtain the desired closed loop input-output dynamics:

$$y + \sum_{k=1}^{r}\gamma_k \frac{d^k y}{dt^k} = y_{sp} \tag{6.66}$$

6.5.1 Reduced Order Realization

One can easily identify two distinct components of the controller. The first component is the dynamic sytem:

$$\begin{aligned} \dot{\zeta} &= A^*\zeta + b^*(y_{sp} - y) \\ y^* &= \zeta_1 \end{aligned} \tag{6.67}$$

It can be easily verified from equation (6.67) that

$$C^*\zeta + \frac{\beta_r}{\gamma_r}(y_{sp} - y) = \sum_{k=0}^{r}\beta_k \frac{d^k y^*}{dt^k} \tag{6.68}$$

Then, the second component of the controller takes the form:

$$\begin{aligned} \dot{w} &= f(w,t) + g(w,t)\frac{\sum_{k=0}^{r}\beta_k \frac{d^k y^*}{dt^k} - \sum_{k=0}^{r}\beta_k \overline{L}_f^k h(w,t)}{\beta_r L_g \overline{L}_f^{r-1} h(w,t)} \\ u &= \frac{\sum_{k=0}^{r}\beta_k \frac{d^k y^*}{dt^k} - \sum_{k=0}^{r}\beta_k \overline{L}_f^k h(w,t)}{\beta_r L_g \overline{L}_f^{r-1} h(w,t)} \end{aligned} \tag{6.69}$$

Reproduced with permission of the copyright owner. Further reproduction prohibited without permission.

It follows from equation (6.56) that

$$\sum_{k=0}^{r}\beta_k\frac{d^k[h(w,t)]}{dt^k} = C^*\zeta + \frac{\beta_r}{\gamma_r}(y_{sp}-y) \tag{6.70}$$

which combined with equation (6.68) yields

$$\sum_{k=0}^{r}\beta_k\frac{d^k[h(w,t)]}{dt^k} = \sum_{k=0}^{r}\beta_k\frac{d^k y^*}{dt^k} \tag{6.71}$$

Thus, if

$$\zeta_i(0) = \overline{L}_f^{i-1}h(w,t)(0),\ i = 1,....,\ r \tag{6.72}$$

it follows that

$$\zeta_i(t) = \overline{L}_f^{i-1}h(w,t),\ i = 1,....,\ r \tag{6.73}$$

Substituting in the dynamic output feedback controller, we obtain the following n-th order realization:

$$\begin{aligned} \dot{w} &= f(w,t)+g(w,t)\frac{(y_{sp}-y)-\sum_{k=1}^{r}\gamma_k\overline{L}_f^k h(w,t)}{\gamma_r L_g\overline{L}_f^{r-1}h(w,t)} \\ u &= \frac{(y_{sp}-y)-\sum_{k=1}^{r}\gamma_k\overline{L}_f^k h(w,t)}{\gamma_r L_g\overline{L}_f^{r-1}h(w,t)} \end{aligned} \tag{6.74}$$

6.6 Linear Time-Varying Systems

Consider a SISO linear time-varying system described by:

$$\begin{aligned} \dot{x} &= A(t)x + B(t)u \\ y &= C(t)x \end{aligned} \tag{6.75}$$

where $A(t)$, $B(t)$ and $C(t)$ are matrices of dimension n x n, n x 1 and n x 1 respectively. This is a special case of (6.1) for:

$$\begin{aligned} f(x,t) &= A(t)x \\ g(x,t) &= B(t) \\ h(x,t) &= C(t)x \end{aligned} \tag{6.76}$$

Reproduced with permission of the copyright owner. Further reproduction prohibited without permission.

Define:

$$\begin{aligned} C_0(t) &= C(t) \\ C_1(t) &= \frac{\partial C(t)}{\partial t} + C(t).A(t) \\ C_2(t) &= \frac{\partial C_1(t)}{\partial t} + C_1(t).A(t) \\ C_3(t) &= \frac{\partial C_2(t)}{\partial t} + C_2(t).A(t) \\ &\cdot \\ &\cdot \\ &\cdot \\ C_k(t) &= \frac{\partial C_{k-1}(t)}{\partial t} + C_{k-1}(t).A(t) \end{aligned} \tag{6.77}$$

It can be easily seen that the modified Lie derivatives are:

$$\begin{aligned} \overline{L}_f^0 h(x,t) &= C_0(t)x \\ \overline{L}_f^1 h(x,t) &= C_1(t)x \\ \overline{L}_f^2 h(x,t) &= C_2(t)x \\ \overline{L}_f^3 h(x,t) &= C_3(t)x \\ &\cdot \\ &\cdot \\ \overline{L}_f^k h(x,t) &= C_k(t)x \end{aligned} \tag{6.78}$$

Applying definition 6.1 we immediately see that for a system of the form (6.75), the relative order r of output y with respect to the manipulated input u is the smallest integer for which:

$$C_{r-1}(t)B(t) \neq 0 \tag{6.79}$$

The state feedback (equation (6.40)) is of the form:

$$u = \frac{v - \sum_{k=0}^{r} \beta_k C_k(t)x}{\beta_r C_{r-1}(t)B(t)} \tag{6.80}$$

Reproduced with permission of the copyright owner. Further reproduction prohibited without permission.

The output feedback controller becomes:

$$\begin{aligned}
\dot{\zeta} &= A^*\zeta + b^*(y_{sp} - y) \\
\dot{w} &= A(t)w + B(t)\frac{C^*\zeta + \frac{\beta_r}{\gamma_r}(y_{sp} - y) - \sum_{k=0}^{r} C_k(t)w}{\beta_r C_{r-1}(t)w} \\
u &= \frac{C^*\zeta + \frac{\beta_r}{\gamma_r}(y_{sp} - y) - \sum_{k=0}^{r} C_k(t)w}{\beta_r C_{r-1}(t)w}
\end{aligned} \tag{6.81}$$

where A^*, b^* and C^* are defined by equations (6.57), (6.58) and (6.59).

6.6.1 Zero Dynamics of Linear Time-Varying Systems

Consider a linear time-varying system of the form (6.75) with relative order r and linearly independent scalar fields $C_0(t)x$, $C_1(t)x$, ..., $C_{r-1}(t)x$. Assume that the components of the vector B are as follows:

$$B(t) = [b_1(t)\ b_2(t) \ldots b_n(t)]^T \tag{6.82}$$

Reproduced with permission of the copyright owner. Further reproduction prohibited without permission.

where $b_n(t) \neq 0$. Then it is not difficult to verify that the transformation:

$$\begin{aligned}
\zeta_1 &= x_1 - \frac{b_1(t)}{b_n(t)}x_n \\
\zeta_2 &= x_2 - \frac{b_2(t)}{b_n(t)}x_n \\
&\vdots \\
\zeta_{n-r} &= x_{n-r} - \frac{b_{n-r}(t)}{b_n(t)}x_n \\
\zeta_{n-r+1} &= C_0(t)x \\
\zeta_{n-r+2} &= C_1(t)x \\
&\vdots \\
\zeta_{n-1} &= C_{r-1}(t)x \\
\zeta_n &= C_r(t)x
\end{aligned} \tag{6.83}$$

is invertible and transforms equation (6.75) to the form represented by equation (6.43).

6.7 Illustrative Example

Reaction mechanisms which involve successive reaction steps are common in many areas of chemistry. The system

$$A \rightleftharpoons B \rightarrow C \tag{6.84}$$

is a well studied system in the presence of bifunctional catalysts (see, for instance, Froment and Bischoff, 1979). For instance the isomerization of paraffin using platinum-silica-alumina catalyst is represented by the above reaction scheme. In this case

Reproduced with permission of the copyright owner. Further reproduction prohibited without permission.

the platinum catalyzes the first reaction and the silica-alumina catalyzes the second reaction and neither catalyzes the reaction of the other component (Eley *et al.*, 1962). Similarly the conversion of Penicillin N to Deacetoxycephalosporin C to Deacetylcephalosporin C in *C. acremonium* is catalyzed by the bifunctional enzyme expandase/hydroxylase (Skatrud *et al.*, 1989). Due to the presence of separate reaction sites on the catalyst, the decay kinetics of these sites is usually different.

In this example we study a regulation problem in a system represented by the above kinetics where the reaction sites catalyzing the second reaction undergo substantial decay whereas the reaction sites catalyzing the first reaction are stable in the time scale of operation. A schematic of the system under consideration is shown in Figure 6.1. We assume that the rates of reaction for the scheme represented by equation (6.84) are given by:

$$\begin{aligned} r_1 &= k_1 e_1 C_A - k_2 e_1 C_B^2 \\ r_2 &= k_3 e_2 C_B^2 \end{aligned} \tag{6.85}$$

where e_1 and e_2 represent the activity of the two reaction sites on the bifunctional catalyst. Figure 6.2 shows the time profile of the activity of the two sites on the catalyst. The activity of the first site is constant whereas the activity of the second site follows second order decay kinetics from 0 - 40 hours due to sintering (Fogler, 1986). Thus:

$$e_2 = \frac{1}{1 + k_D t} \quad 0 \leq t \leq 40$$

The unsteady state mass balances are given by (see the Notation section for explanation of symbols):

$$\frac{d}{dt}\begin{bmatrix} x_1 \\ x_2 \\ x_3 \end{bmatrix} = \begin{bmatrix} 1 - x_1 - Da_1 x_1 + Da_2 x_2^2 \\ Da_1 x_1 - x_2 - Da_2 x_2^2 - Da_3 x_2^2 \\ Da_3 x_2^2 - x_3 \end{bmatrix} + \begin{bmatrix} 0 \\ 1 \\ 0 \end{bmatrix} u \tag{6.86}$$

Reproduced with permission of the copyright owner. Further reproduction prohibited without permission.

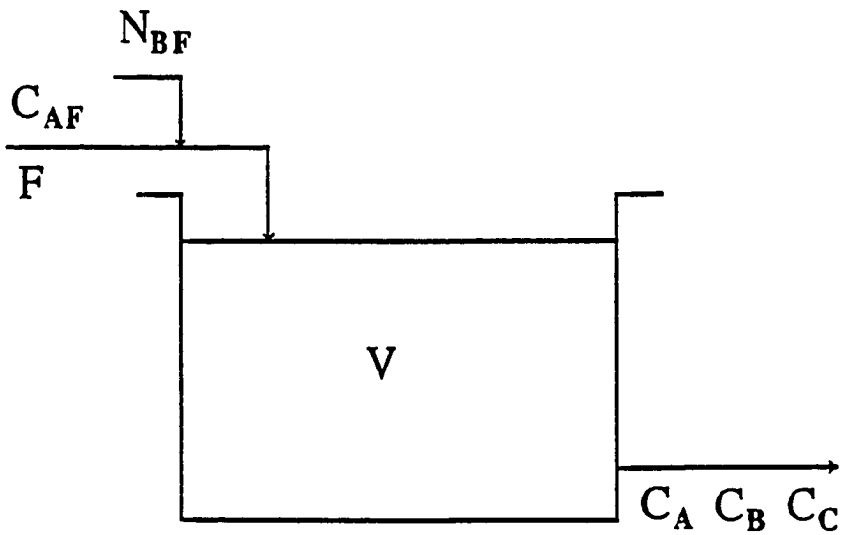

Figure 6.1: A Schematic of the System

Reproduced with permission of the copyright owner. Further reproduction prohibited without permission.

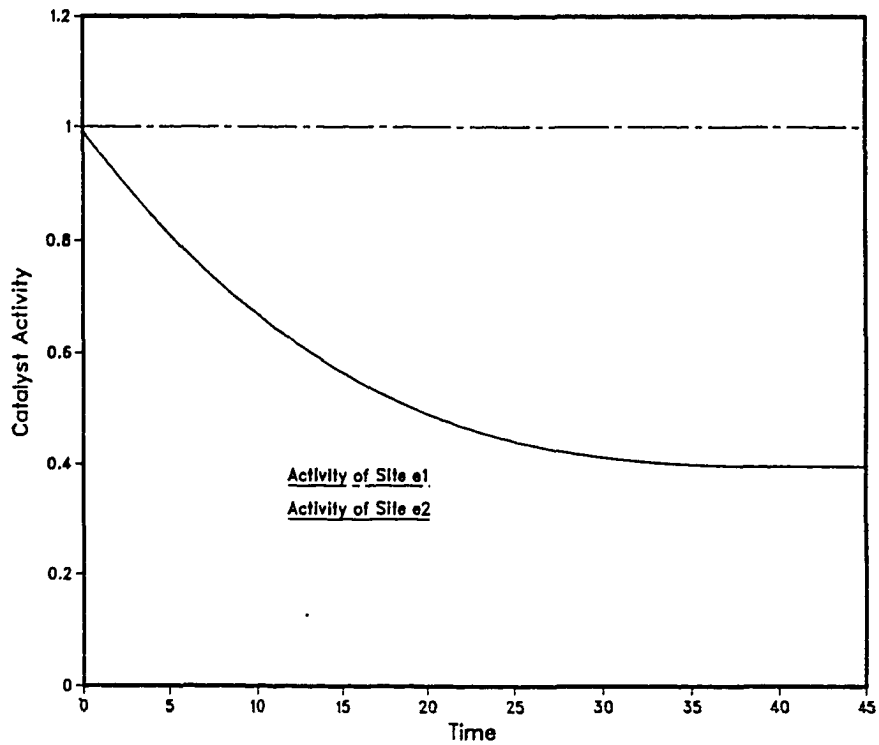

Figure 6.2: Time Profile of Activity of Catalytic Sites

Reproduced with permission of the copyright owner. Further reproduction prohibited without permission.

$$y = x_3 \tag{6.87}$$

Due to the time-varying nature of e_2, the term Da_3 is a time-varying parameter. The system is of the form (6.1) with:

$$x = \begin{bmatrix} x_1 \\ x_2 \\ x_3 \end{bmatrix} ; f(x,t) = \begin{bmatrix} 1 - x_1 - Da_1 x_1 + Da_2 x_2^2 \\ Da_1 x_1 - x_2 - Da_2 x_2^2 - Da_3 x_2^2 \\ Da_3 x_2^2 - x_3 \end{bmatrix} ; g(x,t) = \begin{bmatrix} 0 \\ 1 \\ 0 \end{bmatrix} \tag{6.88}$$

It can be easily seen that $< dh, g > = 0$ and $L_g \overline{L}_f^1 h(x,t) = 2Da_3 x_2 \neq 0$. Thus $r = 2$. Furthermore,

$$\overline{L}_f^1 h(x,t) = Da_3 x_2^2 - x_3 \tag{6.89}$$

$$\overline{L}_f^2 h(x,t) = 2Da_3 x_2 (Da_1 x_1 - x_2 - Da_2 x_2^2 - Da_3 x_2^2) - (Da_3 x_2^2 - x_3) + x_2^2 \frac{\partial Da_3}{\partial t} \tag{6.90}$$

The transformation

$$T = \begin{bmatrix} x_1 \\ x_3 \\ Da_3 x_2^2 - x_3 \end{bmatrix} \tag{6.91}$$

will transform the system into the form (6.33). Let x_{1s}, x_{2s}, x_{3s}, and u_s be the operating point. Define:

$$\begin{aligned} \zeta_1 &= x_1 - x_{1s} \\ \zeta_2 &= x_3 - x_{3s} \\ \zeta_3 &= Da_3(x_2^2 - x_{2s}^2) - (x_3 - x_{3s}) \end{aligned} \tag{6.92}$$

Then, it can be easily shown that the forced zero dynamics are given by

$$\dot{\zeta}_1 = -\zeta_1 - Da_1 \zeta_1 + \frac{Da_2}{Da_3}(\zeta_2 + \zeta_3) \tag{6.93}$$

Clearly, the above equation is stable for exponentially decaying inputs ζ_2 and ζ_3 and so the system (6.86) has stable zero dynamics.

Reproduced with permission of the copyright owner. Further reproduction prohibited without permission.

The performance of the dynamic output feedback (equation 6.56) was evaluated by numerical simulations. The control objective was to regulate the output at $y = 0.500$. The adjustable parameters were chosen as $\beta_0 = 1$, $\beta_1 = \gamma_1 = 2$ and $\beta_2 = \gamma_2 = 1$ in order to obtain a critically damped response.

Figure 6.3 shows the simulated closed-loop response under the assumption that the model is perfect. This case is compared with the case where the time-varying parameter Da_3 is assumed to be constant in the state feedback law. It is observed that the constant-parameter control law is unable to bring the system to set point till $t = 40$ after which the catalyst activity e_2 is virtually constant. This is because in the time interval from $t = 0$ to $t = 40$, the parameter Da_3 decreases continuously and a controller with constant parameters would require additional integral action to drive the system to set-point.

Robustness analysis of the dynamic control law was performed by assuming that there is an error of about 10% in estimating the time-varying parameter Da_3 in the dynamic control law. Figure 6.4 shows the time profile of the time varying parameter Da_3 as well as the estimated profile used in the control law. Figure 6.5 shows the simulated closed-loop response under this error in estimating the time-varying parameter. It is observed that an error of about 10% in the estimation of the parameter Da_3 leads to an error of only 0.6% in tracking the set-point.

Note that the dynamic output feedback is a function of the time-varying parameter Da_3 and its time derivative (see equation (6.90)). If the system states are sampled "fast enough", the term $\frac{\partial Da_3}{\partial t}$ will be small and can be ignored. In this situation, the feedback is equivalent to deriving a feedback law by assuming *constant* parameters and updating this feedback law by new estimates of the time-varying parameter (as is done in adaptive control algorithms).

Reproduced with permission of the copyright owner. Further reproduction prohibited without permission.

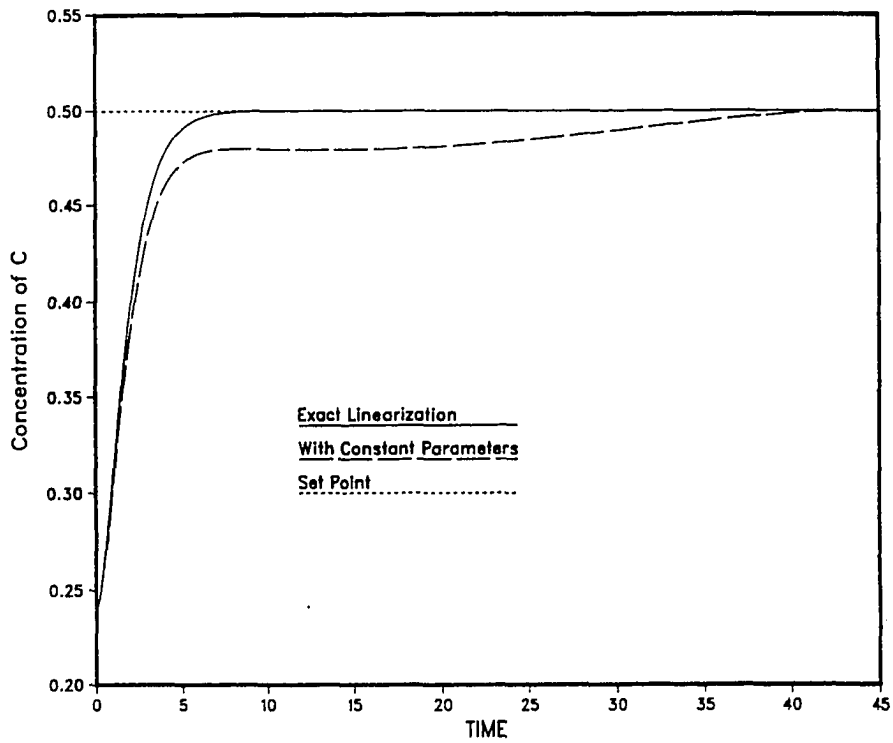

Figure 6.3: Closed Loop Response for Perfect Model

Reproduced with permission of the copyright owner. Further reproduction prohibited without permission.

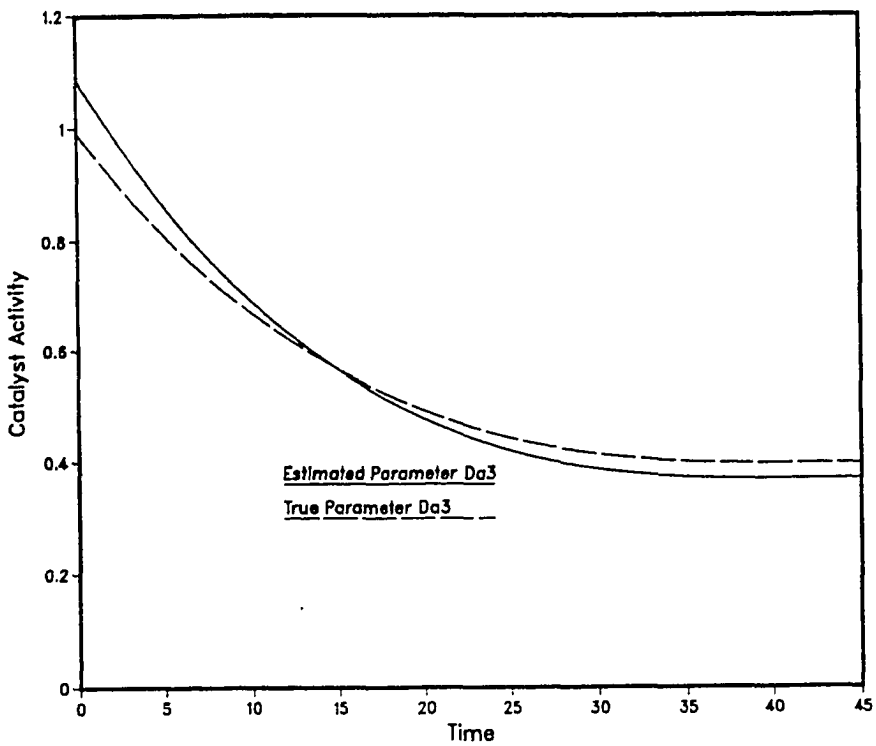

Figure 6.4: Time Varying Parameter Da_3

Reproduced with permission of the copyright owner. Further reproduction prohibited without permission.

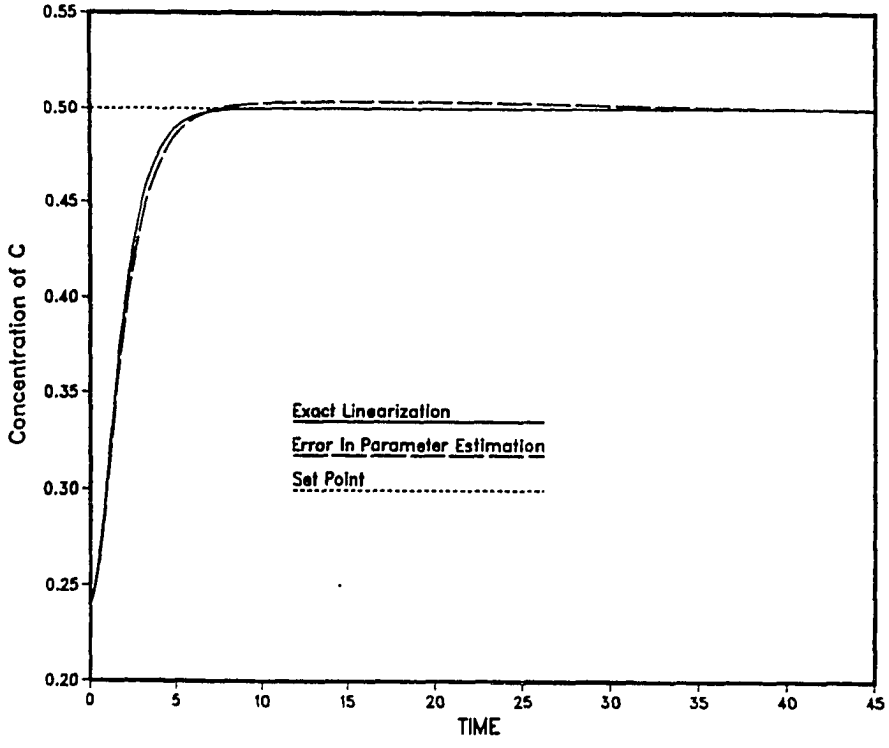

Figure 6.5: Robustness Analysis

Reproduced with permission of the copyright owner. Further reproduction prohibited without permission.

We studied the effect of sampling time through numerical simulations. The results are shown in Figure 6.6. Assuming the same values of the adjustable parameters $\beta_0, \beta_1, \beta_2, \gamma_1$ and γ_2 as in Figure 6.3, we simulated the controller performance for the case where the time-varying parameter in the dynamic feedback law is assumed to be constant but updated with new estimates at certain sampling instants. In this simulation we assume that at each sampling instant, we get a time averaged estimate of the time-varying parameter Da_3 of the previous sampling interval. It is observed from Figure 6.6 that when the sampling is "fast enough" (sampling interval = 1), the "adaptive" feedback law drives the system very close to the set-point. When the sampling interval is increased (sampling interval = 5, 10), the system exhibits damped oscillations.

Reproduced with permission of the copyright owner. Further reproduction prohibited without permission.

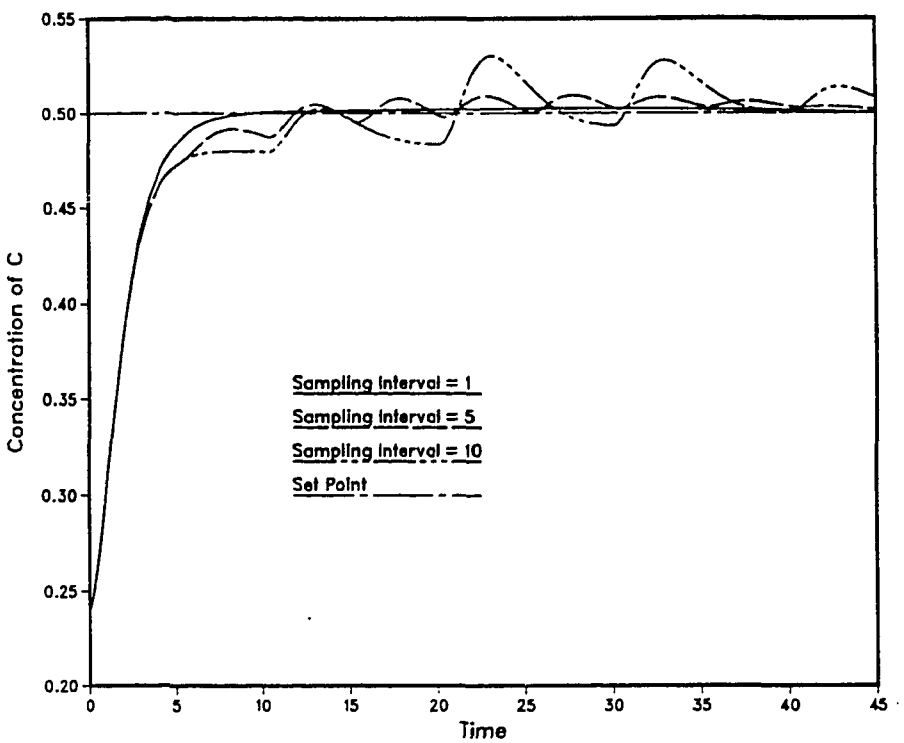

Figure 6.6: Comparison with Adaptive Control

Reproduced with permission of the copyright owner. Further reproduction prohibited without permission.

6.8 Nomenclature

C_A = concentration of species A in reactor

C_{AF} = feed concentration of species A

C_B = concentration of species B in reactor

C_C = concentration of species C in reactor

F = volumetric feed rate

N_{BF} = molar feed rate of species B

k_1 = first order rate constant

k_2, k_3 = second order rate constants

t^* = time

t = t^*F/V

x_1 = C_A/C_{AF}

x_2 = C_B/C_{AF}

x_3 = C_C/C_{AF}

Da_1 = k_1e_1V/F

Da_2 = $k_2e_1C_{AF}/F$

Da_3 = $k_3e_2C_{AF}/F$

Reproduced with permission of the copyright owner. Further reproduction prohibited without permission.

CHAPTER VII

MODELING AND YIELD OPTIMIZATION OF CEPHAMYCIN C FERMENTATION

Microorganisms are among man's best friends and his worst enemies, but it took him a million years to find out.

E. C. Stakman

7.1 Introduction

Given a particular organism, maximizing production from batch bioreactors requires determination of conditions which maximize the genetic potential of the organism. The activity of a batch culture at any point of time is a function of both the environmental state as well as the previous history of the culture. A constant environment is not optimal for fermentations. A particular time sequence of temperature, pH, dissolved oxygen levels, and substrate feeding is required for the culture to synthesize product at its optimal rate.

Due to the inherent complexity of the biological process, the natural question to ask is: how can the optimal operating parameters for the fermentation be calculated ? In this chapter we address this issue by studying the production of cephamycin C. The theory developed in the previous chapters is applied to a mathematical model

Reproduced with permission of the copyright owner. Further reproduction prohibited without permission.

describing the production of cephamycin C. It is shown that when glucose feeding is chosen as the manipulated input for optimization of cephamycin C yield, this leads to an uncontrollable situation. When amino acid feeding is chosen as a manipulated input, this leads to a situation where there is no singular interval and cephamycin C yield is maximized by choosing the maximum feed rate. When the manipulated input chosen is the rate of temperature change, the optimal operating strategy consists of singular, non-singular and constrained regions.

7.2 Microbial Cell Metabolism for Synthesis of Beta-Lactam Antibiotics

We first discuss the key features of microbial cell metabolism. A living cell is a complex chemical reactor in which more than 1000 independent enzyme-catalyzed reactions occur. A schematic representation of the key metabolic processes in a microbial cell is shown in Figure 7.1. The cell utilizes substrates from the environment for production of both energy as well as metabolites. Carbon and nitrogen sources from the medium are utilized for the following purposes:

- Cell growth, energy, and maintenance
- Production of enzymes required to catalyze the secondary metabolic pathway to cephamycin C synthesis
- Production of primary metabolites required for cephamycin C synthesis
- Synthesis of β-lactam antibiotics using the primary metabolites and the necessary enzymes.

The development of cell-free systems from β-lactam producing organisms has led to the establishment of the biosynthetic steps in the pathway of penicillins and cephalosporins. The initial steps in the formation of penicillins in filamentous fungi

Reproduced with permission of the copyright owner. Further reproduction prohibited without permission.

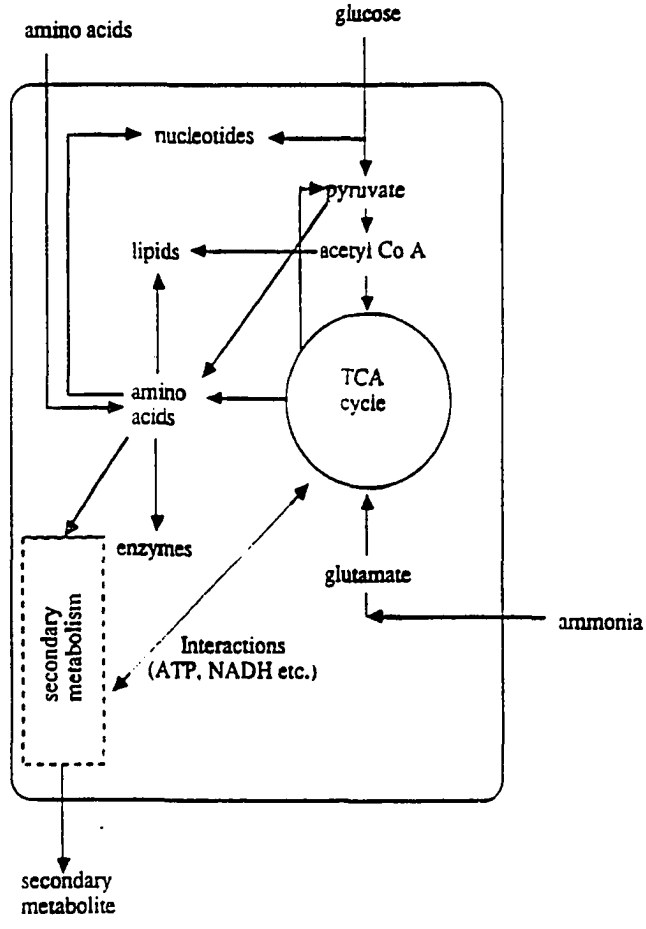

Figure 7.1: Key Metabolic Processes in a Microbial Cell

Reproduced with permission of the copyright owner. Further reproduction prohibited without permission.

and cephalosporins and cephamycins in both prokaryotes and lower eukaryotes are identical. The tripeptide δ-(L-α-aminoadipyl)-L-cysteinyl-D-valine (ACV) is formed from the amino acid precursors L-α-aminoadipate, L-cysteine and L-valine by ACV synthetase. Figure 7.2 shows the biosynthetic pathway leading to the formation of L-α-aminoadipate, L-cysteine and L-valine. The synthesis of these primary metabolites is regulated by the endogenous pool of amino acids in the microbial cell. Depending on the availability of exogenous amino acids and the cellular requirement, the pathway for synthesis of these amino acids from inorganic sources is regulated.

Figure 7.3 shows the biosynthetic pathway leading to the production of penicillins and cephalosporins starting from the amino acid precursors L-α-aminoadipate, L-cysteine and L-valine. The first β-lactam in the pathway is formed by cyclization of the tripeptide yielding isopenicillin N (IPN). After synthesis of IPN, the pathways to cephalosporins and penicillins diverge. In the fungus *C. acremonium* and in the actinomyces *N. lactamdurans* and *S. clavuligerus*, the α-aminoadipyl side chain is isomerised to produce penicillin N (PN). The thiazolidine ring of the penicillin is then expanded to the dihydrothiazine ring to form deacetoxycephalosporin C (DAOCS) using the enzyme deacetoxycephalosporin C synthetase. After the ring expansion, the C-3 methyl group of DAOC is hydrolyzed by DAOC hydroxylase to Deacetylcephalosporin C (DAC). Subsequent conversion to cephamycin C (CMC) involves the hydroxylation at the C-7 position catalyzed by a dioxygenase, methylation of that hydroxyl group by methyltransferase, and the transfer of a carbamoyl group to the C-3 hydroxymethyl group catalyzed by O-carbamoyl-transferase.

The products penicillin V, cephalosporin C and cephamycin C derived from the β-lactam biosynthetic pathway are commercially important.

Reproduced with permission of the copyright owner. Further reproduction prohibited without permission.

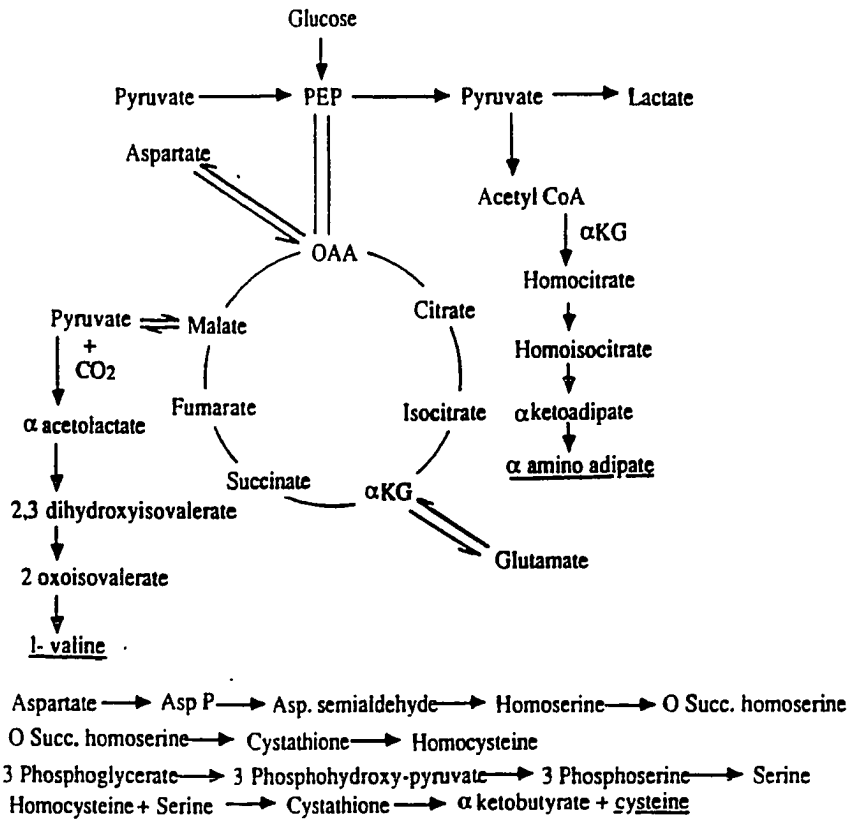

Figure 7.2: Biosynthetic Pathway for α-aminoadipate, Cysteine, and Valine

Reproduced with permission of the copyright owner. Further reproduction prohibited without permission.

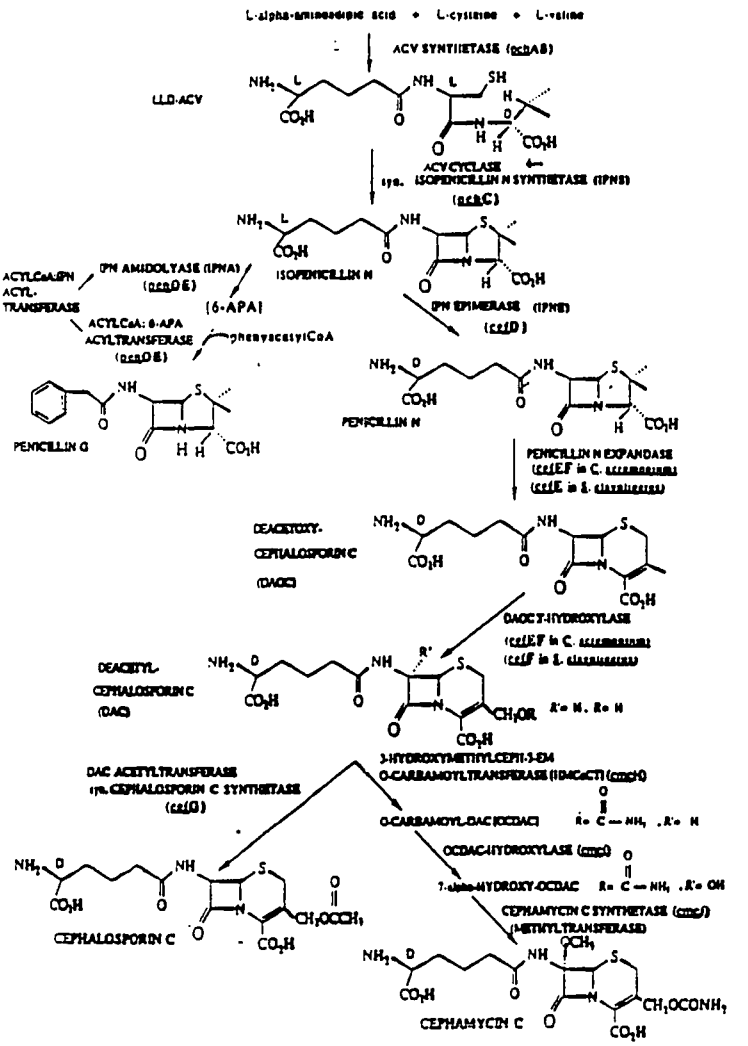

Figure 7.3: Biosynthetic Pathway for β-lactam Antibiotics

Reproduced with permission of the copyright owner. Further reproduction prohibited without permission.

7.3 A Mathematical Model for Synthesis of Beta-Lactam Antibiotics

Based on the above description, a mathematical model is developed which describes the biosynthesis of β-lactam antibiotics. The complexity of the kinetic description which is required and appropriate depends on the intended application of the kinetics. For instance, Bajpai and Reuss (1981) developed a mathematical model to describe the formation of penicillin in *P. chrysogenum*. The formation of cell mass was described by a single lumped equation and the product formation was described by substrate inhibited kinetics. Using this simple, unstructured model with four equations and nine parameters, they were able to verify the experimental results of Mou (1979). Matsumura *et al.* (1981) developed a mathematical model to describe growth and cephalosporin C formation in *C. acremonium*. The cell mass formation was described by a structured model with three different states, namely, hyphae, swollen hyphae, and arthrospores. The product was assumed to be limited by a single enzyme catalyzed reaction. This model consisted of eight equations and twenty eight parameters. Malmberg and Hu (1991) developed a structured model for cephamycin C formation by *S. clavilgerus* using the β-lactam biosynthesis pathway shown in Figure 7.3 to determine the rate limiting reactions. A kinetic analysis was performed on the model to elucidate the rate-limiting enzyme in the biosynthesis pathway.

Clearly, it is not practical or possible to formulate a kinetic model which includes all the features and details of cellular metabolism. In this section, we will develop a model which will primarily include information on secondary metabolism since the ultimate objective of this exercise is use the model for yield optimization of the β-lactam cephamycin C.

Reproduced with permission of the copyright owner. Further reproduction prohibited without permission.

7.3.1 Cell Growth

Cell growth in a batch reactor can be modeled as follows (Bailey and Ollis, 1986):

$$\frac{dX}{dt} = \mu X - k_x X \tag{7.1}$$

where X is the concentration of the cell mass, μ is the specific growth rate, and k_x is the cell death rate constant. This overall description "lumps" together the morphological changes that occur during cell growth and ignores the age distribution of cell population.

7.3.2 Substrate Utilization

Glucose is required for cell growth, maintenance and production of enzymes for secondary metabolism. We can model glucose utilization in a batch bioreactor as (Bailey and Ollis, 1986):

$$\frac{dS}{dt} = -\frac{1}{Y_x}\mu X - m_x X \tag{7.2}$$

The first term in the right hand side of the above equation accounts for the substrate used for growth and the second term accounts for cellular maintenance and non-growth associated usage of the substrate.

The first step in the biosynthesis of cephamycin C involves the utilization of the amino acids α-aminoadipic acid, l-valine and cysteine. The *exogenous* amino acid balance can be written as follows (Matsumura *et al.*, 1981)

$$\frac{d[aa]}{dt} = -\frac{\mu_{aa}[aa]X}{K_{aa} + [aa]} + s_{aa}u_{aa} \tag{7.3}$$

where $[aa]$ refers to the concentration of exogenous amino acids, μ_{aa} is the maximum specific uptake rate of exogenous acids into the cell, s_{aa} is the concentration of amino acids in the feed stream and u_{aa} is the volumetric feed rate of amino acids. Changes

Reproduced with permission of the copyright owner. Further reproduction prohibited without permission.

in the *endogenous* pool of amino acids can be described by considering the material balance: uptake of exogenous amino acids from the culture medium, endogenous amino acid synthesis by inorganic sources, utilization of amino acids for protein synthesis, utilization of amino acids for secondary metabolism.

$$\frac{d[aa_i]}{dt} = \frac{\mu_{aa}[aa]X}{K_{aa}+[aa]} + U_{Apr} - \frac{\mu_{aai}[aa_i]}{K_{aai}+[aa_i]} \tag{7.4}$$

where $[aa_i]$ refers to the concentration of *endogenous* amino acids α-aminoadipic acid, l-valine and cysteine, and the subscript "*pr*" refers to the rate of metabolite produced. When the necessary amino acids are present in the culture medium, the rate of endogenous biosynthesis, U_{Apr}, is very low.

7.3.3 Synthesis of Enzymes Necessary for Synthesis of Cephamycin C

As seen from Figure 7.3, the enzymes ACV synthetase, IPN epimerase, expandase, DAC hydroxylase, O-carbamoyltransferase, OCDAC hydroxylase and cephamycin synthetase are required for the biosynthesis of cephamycin C from α-aminoadipic acid, l-valine and cysteine. The synthesis of each enzyme can be modeled as follows:

$$\frac{dE_i}{dt} = \mu_{E_i}X - k_{E_i}E_i \tag{7.5}$$

where μ_{E_i} is the specific rate of production of enzyme E_i and k_{E_i} is the first order rate constant of degradation of enzyme E_i. High producing strains of cephamycin C have been selected with enzymes which are derepressed with respect to the substrate glucose and so the functions μ_{E_i} should be very weak functions of the substrate.

7.3.4 Synthesis of Intermediates and Product of Secondary Metabolism

Each step in the secondary metabolism pathway can be represented by:

$$S_i \xrightarrow{E_i} S_{i+1}$$

Reproduced with permission of the copyright owner. Further reproduction prohibited without permission.

The rate of change of the $i+1$-th intermediate can be described as follows:

$$\frac{dS_{i+1}}{dt} = k_i E_i S_i - k_{i+1} S_{i+1} \tag{7.6}$$

Thus, we have the following balances leading to the formation of cephamycin C:

Formation of LLD-ACV

$$\frac{d[ACV]}{dt} = k_1 E_{ACVS}[aa] - k_2[ACV] \tag{7.7}$$

Formation of Iso-Penicillin N

$$\frac{d[IPN]}{dt} = k_3 E_{cyclase}[ACV] - k_4[IPN] \tag{7.8}$$

Formation of Penicillin N

$$\frac{d[PN]}{dt} = k_5 E_{epimerase}[IPN] - k_6[PN] \tag{7.9}$$

Formation of DAOC

$$\frac{d[DAOC]}{dt} = k_7 E_{expandase}[PN] - k_8[DAOC] \tag{7.10}$$

Formation of DAC

$$\frac{d[DAC]}{dt} = k_9 E_{hydroxylase}[DAOC] - k_{10}[DAC] \tag{7.11}$$

Formation of OCDAC

$$\frac{d[OCDAC]}{dt} = k_{11} E_{transferase}[DAC] - k_{12}[OCDAC] \tag{7.12}$$

Formation of HOCDAC

$$\frac{d[HOCDAC]}{dt} = k_{13} E_{OCDAC-H}[OCDAC] - k_{14}[HOCDAC] \tag{7.13}$$

Formation of Cephamycin C

$$\frac{d[CMC]}{dt} = k_{15} E_{synthetase}[HOCDAC] - k_{16}[CMC] \tag{7.14}$$

Reproduced with permission of the copyright owner. Further reproduction prohibited without permission.

Some of the kinetic parameters have been identified for specific systems. For instance, Malmberg and Hu (1991) estimated the kinetic parameters for cephamycin C formation by *S. clavilgerus*.

7.4 Yield Optimization of Cephamycin C

The mathematical model developed in the previous section describes the dynamics of the formation of various metabolites and enzymes required for the production of β-lactams. However, such a model is too complex for implementing process control strategies. This generalized model can be reduced to a tractable size for yield optimization of a specific metabolite for specific culture strains and culture media. In this section we consider the yield optimization of cephamycin C produced by a high producting industrial strain of *N. lactamdurans* in a complex medium.

Zhang *et al* (1989) studied the biosynthesis of cephamycin C in a cell-free system of *S. clavuligerus* and showed that there is a control mechanism which affects the synthesis of the tripeptide ACV. Malmberg and Hu (1991) analyzed the kinetic data available in the literature and showed that ACV synthetase activity appears to be parallel with the specific production rate. This suggests that ACV synthetase may be the rate controlling enzyme for the overall flux of the system. If we assume that only one of the steps in the biosynthesis pathway is shown in Figure 7.3 is rate limiting, we have:

$$[aa_i] \xrightarrow{E} [CMC]$$

Thus, the individual balances for the intermediates in the biosynthesis of cephamycin C can be replaced by one enzyme-catalyzed reaction relating cephamycin C to the amino acid concentration.

$$\frac{d[CMC]}{dt} = k_a[aa_i]E - k_{16}[CMC] \tag{7.15}$$

Reproduced with permission of the copyright owner. Further reproduction prohibited without permission.

$$\frac{d[E]}{dt} = \mu_E X - k_E E \tag{7.16}$$

Based on the manipulated input chosen for yield optimization, further simplifications can be made to the model. In this study, we consider three different manipulated inputs: glucose feeding, amino acids feeding and temperature variation in the idiophase.

7.4.1 Effect of Feeding Glucose

The biosynthesis of secondary metabolites proceeds as long as the enzymes catalyzing this pathway are present and the primary metabolites necessary for cephamycin C production (α-aminoadipic acid, l-valine and cysteine) are not depleted.

Replacing the biosynthesis pathway by one enzyme catalyzed reaction, we obtain the following model for fed-batch fermentation of cephamycin C.

$$\begin{aligned} \frac{ds}{dt} &= -\frac{1}{Y_x}\mu_x x - m_x x + s_F u_g \\ \frac{dp}{dt} &= k_a \frac{[a_i]}{V} e - k_{16} p \\ \frac{dV}{dt} &= u_g - u_{evap} \end{aligned} \tag{7.17}$$

where s, $[a_i]$, p and e refer to the *amounts* of glucose, amino acids, cephamycin C and rate limiting enzyme,V represents the fermentor volume, u_g refers to the volumetric flow rate of glucose, and u_{evap} represents the evaporative losses. There is no change in cell mass in the idiophase. By feeding glucose continuously to the system, the cell is able to generate energy for maintenance as well as for producing the enzymes necessary for cephamycin C synthesis. After an initial rapid growth phase of about 40 hours, the increase in biomass is small and glucose is used primarily for maintenance and enzyme synthesis. If the glucose in the medium is depleted, the cell attempts to assemble the necessary enzymes from the amino acids in the medium

Reproduced with permission of the copyright owner. Further reproduction prohibited without permission.

and synthesis of cephamycin C stops when the amino acids in the medium run out. High producing industrial strains are derepressed with respect to high concentrations of glucose. Figure 7.4 shows the effect of glucose on product in a typical industrial strain. It is clear that glucose feed rate in the range 9 ml/hr to 18 ml/hr does not significantly affect the productivity of cephamycin C. In this concentration region, the effect of substrate feeding on cell mass and product yield is weak in the sense that overfeeding will not change the productivity but stopping the glucose feed would eventually lead to loss of productivity (because synthesis of enzymes required for secondary metabolism would stop).

This model is in the form (4.15) with

$$f(x,t) = \begin{bmatrix} -\frac{1}{Y_x}\mu_x x - m_x x \\ k_a \frac{[a_i]}{V} e - k_{16} p \\ -u_{evap} \end{bmatrix} \quad g(x,t) = \begin{bmatrix} s_F \\ 0 \\ 1 \end{bmatrix} \tag{7.18}$$

For controllability:

$$det \left[g \; \vdots \; \overline{ad}_f^1 g \; \vdots \; \overline{ad}_f^2 g \right] \not\equiv 0 \tag{7.19}$$

It can be easily verified that the controllability assumption is violated. This makes sense intuitively because the substrate balance and the volume balance are not independent. Substituting u_g in the first equation of (7.17) by $\left(\frac{dV}{dt} + u_{evap}\right)$, one can solve for s in terms of V. Thus, there are only two independent equations, namely the balance for the product and the volume balance. It can be easily seen that since the volume appears as a denominator term in the product balance, the optimal operating strategy to maximize product formation is to keep the flowrate at its minimum value of 9 ml/hr to minimize the volume.

Reproduced with permission of the copyright owner. Further reproduction prohibited without permission.

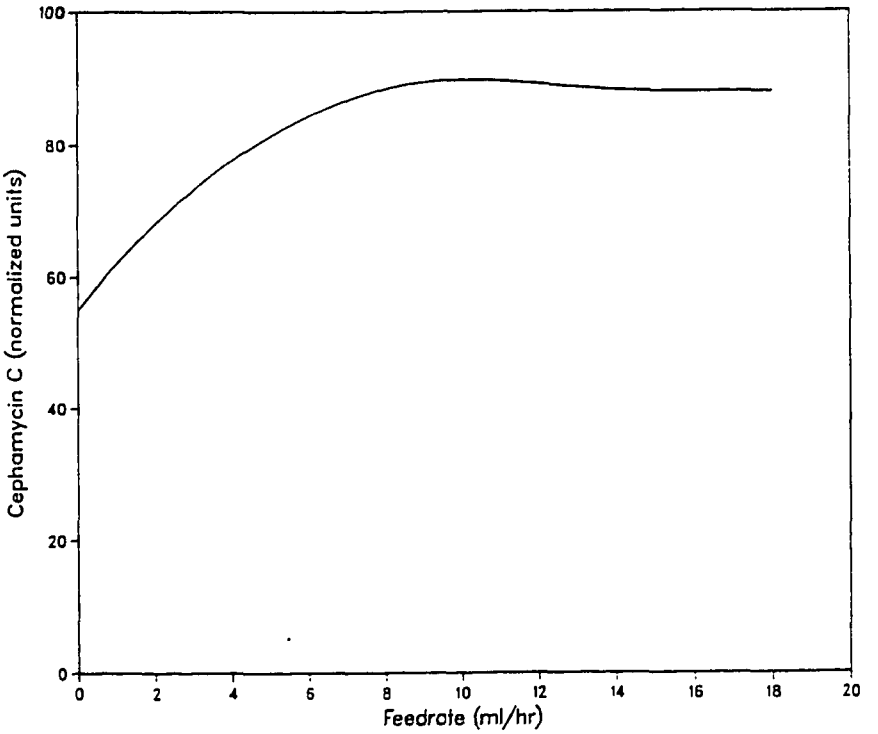

Figure 7.4: Effect of Glucose Feeding on Product

Reproduced with permission of the copyright owner. Further reproduction prohibited without permission.

7.4.2 Effect of Feeding Amino Acids

When sufficient glucose is available, the flow of precursors α-aminoadipic acid, l-valine and cysteine could determine the yield of the β-lactam product. For instance Jaklitsch *et al.* (1986) examined four different strains of *P. chrysogenum.* It was observed that the pool content of α-aminoadipic acid was highest in the high producing strain (0.7 %) and lowest in the low producing strain (0.05 %). Similarly, it has been reported (Inamine and Birnbaum, 1973) that the addition of α-aminoadipic acid at concentrations ranging from $0.025 - 0.05$ % in *S. clavuligerus* and $0.3 - 0.5$ % in *N. lactamdurans* increases cephamycin C production.

Figure 7.5 shows the effect of various endogenous amino acid profiles on the cephamycin C profile at a constant activity of the rate limiting enzyme. Since the endogenous amino acid concentration appears linearly in the product balance (equation 7.15), it is clear that maximizing the product concentration is equivalent to maximizing the concentration of endogenous amino acid pool. We drop the cell mass and substrate balances since these are not affected by amino acids feeding. Thus, the reduced model consists of the following equations:

$$\begin{aligned} \frac{d[aa]}{dt} &= -\frac{\mu_{aa}[aa]}{K_{aa}+[aa]}X + s_{aa}u_{aa} \\ \frac{d[aa_i]}{dt} &= \frac{\mu_{aa}[aa]}{K_{aa}+[aa]}X + U_{Apr} - \frac{\mu_{aai}[aa_i]}{K_{aai}+[aa_i]} \end{aligned} \tag{7.20}$$

This model is of the form (4.15) with

$$f(x,t) = \begin{bmatrix} -\dfrac{\mu_{aa}[aa]}{K_{aa}+[aa]}X \\ \dfrac{\mu_{aa}[aa]}{K_{aa}+[aa]}X + U_{Apr} - \dfrac{\mu_{aai}[aa_i]}{K_{aai}+[aa_i]} \end{bmatrix}; g(x,t) = \begin{bmatrix} s_{aa} \\ 0 \end{bmatrix} \tag{7.21}$$

Using the controllability assumption (4.17), it can be easily verified that the controllability assumption is satisfied. Furthermore, the degree of singularity $s = \infty$.

Reproduced with permission of the copyright owner. Further reproduction prohibited without permission.

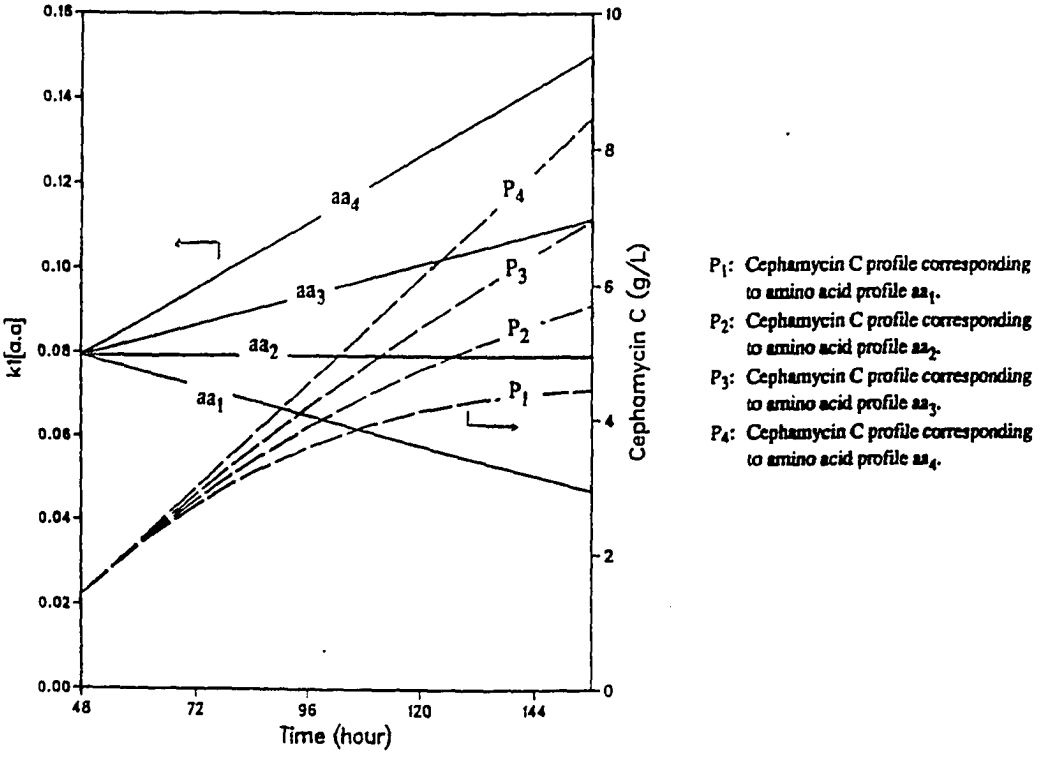

Figure 7.5: Effect of Feeding Amino Acids on Product

Reproduced with permission of the copyright owner. Further reproduction prohibited without permission.

Thus, a necessary condition for a singular extremal to exist is

$$det[g(x,t)\,\overline{ad}_f^1 g(x,t)] = \frac{\partial}{\partial[aa]}\left(\frac{[aa]}{K_{aa}+[aa]}\right) = 0 \qquad (7.22)$$

It is clear that in this case a singular region does not exist and so the optimal operating strategy is to use the maximum feed rate possible.

Increasing the rate of amino acid feed will increase the concentration of cephamycin C formed till the point where one of the key rate-limiting enzymes involved in the biosynthesis pathway gets saturated. Beyond this point, increasing the feedrate of amino acids does not change the productivity. It has been shown that high producing strains of β-lactam producing organisms possess superior enzyme systems as compared to their low producing counterparts (Shen *et al.*, 1986). Thus, if glucose and amino acid precursors are fed in sufficient quantities (as determined in the previous subsections), one of the enzymes involved in β-lactam biosynthesis becomes rate-limiting. Increased feeding of precursors only leads to accumulation of precursors since the rate-limiting enzyme is saturated. The yield of the β-lactam product can be increased by increasing the activity of the rate-limiting enzyme. In *S. clavuligerus*, this rate limiting enzyme is probably ACV synthetase (Malmberg and Hu, 1991). Skatrud *et al.* (1989) showed that in *C. acremonium*, the enzyme expandase which is responsible for converting penicillin N to DAOC can be rate limiting. By the use of recombinant DNA technology, an extra copy of the gene responsible for the production of expandase (*cef*EF gene) was introduced in a recombinant strain of *C. acremonium*. This led to a substantial decrease in penicillin N and a substantial increase in the amount of cephaposporin C.

When sufficient glucose and precursors are being fed, the model can be reduced

Reproduced with permission of the copyright owner. Further reproduction prohibited without permission.

as follows to study the effect of changing enzyme activity:

$$\begin{aligned} \frac{dE}{dt} &= \mu_E X - k_E E \\ \frac{d[CMC]}{dt} &= k_a E[aa_i] - k_{16}[CMC] \end{aligned} \tag{7.23}$$

Figure 7.6 shows the effect of changing enzyme activity on the yield of cephamycin C. It is observed that if sufficient amino acid precursers are available, increasing the activity of the rate-limiting enzyme leads increased yield of cephamycin C. Increasing the activity of the rate-limiting enzyme allows for a higher amount of precursor to be used, thus leading to a higher yield of cephamycin C.

7.4.3 Effect of Changing Temperature

Temperature can profoundly affect the productivity of the bioreactor. Constantinides *et al.* (1970) calculated optimal temperatures for the tropophase and idiophase in a penicillin fermentation. However, they did not consider the effect of changing the temperature in the idiophase alone. Temperature affects both the synthesis rate as well as the degradation rate of each intermediate in the biosynthesis of cephamycin C. Thus, it is important to study the effect of temperature in the idiophase alone.

The reduced model does not have balances for cell mass and glucose utilization since the effect of feeding substrate on cell mass is weak as long as the glucose feed rate is between 9 ml/hr and 18 ml/hr. Assuming that the activity of the rate limiting enzyme is not affected by temperature, the reduced model becomes:

$$\begin{aligned} \frac{d[CMC]}{dt} &= k_a(T)E[aa_i] - k_{16}(T)[CMC] \\ \frac{dT}{dt} &= q \end{aligned} \tag{7.24}$$

where q is a measure of the heat input and is proportional to the rate of change of

Reproduced with permission of the copyright owner. Further reproduction prohibited without permission.

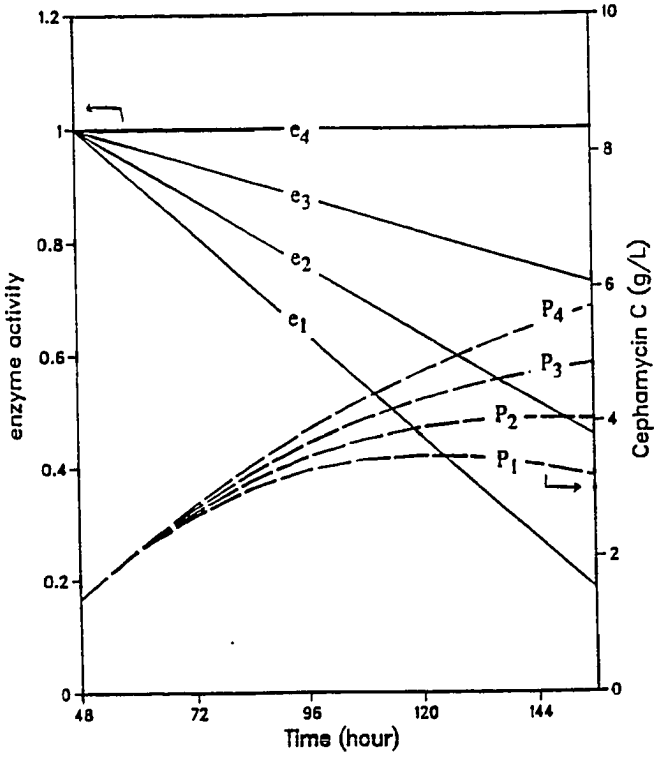

P_1: Cephamycin C profile corresponding to enzyme profile e_1.
P_2: Cephamycin C profile corresponding to enzyme profile e_2.
P_3: Cephamycin C profile corresponding to enzyme profile e_3.
P_4: Cephamycin C profile corresponding to enzyme profile e_4.

Figure 7.6: Effect of Enzyme Activity on Product

Reproduced with permission of the copyright owner. Further reproduction prohibited without permission.

temperature. The exogenous and endogenous amino acid balances are given by:

$$\begin{aligned} \frac{d[aa]}{dt} &= -\frac{\mu_{aa}[aa]X}{K_{aa}+[aa]} + s_{aa}u_{aa} \\ \frac{d[aa_i]}{dt} &= \frac{\mu_{aa}[aa]X}{K_{aa}+[aa]} + U_{Apr} - \frac{\mu_{aai}[aa_i]}{K_{aai}+[aa_i]} \end{aligned} \tag{7.25}$$

Temperature affects the parameters k_a, k_{16} and the amino acid utilization rate U_{Au}. We assume that the parameters k_a and k_{16} follow an Arrhenius type relationship with temperature. Thus

$$\begin{aligned} k_a &= k_{a0}exp\left(\frac{-\Delta E_a}{RT}\right) \\ k_{16} &= k_{160}exp\left(\frac{-\Delta E_{16}}{RT}\right) \end{aligned} \tag{7.26}$$

Due to the nonlinear relationship between temperature and the parameters k_a and k_{16}, cephamycin C yield would be maximized by following an optimal temperature *profile* instead of a *constant* temperature in the production phase. Typically, the activation energy of product degradation is greater than the activation energy of product formation by a factor of three (Wang *et al.*, 1979). In other words, the degradation rate is more sensitive to temperature than is the formation rate. Thus, intuitively, one would expect a continuously *decreasing* temperature profile to provide the optimal product yield. From the data of Constantinides *et al.* (1970) we estimated the activation energy of degradation of the β-lactam penicillin to be about $50,000$ *Joules/mole*. We consider the effect of temperature on a system described by $[aa_i] \longrightarrow [CMC]$ with $\Delta E_a = 16,000$ *Joules/mole* and $\Delta E_{16} = 50,000$ *Joules/mole*. We compare the product profiles for three different constant temperatures T_1, T_2 and T_3 where $T_1 > T_2 > T_3$. The results are shown in Figure 7.7. It is observed that at temperature T_1 (the highest temperature), the initial part of product concentration profile is high due to the higher synthesis rate but the product profile levels off quickly due to the increased degradation rate. At temperature T_3 (the lowest temperature), the initial part of the product concentration

Reproduced with permission of the copyright owner. Further reproduction prohibited without permission.

profile is lower than that for temperature T_1. However, due to the lower degradation rate, the product synthesis continues for a longer time, eventually leading to a higher product yield. At temperature T_2 it is observed that the final product yield is higher than that for temperatures T_1 and T_3 since at temperature T_2, the synthesis rate of product is higher than the synthesis rate at temperature T_3 and the degradation rate of product is lower than the degradation rate at temperature T_1. Thus, it is clear that a continuously changing temperature *profile* rather than a constant temperature would provide the maximum product yield.

It can be easily seen that the controllability assumption is satisfied. Furthermore, $s = \infty$ and in the singular region the optimal profile of the manipulated input q can be calculated by equation (4.9) which yields:

$$q = -\frac{[CMC]\Delta E_{16}k_{16}^2 - E[aa_i]\Delta E_{16}k_a k_{16} + E[aa_i]\Delta E_a k_a - [CMC]\Delta E_{16}k_{16}}{E[aa_i]k_a\frac{\Delta E_a^2}{RT^2} - [CMC]k_{16}\frac{\Delta E_{16}^2}{RT^2}} \tag{7.27}$$

in the singular region. Figure 7.8 shows the optimal temperature profile and the corresponding product profile calculated from the above formula. It is clear that the temperature profile rather than a constant temperature leads to increased product yield.

In practice, the optimal temperature profile is bounded by a maximum temperature T_{max} (above which the cells die catastrophically) and a minimum temperature T_{min} (below which the cellular processes slow down to the extent that no product is formed). Beta-lactam fermentations normally synthesize products in the temperature range $20 - 35^{\circ}$ C. Using the system parameters given in Table 7.1 we calculated the optimum temperature profile to maximize cephamycin C yield. The results are shown in Figure 7.9. There is an initial rise in temperature which leads to an en-

Reproduced with permission of the copyright owner. Further reproduction prohibited without permission.

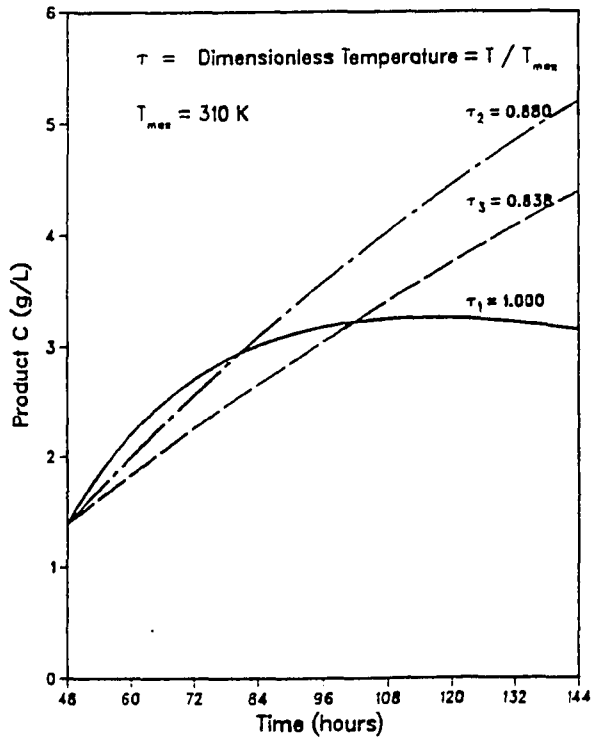

Figure 7.7: Effect of Changing Temperature on Product

Reproduced with permission of the copyright owner. Further reproduction prohibited without permission.

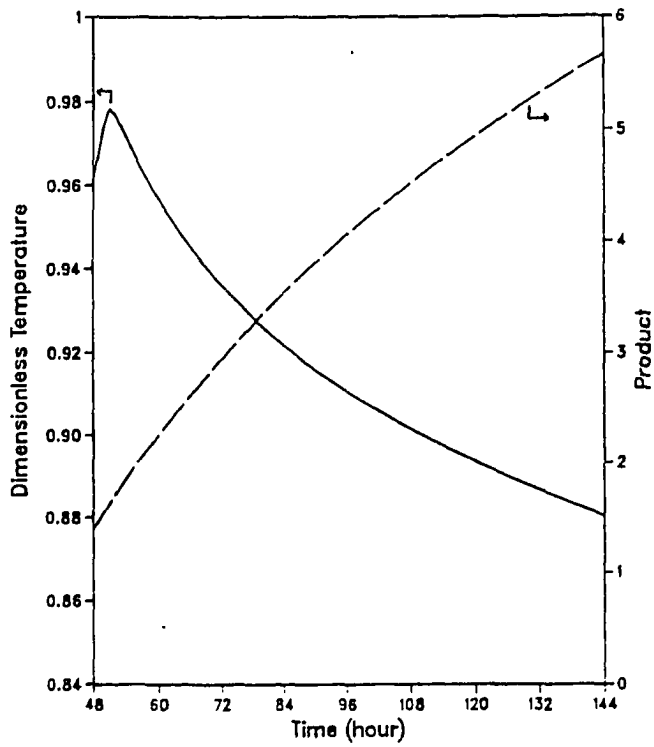

Figure 7.8: Optimal Temperature and Product Profiles

Reproduced with permission of the copyright owner. Further reproduction prohibited without permission.

hanced synthesis rate of cephamycin C. The temperature decreases from 52 hours to 67 hours to reduce the degradation rate of cephamycin C. At 67 hours, the temperature profile hits the lower temperature bound, T_{min}. At this point, the optimal operating strategy is to maintain the fermentation at the lower bound. Operating the fermentation at a higher temperature would lead to higher product degradation rate and operating the fermentation at a lower temperature would result in shut down of cellular metabolism and product synthesis.

7.4.4 Effect of Changing Temperature on Amino Acid Feeding

The optimal temperature profile calculated by equation (7.27) was based on the assumption that sufficient *endogenous* amino acids are present. However, by decreasing temperature, the utilization rate of amino acids decreases. Thus, maintaining a constant feed of amino acids would result in accumulation of exogenous amino acids. Since it is expensive to feed amino acids, it is desirable to have a separate control loop for amino acids feed. As the temperature decreases, the amino acid feed has to be decreased in such a way that there is very little accumulation of amino acids in the fermentation broth. This strategy of controlling amino acids while keeping the fermentation on the optimal temperature profile would minimize the use of amino acids as well as maximize the formation of cephamycin C.

7.5 Conclusions

We have shown how a detailed structured model can be reduced for yield optimization depending on the manipulated input chosen. Even though the same biosynthesis pathway for cephamycin C production is followed in different microorganisms and different strains of the same microorganism, the model parameters of the reduced

Reproduced with permission of the copyright owner. Further reproduction prohibited without permission.

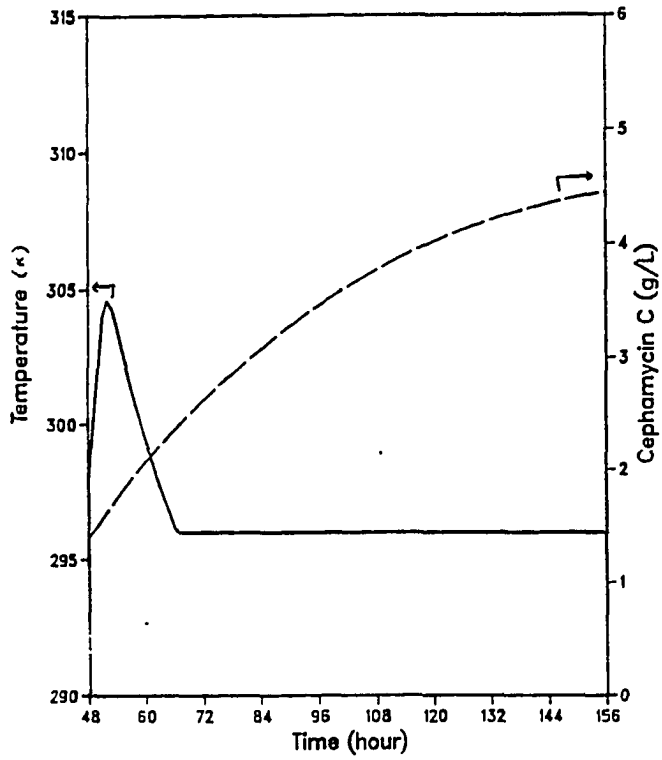

Figure 7.9: Optimal Temperature and Product Profiles (Constrained Optimization)

Reproduced with permission of the copyright owner. Further reproduction prohibited without permission.

ΔE_a	16744 $J/mole$ (4 $KCal/mole$)
ΔE_{16}	49600 $J/mole$ (11.85 $KCal/mole$)
k_{a0}	823.18
k_{160}	5.578 x 10^6
T_{min}	296 K
T_{max}	305 K

Table 7.1: Model Parameters

model differ in different systems. Thus, the optimum operating conditions have to be set separately for each system. Optimal cephamycin C production can be achieved by:

- Feeding glucose at a rate of 9 ml/hr.
- Using the optimal temperature profile to maximize the production of cephamycin C.
- Feeding amino acid precursers so that the rate limiting enzyme is saturated and at the same time adjust the feed rate with temperature so that there is no accumulation of amino acids in the fermentation broth.

Reproduced with permission of the copyright owner. Further reproduction prohibited without permission.

CHAPTER VIII

CONCLUSIONS AND FUTURE WORK

Were I to await perfection, my book would never be finished.

Tai T'ung

In batch reactors, the major objective is to minimize an objective function at the *end* of the batch cycle. The traditional approach to end-point optimization provides an *open-loop* scheme through the solution of a two-point boundary value problem. However, this approach is inappropriate when the model parameters and initial conditions of the process model are not accurately known and there are external disturbances to the process. In this situation optimal closed-loop schemes have been developed in the literature for only *specific* cases.

In this thesis, the *general* problem of synthesizing optimal state feedback laws for end-point optimization was addressed. First, it was shown that geometric tools can be used to obtain a more concrete and transparent representation of the necessary conditions for optimality. These results were then used to develop a general framework for end-point optimal state feedback synthesis. Explicit synthesis formulae for the state feedback laws were obtained for the case where the final time is fixed and there are no state inequality constraints. The degree of singularity of the system was defined in terms of the Lie bracket structure of the system dynamics. It was shown

Reproduced with permission of the copyright owner. Further reproduction prohibited without permission.

that when the system possesses an infinite degree of singularity, the optimization problem is equivalent to a regulation problem. For finite degree of singularity static and dynamic state feedback laws were developed for end-point optimization. Utilizing the same methodology, feedback laws were derived for end-point optimization when the final time is free and there is a state inequality constraint. As illustrative examples of application of the proposed methodology, several end-point optimization problems in batch chemical and biochemical reactors were considered.

It was observed that under certain conditions the end-point optimization problem is equivalent to a regulation problem in a time-varying system. Feedback laws were derived to solve this regulation problem. A nonlinear transformation was derived which provides a linear time-invariant input-output response. A standard linear controller with integral action was then used for offsetless tracking of the desired trajectory. Internal stability results under the state feedback were derived. Then, a dynamic output feedback controller for the time-varying system was synthesized. Finally, end-point optimization of cephamycin C, an industrially important β-lactam antibiotic, was considered. Three different manipulated inputs, namely, glucose feeding, amino acids feeding and temperature, are considered. It was shown how the theory developed in this thesis can be used for end-point optimization for each case.

In this thesis, a general state feedback approach has been formulated for end-point optimization of batch processes. Using this methodology it is possible to calculate the optimal input profile to minimize an objective function for *any* batch process described by a system of ordinary differential equations. The formulation of the optimization strategy as a state feedback law has several advantages over the traditional open-loop approach. Disturbances to the process and uncertainties in the initial conditions can be attenuated. If the model parameters are time-varying, they

Reproduced with permission of the copyright owner. Further reproduction prohibited without permission.

can be updated *on-line*. This formulation provides a uni-directional algorithm for the calculation of the optimal strategy.

In this thesis, optimal state feedback laws were derived for a system with a *single* manipulated input. The methodological framework introduced in this thesis can be generalized to end-point optimization problems using *multiple* manipulated inputs. Possible applications for such feedback laws would be, for instance, in yield optimization of semi-batch reactors by manipulating both feed rate of substrate as well as the batch temperature. Future work in *practical* implementation of the theory developed in this thesis is necessary. The optimal state feedback laws developed in this thesis can be coupled with state and parameter estimation algorithms to provide an on-line *adaptive* optimization scheme. The development of efficient state and parameter algorithms for complex systems is an open issue in the literature and needs further investigation. Other practical issues include the development of software packages within a symbolic computation environment to calculate analytical expressions for the feedback laws and finally the experimental application of these methods.

Reproduced with permission of the copyright owner. Further reproduction prohibited without permission.

APPENDICES

Reproduced with permission of the copyright owner. Further reproduction prohibited without permission.

APPENDIX A

PROOFS OF THEOREMS IN CHAPTER IV

A.1 Proof of Theorem 4.1

Proof for (i): We prove this part of the theorem by contradiction. Let us assume that a singular extremal exists for the system (4.2) with degree of singularity $s = \infty$. The first order necessary conditions on the singular extremal are as follows:

$$\begin{aligned} \lambda^T g(x) &= 0 \\ \lambda^T ad_f^1 g(x) &= 0 \\ \lambda^T ad_f^2 g(x) &= 0 \\ &\cdot \\ &\cdot \\ &\cdot \\ \lambda^T ad_f^{n-1} g(x) &= 0 \\ &\cdot \\ &\cdot \\ &\cdot \end{aligned} \tag{A.1}$$

The first n equations can be written in compact form as:

$$\lambda^T \left[g(x) \,|\, ad_f^1 g(x) \,|\, \ldots \,|\, ad_f^{n-1} g(x) \right] = 0 \tag{A.2}$$

Reproduced with permission of the copyright owner. Further reproduction prohibited without permission.

Since $\lambda(t)$ is an absolutely continuous non-zero vector function in $\mathbb{R}^n$, it follows that:

$$det\left[g(x)\,|ad_f^1 g(x)\,|\ldots|ad_f^{n-1}g(x)\right] = 0$$

for all x in some non-empty set in $\mathbb{R}^n$. This contradicts the assumption of global linear independence of $g(x)$, $ad_f^1 g(x)$, ..., $ad_f^{n-1}g(x)$.

Proof for (ii): The first order necessary conditions on the singular extremal are given by equation (4.7). Using exactly the same argument as in the proof of (i), we conclude that the state trajectories corresponding to the singular control must lie on the surface:

$$S(x) = 0$$

A.2 Proof of Corollary 4.1

Consider a single-input controllable linear system of the form:

$$\dot{x} = Ax + bu$$

For this system $ad_f^k g(x) = (-1)^k A^k b$ for all $k = 0,1,2,\ldots$. Hence

$$[g, ad_f^k g](x) = 0 \ \textit{for all}\ k = 0,1,2,\ldots$$

Thus $s = \infty$. Since the system under consideration is controllable for all x, vector fields defined by $ad_f^k g(x)$ for $k = 0,1,2,\ldots(n-1)$ are linearly independent. Thus, from Theorem 4.1 the system under consideration does not possess a singular extremal.

A.3 Proof of Corollary 4.2

From the involutivity assumption:

$$[g, ad_f^k g](x) = \sum_{j=0}^{n-2} \alpha_{jk}(x) ad_f^k g(x)$$

Reproduced with permission of the copyright owner. Further reproduction prohibited without permission.

where $\alpha_{jk}(x)$ are scalar fields in x.

Hence $s > (n-2)$. But $s \leq (n-2)$ if finite. Thus $s = \infty$. Since the vector fields defined by $ad_f^k g(x)$ for $k = 0, 1, 2, ...(n-1)$ are linearly independent for all x, from Theorem 4.1 the system under consideration does not possess a singular extremal.

A.4 Proof of Theorem 4.2

The first-order necessary conditions for $s = n-2$ can be written as:

$$\lambda^T g(x) = 0$$

$$\lambda^T ad_f^1 g(x) = 0$$

$$\vdots$$

$$\lambda^T ad_f^{n-2} g(x) = 0$$

$$\lambda^T ad_f^{n-1} g(x) + \lambda^T [g, ad_f^{n-2} g](x) u = 0$$

Since these are n equations in n adjoint states, we can eliminate the adjoint states $\lambda^T = [\lambda_1 \ \lambda_2 \ ... \ \lambda_n]$ to obtain expression (4.12).

Reproduced with permission of the copyright owner. Further reproduction prohibited without permission.

A.5 Proof of Theorem 4.3

From Proposition 4.2, the first order necessary conditions for singular extremal are:

$$\begin{aligned}
\lambda^T g(x) &= 0 \\
\lambda^T ad_f^1 g(x) &= 0 \\
&\vdots \\
\lambda^T ad_f^s g(x) &= 0 \\
\lambda^T ad_f^{s+1} g(x) + \lambda^T [g, ad_f^s g](x)u(t) &= 0
\end{aligned} \tag{A.3}$$

which constitute $s+2$ equations in n adjoint states. Differentiating the last equation $(n-s-2)$ times we obtain $(n-s-2)$ more equations:

$$\begin{aligned}
&\lambda^T \left(ad_f^{s+2} g(x) + [g, ad_f^{s+1} g](x)u(t) \right) + \\
&\qquad \lambda^T \left(\left(I\frac{d}{dt} - \frac{\partial f(x)}{\partial x} - \frac{\partial g(x)}{\partial x}u(t) \right) ([g, ad_f^s g](x)u(t)) \right) = 0 \\
&\lambda^T \left(ad_f^{s+3}(g(x)) + [g, ad_f^{s+2}(g)](x)u(t) \right) + \\
&\qquad \lambda^T \left(\left(I\frac{d}{dt} - \frac{\partial f(x)}{\partial x} - \frac{\partial g(x)}{\partial x}u(t) \right) ([g, ad_f^{s+1} g](x)u(t)) \right) + \\
&\qquad \lambda^T \left(I\frac{d}{dt} - \frac{\partial f(x)}{\partial x} - \frac{\partial g(x)}{\partial x}u(t) \right)^2 ([g, ad_f^s g](x)u(t)) = 0 \\
&\vdots \\
&\lambda^T \left(ad_f^{n-1} g(x) + \sum_{k=0}^{n-s-2} \left(I\frac{d}{dt} - \frac{\partial f(x)}{\partial x} - \frac{\partial g(x)}{\partial x}u(t) \right)^k \left([g, ad_f^{n-k-2} g](x)u(t) \right) \right) = 0
\end{aligned} \tag{A.4}$$

Equations (A.3) and (A.4) constitute a set of n equations in n adjoint variables which can be eliminated to give the dynamic state feedback law. This is obtained by setting the determinant of the vector fields in (4.13) equal to zero.

Reproduced with permission of the copyright owner. Further reproduction prohibited without permission.

A.6 Proof of Theorem 4.4

Proof for (i): We prove this part of the theorem by contradiction. Let us assume that a singular extremal exists for the system (4.15) with degree of singularity $s = \infty$. The first order necessary conditions on the singular extremal are as follows:

$$\begin{aligned}
\lambda^T g(x) &= 0 \\
\lambda^T \overline{ad}_f^1 g(x,t) &= 0 \\
\lambda^T \overline{ad}_f^2 g(x,t) &= 0 \\
&\cdot \\
&\cdot \\
&\cdot \\
\lambda^T \overline{ad}_f^{n-1} g(x,t) &= 0 \\
&\cdot \\
&\cdot \\
&\cdot
\end{aligned} \tag{A.5}$$

The first n equations can be written in compact form as:

$$\lambda^T \left[g(x,t) \,\vdots\, \overline{ad}_f^1 g(x,t) \,\vdots\, \ldots \,\vdots\, \overline{ad}_f^{n-1} g(x,t) \right] = 0 \tag{A.6}$$

Since $\lambda(t)$ is an absolutely continuous non-zero vector function in $\mathbb{R}^n$, it follows that:

$$det \left[g(x,t) \,\vdots\, \overline{ad}_f^1 g(x,t) \,\vdots\, \ldots \,\vdots\, \overline{ad}_f^{n-1} g(x,t) \right] = 0$$

for all x and t in some non-empty set in $\mathbb{R}^n \times \mathbb{R}$. This contradicts the assumption of global linear independence of $g(x,t)$, $\overline{ad}_f^1 g(x,t)$, ..., $\overline{ad}_f^{n-1} g(x,t)$.

Proof for (ii): The first order necessary conditions on the singular extremal are given by equation (4.21). Using exactly the same argument as in proof of (i), we conclude that the state trajectories corresponding to the singular control must satisfy the

Reproduced with permission of the copyright owner. Further reproduction prohibited without permission.

following relationship:

$$\overline{S}(x,t) = 0$$

A.7 Proof of Theorem 4.5

Proof for (i): For $s = n-2$, the first order necessary conditions can be written as:

$$\begin{aligned}
\lambda^T g(x,t) &= 0 \\
\lambda^T \overline{ad}_f^1 g(x,t) &= 0 \\
\lambda^T \overline{ad}_f^2 g(x,t) &= 0 \\
&\cdot \\
&\cdot \\
&\cdot \\
\lambda^T \overline{ad}_f^s g(x,t) &= 0 \\
\lambda^T \overline{ad}_f^{n-1} g(x,t) + \lambda^T [g, \overline{ad}_f^{n-2} g](x,t) u &= 0
\end{aligned} \tag{A.7}$$

Since there are n equations in n adjoint states, we can eliminate the adjoint states $\lambda^T = [\lambda_1, \lambda_2, ..., \lambda_n]$ to obtain expression (4.24).

Proof for (ii): For $s \leq n-3$, the first order necessary conditions can be written as equation (4.21) which constitute $s+2$ equations in n adjoint states. Differentiating

Reproduced with permission of the copyright owner. Further reproduction prohibited without permission.

the last equation in (4.21) $(n-s-2)$ times we obtain $(n-s-2)$ more equations:

$$\lambda^T\left(\overline{ad}_f^{s+2}g(x,t)+[g,\overline{ad}_f^{s+1}g](x,t)u(t)\right)+$$
$$\lambda^T\left(\left(I\frac{d}{dt}-\frac{\partial f(x,t)}{\partial x}-\frac{\partial g(x,t)}{\partial x}u(t)\right)([g,\overline{ad}_f^{s}g](x,t)u(t))\right)\;=\;0$$
$$\lambda^T\left(\overline{ad}_f^{s+3}(g(x,t))+[g,\overline{ad}_f^{s+2}(g)](x,t)u(t)\right)+$$
$$\lambda^T\left(\left(I\frac{d}{dt}-\frac{\partial f(x,t)}{\partial x}-\frac{\partial g(x,t)}{\partial x}u(t)\right)([g,\overline{ad}_f^{s+1}g](x,t)u(t))\right)+$$
$$\lambda^T\left(I\frac{d}{dt}-\frac{\partial f(x,t)}{\partial x}-\frac{\partial g(x,t)}{\partial x}u(t)\right)^2([g,\overline{ad}_f^{s}g](x,t)u(t))\;=\;0$$

.

.

.

$$\lambda^T\left(\overline{ad}_f^{n-1}g(x,t)\right)+$$
$$\lambda^T\left(\sum_{k=0}^{n-s-2}\left(I\frac{d}{dt}-\frac{\partial f(x,t)}{\partial x}-\frac{\partial g(x,t)}{\partial x}u(t)\right)^k\left([g,\overline{ad}_f^{n-k-2}g](x,t)u(t)\right)\right)\;=\;0 \tag{A.8}$$

Equations (4.21) and (A.8) constitute a set of n equations in n adjoint variables which can be eliminated to give the dynamic state feedback law. This is obtained by setting the determinant of the vector fields in (4.25) equal to zero.

Reproduced with permission of the copyright owner. Further reproduction prohibited without permission.

APPENDIX B

PROOFS OF CHAPTER V

B.1 Proof of Theorem 5.1

The first order necessary conditions on the singular extremal are as follows:

$$\begin{aligned}
\lambda^T g(x) &= 0 \\
\lambda^T ad_f^1 g(x) &= 0 \\
\lambda^T ad_f^2 g(x) &= 0 \\
&\cdot \\
&\cdot \\
&\cdot \\
\lambda^T ad_f^{n-2} g(x) &= 0 \\
\lambda^T ad_f^{n-1} g(x) &= 0
\end{aligned} \tag{B.1}$$

Eliminating the n-vector of adjoint states to obtain the singular surface (5.12) on which the state trajectories corresponding to the singular extremal evolve.

Reproduced with permission of the copyright owner. Further reproduction prohibited without permission.

B.2 Proof of Theorem 5.2

Proof for (i): The first order necessary conditions are given by:

$$\begin{aligned}
\lambda^T f(x) &= 0 \\
\lambda^T g(x) &= 0 \\
\lambda^T ad_f^1 g(x) &= 0 \\
\lambda^T ad_f^2 g(x) &= 0 \\
&\cdot \\
&\cdot \\
&\cdot \\
\lambda^T ad_f^{n-2} g(x) &= 0
\end{aligned} \tag{B.2}$$

Eliminating the n adjoint states from the above n independent equations, we obtain the singular surface (5.13) on which the state trajectories corresponding to the singular extremal evolve.

Proof for (ii): The first-order necessary conditions are given by:

$$\begin{aligned}
\lambda^T g(x) &= 0 \\
\lambda^T ad_f^1 g(x) &= 0 \\
&\cdot \\
&\cdot \\
&\cdot \\
\lambda^T ad_f^{n-2} g(x) &= 0 \\
\lambda^T ad_f^{n-1} g(x) + \lambda^T [g, ad_f^{n-2} g](x) u &= 0
\end{aligned}$$

Since these are n equations in n adjoint states, we can eliminate the adjoint states $\lambda^T = [\lambda_1 \ \lambda_2 \ ... \ \lambda_n]$ to obtain the static state feedback represented by equation (5.14).

Reproduced with permission of the copyright owner. Further reproduction prohibited without permission.

B.3 Proof of Theorem 5.3

Proof for (i) : The first-order necessary conditions for $s = n-3$ can be written as:

$$\lambda^T f(x) = 0$$

$$\lambda^T g(x) = 0$$

$$\lambda^T ad_f^1 g(x) = 0$$

$$\vdots$$

$$\lambda^T ad_f^{n-3} g(x) = 0$$

$$\lambda^T ad_f^{n-2} g(x) + \lambda^T [g, ad_f^{n-3} g](x) u = 0$$

Since these are n equations in n adjoint states, we can eliminate the adjoint states $\lambda^T = [\lambda_1 \ \lambda_2 \ ... \ \lambda_n]$ to obtain the static state feedback represented by equation (5.14).

Proof for (ii) : From Proposition 5.2, the first order necessary conditions for singular extremal are:

$$\lambda^T g(x) = 0$$

$$\lambda^T ad_f^1 g(x) = 0$$

$$\vdots \qquad \text{(B.3)}$$

$$\lambda^T ad_f^{n-3} g(x) = 0$$

$$\lambda^T ad_f^{n-2} g(x) + \lambda^T [g, ad_f^{n-3} g](x) u(t) = 0$$

which constitute $n-1$ equations in n adjoint states. Differentiating the last equation

Reproduced with permission of the copyright owner. Further reproduction prohibited without permission.

once we obtain an additional equation:

$$ad_f^{n-1}g(x) + [g, ad_f^{n-2}g](x)u(t) + \left(I\frac{d}{dt} - \frac{\partial f(x)}{\partial x} - \frac{\partial g(x)}{\partial x}u(t)\right)\left([g, ad_f^{n-3}g](x)u(t)\right) = 0 \tag{B.4}$$

The above equations constitute a set of n equations in n adjoint variables which can be eliminated to give the dynamic state feedback law. This is obtained by setting the determinant of the vector fields in (5.17) equal to zero.

B.4 Proof of Theorem 5.4

Proof for (i): The first order necessary conditions for singular extremal are:

$$\begin{aligned}
\lambda^T f(x) &= 0 \\
\lambda^T g(x) &= 0 \\
\lambda^T ad_f^1 g(x) &= 0 \\
&\cdot \\
&\cdot \\
&\cdot \\
\lambda^T ad_f^{s-1} g(x) &= 0 \\
\lambda^T ad_f^s g(x) + \lambda^T [g, ad_f^{s-1} g](x)u(t) &= 0
\end{aligned} \tag{B.5}$$

Reproduced with permission of the copyright owner. Further reproduction prohibited without permission.

which constitute $s+2$ equations in n adjoint states. Differentiating the last equation $(n-s-3)$ times we obtain $(n-s-3)$ more equations:

$$\lambda^T\left(ad_f^{s+1}g(x)+[g,ad_f^s g](x)u(t)\right)+ \lambda^T\left(\left(I\frac{d}{dt}-\frac{\partial f(x)}{\partial x}-\frac{\partial g(x)}{\partial x}u(t)\right)([g,ad_f^{s-1}g](x)u(t))\right) = 0$$

$$\lambda^T\left(ad_f^{s+2}(g(x))+[g,ad_f^{s+1}(g)](x)u(t)\right)+ \lambda^T\left(\left(I\frac{d}{dt}-\frac{\partial f(x)}{\partial x}-\frac{\partial g(x)}{\partial x}u(t)\right)([g,ad_f^s g](x)u(t))\right)+ \lambda^T\left(I\frac{d}{dt}-\frac{\partial f(x)}{\partial x}-\frac{\partial g(x)}{\partial x}u(t)\right)^2([g,ad_f^{s-1}g](x)u(t)) = 0$$

.

.

.

$$\lambda^T\left(ad_f^{n-2}g(x)+\sum_{k=0}^{n-s-3}\left(I\frac{d}{dt}-\frac{\partial f(x)}{\partial x}-\frac{\partial g(x)}{\partial x}u(t)\right)^k\left([g,ad_f^{n-k-3}g](x)u(t)\right)\right) = 0 \tag{B.6}$$

The above equations constitute a set of n equations in n adjoint variables which can be eliminated to give the dynamic state feedback law. This is obtained by setting the determinant of the vector fields in (5.18) equal to zero.

Proof for (ii) : The first order necessary conditions for singular extremal are:

$$\begin{aligned}
\lambda^T g(x) &= 0\\
\lambda^T ad_f^1 g(x) &= 0\\
&\cdot\\
&\cdot\\
&\cdot\\
\lambda^T ad_f^s g(x) &= 0\\
\lambda^T ad_f^{s+1} g(x) + \lambda^T[g,ad_f^s g](x)u(t) &= 0
\end{aligned} \tag{B.7}$$

which constitute $s+2$ equations in n adjoint states. Differentiating the last equation

Reproduced with permission of the copyright owner. Further reproduction prohibited without permission.

$(n-s-2)$ times we obtain $(n-s-2)$ more equations:

$$\lambda^T \left(ad_f^{s+2} g(x) + [g, ad_f^{s+1} g](x)u(t)\right) + \lambda^T \left(\left(I\frac{d}{dt} - \frac{\partial f(x)}{\partial x} - \frac{\partial g(x)}{\partial x}u(t)\right)([g, ad_f^s g](x)u(t))\right) = 0$$

$$\lambda^T \left(ad_f^{s+3}(g(x)) + [g, ad_f^{s+2}(g)](x)u(t)\right) + \lambda^T \left(\left(I\frac{d}{dt} - \frac{\partial f(x)}{\partial x} - \frac{\partial g(x)}{\partial x}u(t)\right)([g, ad_f^{s+1} g](x)u(t))\right) + \lambda^T \left(I\frac{d}{dt} - \frac{\partial f(x)}{\partial x} - \frac{\partial g(x)}{\partial x}u(t)\right)^2 ([g, ad_f^s g](x)u(t)) = 0$$

.

.

.

$$\lambda^T \left(ad_f^{n-1} g(x) + \sum_{k=0}^{n-s-2} \left(I\frac{d}{dt} - \frac{\partial f(x)}{\partial x} - \frac{\partial g(x)}{\partial x}u(t)\right)^k \left([g, ad_f^{n-k-2} g](x)u(t)\right)\right) = 0 \tag{B.8}$$

The above equations constitute a set of n equations in n adjoint variables which can be eliminated to give the dynamic state feedback law. This is obtained by setting the determinant of the vector fields in (5.19) equal to zero.

Reproduced with permission of the copyright owner. Further reproduction prohibited without permission.

BIBLIOGRAPHY

Reproduced with permission of the copyright owner. Further reproduction prohibited without permission.

BIBLIOGRAPHY

[1] Aiba, S., A. E. Humphery, and N. F. Millis, *Biochemical Engineering*, University of Tokyo Press, Tokyo, p. 148, 1973

[2] Bailey, J. E., and D. F. Ollis, *Biochemical Engineering Fundamentals*, McGraw-Hill, Inc., 1986

[3] Bajpai, R. K., and M. Reuss, "Evaluation of Feeding Strategies in Carbon-Regulated Secondary Metabolite Production through Mathematical Modelling", *Biotechnol. Bioeng.*, **23**, 717 (1981)

[4] Bell, D. J., and W. Tsang, "Invertibility and Decoupling of Linear Time-Varying Systems ", *Int. J. Control*, **52**, 4, 983 (1990)

[5] Bryson, A. E., and Y. C. Ho, *Applied Optimal Control*, John Wiley and Sons, Inc., New York, 1975

[6] Byrnes, C. I., and Isidori, A., "Global Feedback Stabilization of Nonlinear Systems", *Proc. 24th IEEE CDC*, Ft. Lauderdale, 1031 (1985)

[7] Chen, S. A., and W. F. Jeng, "Minimum End Time Policies for Batchwise Radical Chain Polymerization", *Chem. Eng. Sci.*, **33**, 735 (1978)

[8] Chen, S. A., and N. W. Huang, "Minimum End Time Policies for Batchwise Radical Chain Polymerization - III: The Initiator Addition Policies", *Chem. Eng. Sci.*, **36**, 1295 (1981)

[9] Chu, W.B., *Modeling, Optimization and Computer Control of the Cephalosporin C Fermentation Process*, Ph.D Thesis, Rutgers, The State University of New Jersey, New Brunswick, 1987

[10] Claude, D., M. Fliess, and A. Isidori, "Immersion, direct et par bouclage, d' um systeme non lineaire dans un lineaire", *C. R. Acad. Sc. Paris*, **296**, 237 (1983)

[11] Constantinides, A., J. L. Spencer, and E. L. Gaden, Jr., "Optimization of Batch Fermentation Processes II. Optimum Temperature Profiles for Batch Penicillin Fermentation", *Biotechnol. Bioeng.*, **12**, 1087 (1970)

[12] Daoutidis, P., and Kravaris, C., "Dynamic Output Feedback Control of Minimum-Phase Nonlinear Processes", *Chem. Eng. Sci.*, **47**, 4, 837 (1992)

Reproduced with permission of the copyright owner. Further reproduction prohibited without permission.

[13] Denn, M. M., *Optimization by Variational Methods*, McGraw-Hill Inc., New York, 1969

[14] Denn, M. M., *Process Modelling*, Longman Scientific and Technical, 1986

[15] Dykstra, K. H., X. M. Li, and H. Y. Wang, "Computer Modeling of Antibiotic Fermentation with Online Product Removal", *Biotechnol. Bioeng.*, **32**, 356 (1988)

[16] Edwards, V. H., "The Influence of High Substrate Concentrations on Microbial Kinetics", *Biotechnol. Bioeng.*, **12**, 679 (1970)

[17] Eley, D. D., P. W. Selwood, and P. B. Weisz, *Advances in Catalysis*, Vol. 13, Academic Press, 1962

[18] Ellis, M. F., T. W. Taylor, V. Gonzalez, and K. F. Jensen, "Estimation of the Molecular Weight Distribution in Batch Polymerization", *A.I.Ch.E. J.*, **34**, 8, 1341 (1988)

[19] Fishman, V. M., and V. V. Biryukov, "Kinetic Model of Secondary Metabolite Production and its Use in Computation Optimal Conditions", *Biotechnol. Bioeng. Symp.*, **4**, 647 (1974)

[20] Fogler, H. S., *Elements of Chemical Reaction Engineering*, Prentice-hall, Inc., 1986

[21] Freund, E., "Design of Time-Variable Multivariable Systems bu Decoupling and by the Inverse ", *IEEE Trans. Automatic Control*, **16**, 183 (1971)

[22] Froment, G. F., and K. B. Bischoff, *Chemical Reactor Analysis and Design*, John Wiley and Sons, Inc., 1979

[23] Gabasov, R., and F. M. Kirillova, "Higher Order Necessary Conditions for Optimality", *SIAM J. on Control*, **10** (1), 127 (1972)

[24] Harmon, J., Svoronos, S. A., and Lyberatos, G., "Adaptive Steady State Optimization of Biomass Productivity in Continuous Fermentors", *Biotechnol. Bioeng.* , **30**, 335 (1987)

[25] Hicks, J., A. Mohan, and W. H. Ray, "The Optimal Control of Polymerization Reactors", *Can. J. Chem. Eng.*, **47**, 590 (1969)

[26] Hirschorn, R. M., "Output Tracking in Multivariable Nonlinear Systems", *IEEE Trans. Automatic Control*, **26**, 593 (1981a)

[27] Hirschorn, R. M., "(A-B) Invariant Distributions and Disturbance Decoupling of Nonlinear Systems", *SIAM J. Contr. Optimiz.*, **19**, 1 (1981b)

[28] Hunt, L. R., "Sufficient Conditions for Controllability", *IEEE Trans. Circuits and Systems*, Vol. CAS-29, 5, 285 (1982)

Reproduced with permission of the copyright owner. Further reproduction prohibited without permission.

[29] Hunt, L. R., R. Su and G. Meyer,"Global Transformations of Nonlinear Systems," *IEEE Trans. Automat. Contr.*, **AC-28**, 24 (1983)

[30] Inamine E., and J. Birnbaum, U.S Patent 3,770,590 (Nov. 6, 1973)

[31] Isidori, A., *Nonlinear Control Systems, 2nd ed.*, Springer-Verlag, 1989

[32] Isidori, A., and A. Ruberti, "On the Synthesis of Linear Input-Output Responses for Nonlinear Systems", *Syst. Contr. Let.*, **4**, 17 (1984)

[33] Jaklitsch, W. M., W. Hampel, M. Rohr, and C. P. Kubicek, "α-Aminoadipate Pool Concentration and Penicillin Biosynthesis in Strains of *Penicillium chrysogenum* ", *Can. J. Microbiol.*, **32**, 473 (1986)

[34] Jakubcsyk, B. and W. Respondek, "On Linearization of Control Systems", *Bull. Acad. Polonaise Sci. Ser. Sci. Math.*, **28**, 60 (1982)

[35] Jazwinski, A. H., *Stochastic Processes and Filtering Theory*, Academic Press, New York, 1970

[36] Joshi, A., and Palsson, B., "*Escherichia coli* Growth Dynamics: A Three-Pool Biochemically Based Description", *Biotech. Bioengg.*, **31**, 3, 102 (1988)

[37] Kelley, H. J., R. E. Kopp, and H. G. Moyer, "Singular Extremals", *Topics in Optimization*, G. Leitmann, ed., Academic Press, New York, 63, 1967

[38] Kern, D. Q., *Process Heat Transfer*, McGraw Hill, 1950

[39] Kopp, R. E., and H. G. Moyer, "Necessary Conditions for Singular Extremals", *AIAA J.*, **3**, 1439 (1965)

[40] Kravaris, C., and Chung, C. B., "Nonlinear State Feedback Synthesis by Global Input Output Linearization", *AIChE J.*, **33**, 4, 592 (1987)

[41] Krener, A. J., "The Higher Order Maximal Principle and its Application to Singular Extremals", *SIAM Journal on Control and Optimization*, **15**(2), 256 (1977)

[42] Lamnabhi-Lagarrigue, F., and G. Stefani, "Singular Optimal Control Problems: On the Necessary Conditions of Optimality", *SIAM J. Control and Optimization*, **28**, 823 (1990)

[43] Lewis, R. M., "Definitions of Order and Junction Conditions in Singular Optimal Control Problems", *SIAM J. Control and Optimization*, **18**, 21 (1980)

[44] Lim,H. C., J. M. Modak, and P. Bonte, "Computational Algorithms for Optimal Feed Rates for a Class of Fed-Batch Fermentation: Numerical Results for Penicellin and Cell Mass Production", *Biotechnol. Bioeng.*, **28**, 1408 (1986)

Reproduced with permission of the copyright owner. Further reproduction prohibited without permission.

[45] Ljung, L, "Estimation of Parameters is Dynamical Systems", in *Handbook of Statistics*, Vol. 5, E. J. Hannan, P. R. Krishnaiah, M. M. Rao eds., Elsevier Science Publishers (1985)

[46] Malmberg, L. H., and W. S. Hu, "Kinetic Analysis of Cephalosporin Biosynthesis in *Streptomyces clavilgerus*", *Biotechnol. Bioeng.*, **38**, 941 (1991)

[47] Matsumura, M., T. Imanaka, T. Yoshida, and H. Taguchi, "Modeling of Cephalosporin C Production and its Application to Fed-Batch Culture", *J. Ferment. Tech.*, **59**, 115 (1981)

[48] Maurer, H., "On optimal control problems with bounded state variables and control control appearing linearly", *SIAM J. Control and Optimization*, **15**, 3, 345 (1977)

[49] McDanell, J. P., and W. F. Powers, "Necessary Conditions for joining Optimal Singular and Nonsingular Subarcs", *SIAM Journal on Control*, **9**(2), 161 (1971)

[50] Menawat, A., R. Muthurasan, and D. R. Coughanowr, "Singular Control Strategy for a Fed-Batch Bioreactor: Numerical Approach", *A.I.Ch.E J.*, **33**, 776 (1987)

[51] Miura, Y., K. Tsuchiya, H. Yamamoto, M. Okazaki, *J. Ferment. Technol.*, **53**, 67 (1975)

[52] Modak, J. M., *A Theoretical and Experimental Optimization of Fed-Batch Fermentation Processes, Ph.D Thesis*, Purdue University, West Lafayette, 1988

[53] Modak, J. M., and H. C. Lim, "Feedback Optimization of Fed-Batch Fermentation", *Biotechnol. Bioeng.*, **30**, 528 (1987)

[54] Mou, D. G., *Toward an Optimum Penicillin Fermentation by Monitoring and Controlling Growth Through Computer-Aided Mass Balancing , Ph.D Thesis*, M.I.T., Cambridge, 1979

[55] Ohno, H., E. Nakanishi and T. Takamatsa, "Optimal Control of a Semi-Batch Fermentation", *Biotechnol. Bioeng.*, **18**, 847 (1976)

[56] Palanki, S., Kravaris, C., and Wang, H.Y., " Synthesis of state feedback laws for end-point optimization in batch processes", *Chem. Eng. Sci., (in press)* (1992)

[57] Ray, W. H., *Advanced Process Control*, McGraw-Hill Inc., NY, 1981

[58] Robbins, H. M., "A Generalized Legendre Condition for Singular Optimal Control Problems", Report No. SRRC-RR-64-95, Sperry Rand Research Center, Sudbury, Massachusetts (1967)

[59] Rouff, M, and F. Lamnabhi-Lagarrigue, "A New Approach to Nonlinear Optimal Feedback Law", *Sys. Control Lett.*, **7**, 411 (1986)

Reproduced with permission of the copyright owner. Further reproduction prohibited without permission.

[60] Sacks, M. E., S. Lee, and J. A. Biesenberger, "Optimal Policies for Batch, Chain Addition Polymerizations", *Chem. Eng. Sci.*, **27**, 2281 (1972)

[61] Schuler, H., and S. Papadopoulou, "Real-Time Estimation of the Chain-Length Distribution in a Polymerization Reactor:II. Comparison of Estimated and Measured Distribution Functions", *Chem. Eng. Sci.*, **41**, 2681 (1986)

[62] Shen, Y. Q., S. Wolfe, and A. L. Demain, " Levels of Isopenicillin N Synthetase and Deacetoxycephalosporin C Synthetase in *Cephalosporium acremonium* Producing High and Low Levels of Cephalosporin C", *BioTechnology*, **4**, 61 (1986)

[63] Silverman, L. M., "Properties and Application of Inverse Systems ", *IEEE Trans. Automatic Control*, **13**, 436 (1968)

[64] Skatrud, P. L., A. J. Tietz, T. D. Ingolia, C. A. Cantwell, D. L. Fisher, J. L. Chapman, and S. W. Queener, " Use of Recombinant DNA to Improve Production of Cephalosporin C *Cephalosporium acremonium*", *BioTechnology*, **7**, 477 (1989)

[65] Speyer, J. L., and Bryson, A. E., " Optimal Programming Problems with a Bounded State Space", *AIAA J.*, **6**, 8, 1488 (1968)

[66] Staniskis, J., and D. Levisauskas, "An Adaptive Control Algorithm for Fed-Batch Culture", *Biotechnol. Bioeng.* , **26**, 419 (1984)

[67] Stephanopoulos, G., and K. Y. San, "Studies on On-Line Bioreactor Identification. I. Theory", *Biotechnol. Bioeng.*, **26**, 1176 (1984)

[68] Stutts, B. E., *An Improved Algorithm for Singular Control Problems with Application to the Optimization of Fed-Batch Penicillin Fermentation, Ph.D Thesis*, Purdue University, West Lafayette, 1983

[69] Su, R., "On the Linear Equivalents of Nonlinear Systems", *Syst. Contr. Let.*, **2**, 48 (1982)

[70] Thomas, I. M., and C. Kiparissides, "Computation of Near-Optimal Temperature and Initiator Policies for a Batch Polymerization Reactor", *Can. J. Chem. Eng.*, **62**, 284 (1984)

[71] Vidyasagar, M., *Nonlinear Systems Analysis*, Prentice-hall, Inc., 1978

[72] Wang, D. I. C., C. L. Cooney, A. L. Demain, P. Dunnill, A. E. Humphrey, and M. D. Lilly, *Fermentation and Enzyme Technology*, John Wiley and Sons, Inc., New York, 1979

[73] Weigand, W. A., "Maximum Cell Productivity by Repeated Fed-Batch Cultures for Constant Yield Case", *Biotechnol. Bioeng.*, **23**, 249 (1981)

Reproduced with permission of the copyright owner. Further reproduction prohibited without permission.

[74] Wonham, W. M., "Linear Multivariable Control: A Geometric Approach", *Lecture Notes on Control and Information Science, 2nd Ed.*, **10**, Springer-Verlag, 1979

[75] Zhang, J., S. Wolfe, and A. L. Demain, "Ammonium Ions Repress δ-(L-α-aminoadipyl)-L-cysteinyl-D-valine synthetase in *streptomyces clavilgerus* NRRL 3585", *Can. J. Microbiol.*, **35**, 399 (1989)

Reproduced with permission of the copyright owner. Further reproduction prohibited without permission.